SOLID/LIQUID PHASE TRANSFORMATIONS

by

James H. Whittam

A dissertation submitted to the Graduate Faculty in Chemistry in partial fulfillment of the requirements for the degree of Doctor of Philosophy, The City University of New York

1975

This manuscript has been read and accepted for the Graduate Committee in Chemistry in satisfaction of the dissertation requirement for the degree of Doctor of Philosophy.

June 24, 1975
date

Henri L. Rosano.
Chairman of Examining Committee

June 24, 1975
date

Leonard H. Schwartz
Executive Officer

Joseph Rennert
Dr. Joseph Rennert

Henri L. Rosano.
Dr. Henri L. Rosano

Angelo Santoro
Dr. Angelo Santoro

Supervisory Committee

The City University of New York

Abstract

Solid/Liquid Phase Transformations

by

James H. Whittam

Adviser: Professor Henri L. Rosano

Evidence of the importance of phase transformations and the solid/liquid interface is observed from studies on three model systems:

A. Aqueous Solutions

In depth experimentation on the dendrite interface structure of aqueous solutions has established that not only are diffusion and concentration factors important to the interface configuration but the rate of heat extraction from the interface (heat transfer) and associated water play important roles.

B. Enzyme Systems

The change in the activity of α amylase is controlled by the rate of freezing, rate of thawing and the concentration of so-called protective agents. This appears to be due to the solute building up at the solid/liquid interface. Very small concentrations of small molecular weight protective agents lower the activity of the enzyme

after a given freeze thaw cycle more than the unprotected enzyme system would do under similar conditions.

C. Saturated Monoacid Triglycerides

Triglycerides were chosen as a third area of study since they exist in almost all fatty materials and their polymorphic states are due to three principle cross sectional arrangements of long chains α, β' and β. This dissertation presents evidence on the physical aging of pure monoacid triglycerides. A technique is also described using a polarizing microscope and a temperature gradient microscope stage which supplies supplementary information to compliment thermal, x-ray I.R. and NMR methods. This apparatus may also be used as a simple device to determine the temperature stability of various fatty systems. More important, it eliminates many three dimensional heat transfer problems and provides a direct method for observing the phenomena of physical aging of triglycerides.

Physical aging or solid/solid phase transformations occurs as a result of the formation of the meta-stable α and β' polymorphs. Prevention of physical aging may be accomplished by solidifying the triglyceride below the critical rate of freezing for α formation or by the addition of low melting triglyceride impurities (such as trilaurin).

Finally, nucleation data is presented for these pure saturated monoacid triglycerides. Estimates of γ, the surface free energy, for these triglycerides is of the order of 14-17 ergs/cm^2.

Scientific
Involvement
Bridges
Yesterday's
Legends to
Learned
Explanations

Preface

Many individuals, pursuing a project of this magnitude alone and accomplishing its goal, feel they achieve ultimate satisfaction. To this author few individuals reach this pinnacle of success and enjoy it without the help of some excellent support.

Likewise, this dissertation at hand is the product of one person striving to attain formal acknowledgment in the field of Chemistry; however, the support which served as the foundation and guidance of this individual effort must not go unrecognized. To all those individuals involved, I express my deepest appreciation.

I am extremely grateful to my family who throughout the years has helped guide, advise, support, and "put up" with my many antics and activities that have brought me to this very promising frontier of my life. To them I always will be indebted.

Beyond no reasonable doubt, the next most influential person in my life has been Professor Henri L. Rosano. Since my undergraduate days his persistance "to solve zee problum" combined with his overall dynamic personality has left an indelible mark in my mind. I have learned much and benefited greatly from his broad knowledge and experience not only in chemistry but in all aspects of life. According to the words of Gibran, "he who is wise does not bid you enter the house of wisdom but rather leads you to the threshold of your own mind." This sums up my education with Henri L. Rosano.

To thank in one line all the other people whom I have had the fortune to meet during the development of this thesis would be a gross injustice since no one would realize the role they played. The following is a brief account of three years at City College.

The genesis of this thesis first "saw light" during the summer of 1971 at C.C.N.Y. At this time I was doing research as an undergraduate with H.L.R. in the Marlies Lab of Old Baskerville Hall. My summer project was suggested by Mr. R. Pfluger of the Maxwell Division, General Foods Corporation and involved a study on the freeze drying of coffee. The following academic year I assisted Mr. M. Freedman (who was working on his Master's thesis) with research involving the freezing of aqueous solutions. Along with the deligent help of Dr. K.A. Jackson and Mr. W. Miller of the Bell Telephone Laboratories, Murray Hill, New Jersey we designed a unique microscope freeze drying stage. Dr. Jackson's expertise in the field of solidification also served as a bank of knowledge where I could often refer for discussion in my current work.

In June 1972 I made an important decision in my educational career. I had just graduated with my bachelor's degree in chemical engineering when I decided (with some convincing from H.L.R.) to accept a teaching fellowship at the City University of New York and progress on towards a Ph'D in Physical Chemistry. At this time it was also decided that I continue my work on aqueous solutions. In addition, the in-

vestigation of aqueous enzyme systems (the second phase of this work) was provoked in discussions by Dr. C. J. Cante and Dr. R. Guardia of the General Foods Corporation, Tarrytown, New York and Dr. Rosano. As a result, α amylase was chosen as a model system which could be related to a practical problem namely, freezing of foods.

During the summer of '72, I was fortunate enough to be employed with the Lever Bros Co. in Edgewater, New Jersey. Under the direction of Dr. E. D. Goddard (now with Union Carbide) I learned some of the techniques to study fats and fat emulsion systems. This experience was invaluable since I could relate some of the concepts I learned in college to solve some practical problems.

That September, the start of the new school year I was admitted into the PhD Program. I began to extend my study on freezing and solidification problems in solutions and enzyme systems. During this year, thoughts on the third system discussed in this thesis were developed by my good friend Dr. Cante, Dr. Rosano and myself. The crystal behavior of triglyceride systems was chosen because of the importance of solidification processes on their crystal form and because of the many inherent problems associated with products containing fats. With the help of my undergraduate friends H. Ragin, M. Petko and A. Garuba a great deal of information was collected on the kinetics of phase transformations also referred as physical aging.

The following years at City, I had the real fortune of working with some fine people. Dr. William Gerbacia who received his PhD in February 1974, and is now working for Chevron Oil Field Research Co. in La Habra California, en riched my educational background in this field of micro-emulsions. Today he is using these systems in hope of de-veloping an economically feasible process for tertiary oil recovery. Bill and I also played a fine game of tennis to-gether especially when our opponents didn't show up. When the other team did manage to play us our usual emulsified continuity would rapidly break down. Then there was Shu Hsien Chen (The Oriental Flower) who enlightened me in the field of monolayers to such an extent that we published the "world famous theory" on Surface Drag Viscosity. The original dubious theory was developed by a Bulgarian scientist and smuggled out of that country by Dr. Rosano who was working for the French government which in turn was paid by the C.I.A.

One often hears that the environment for a PhD must have a certain critical mass. In Rosano's lab, I'm sure we always ran above this critical. I therefore wish to extend thanks to all the other members of our lab; E. LaGamma, M. Mughelli, S. Schecter, A. Weiss, T. Forman and L. Kennberg. If there is anything we will all remember, it is that we had the best lunch hours in the entire college. This group also exhibited the greatest enthusiasm for having a party. No matter what the situation was we could always find an excuse to celebrate.

I must also acknowledge Dr. J. Rennert and Dr. A. Santoro

for their thoughts on this project especially in the final stages of preparation and oh yes, the vocal renditions of Prof. H. Salzberg as he walked through the halls singing, Figaro Figaro, the Russian National Anthem or Manon.

Finally, I wish to thank the "shop", especially J. Cannella and B. Cope for their help in designing some of the equipment used in this project and the tireless efforts of Mrs. C. Silver in the Chemistry office for translating "our scribbled thoughts.

Respectfully,

James H. Whittam

CONTENTS

ILLUSTRATIONS

CHAPTER I

CHAPTER II

CHAPTER III

CHAPTER IV

CHAPTER V

TABLES

I

Introduction

This dissertation concenters on the study of phase transformations and the solid/liquid interface. The experimental work was conducted on three model systems (aqueous solutions, enzyme systems and saturated monoacid triglycerides). Although similar systems have been studied, little information exists on the kinetics of phase transformations (especially in fats) in spite of the technological importance of this phenomena.

Willard J. Gibbs (1878) developed a consistant phenomenological (thermodynamic) treatment of the equilibrium problem (1), which is still essential as an introduction to the study of crystal growth. This treatment is made possible through the existence of the principles of thermodynamics and does not consider the atomic structure of matter. Unfortunately, the thermodynamic treatment does not explain all the facets of crystal growth, therefore it is necessary to use more involved methods of statistical mechanical methods and the atomic structure in order to develop a complete theory and to bring out the possible atomic processes for the crystal growth.

The term freezing is "synonymus" with solidification. The former term is usually applied to aqueous systems. These terms imply the formation of a crystalline phase from its molten or liquid form. The phase transformation is driven by the extraction of heat from the liquid state,

and the progress of the transformation is properly separated into two parts:

1) the initial nucleation of crystals
2) the growth of these nuclei by the accretion of atoms from the liquid.

In addition, some transformation processes must include a third step:

3) solid/solid crystal changes

One of the difficulties associated with studying solid/liquid transformations is that the difference is structure between the liquid and the solid phases of a substance is far less dramatic than the difference between the solid and the gaseous phase. Liquid metals occupy only about 4% more volume than do solid metals and the internal energy of a liquid metal exceeds the internal energy of the crystal by only 4 to 5% of the latent heat of vaporization (in the case of copper, the heat of fusion is 3.1 kcal./mole; the heat of vaporization is 80 kcal./mole). Since liquids and solids are energetically alike, the nearest atom neighbor - distance is similar in the liquid and in the solid; most of the atoms of the liquid have a configuration very much like that of the solid.

Despite all the hypothesis, and theories which maybe developed on this subject the end result must be backed up by experimental evidence. Often, however, new and improved theories must wait to be tested by new and improved experimental approach. This thesis combines new techniques to explain various theoretical hypothesis at the solid/liquid interface.

Chapter I

Solidification in General

1.1 On the Nature of Solids and Liquids

A crystalline solid may be considered as a regular display of atoms which may or may not be identical. Each atomic site is specifically defined in space so that electrostatic and magnetic forces are balanced to produce minimum repulsions. The thermal energy of the crystal would simply be the sum of the individual vibrations of all the atoms. A complete description of the crystalline state would also include the imperfections that exist in the crystals.

Liquids are much more difficult to describe on an atomic scale as can be seen by the divergence of opinion on their structure. Chalmers (2) describes the liquid as a random array of atoms all undergoing thermal vibration. The configuration when averaged over times that are long compared to $^{1}/\nu$ (time of one vibration) appears to be random. The random appearance is restricted however in the sense that no two centers may be closer together than the atomic diameter. This specification would explain the lact of crystallinity as determined by Xray diffraction patterns however short range order could exist in the sense that each atom may be related to some of its neighboring atoms.

1.2 The Solid/Liquid Interface--Free Energy

Solidification may be defined as a process by which a solid grows at the expense of a liquid with which it is in contact (3). Equilibrium is obtained when there is no

further change in the solid/liquid interface boundary.

Thermodynamically, at equilibrium a pure material can exist in two phases when the free energy is equal in each phase:

$$F_{liquid} = F_{Solid}$$

$$E_L - T_E S_L = E_S - T_E S_S \qquad 1\text{-}1$$

where T_E = equilibrium temperature

$$(E_L - E_S) = T_E (S_L - S_S)$$

but $(E_L - E_S)$ is the change of internal energy on melting and is therefore the latent heat of fusion. At temperatures other than the equilibrium temperature, the difference of free energy per unit mass is calculated as follows:

$$\Delta F = \Delta E - T\Delta S \qquad 1\text{-}2$$

This is equal to zero when $T = T_E$ the melting point.

Therefore $\Delta S = \frac{\Delta E}{T_E}$ 1-3

If it is assumed that the latent heat of fusion (ΔE) and the entropy of fusion (ΔS) does not change with temperature then:

$$\Delta F = \Delta E - T\frac{\Delta E}{T_E} = \Delta E \frac{(T_E - T)}{T_E} = \frac{(\Delta E)(\Delta T)}{T_E} \qquad 1.4$$

where ΔT is the departure from the equilibrium temperature.

1.3 Nucleation from the Melt

The nucleation of crystals in an undercooled melt can

occur by a variety of processes. Essentially these processes are related in two catagories; 1) homogeneous nucleation 2) heterogeneous nucleation. In the former case nucleation occurs because of configurational fluctuations in an otherwise homogeneous liquid. The nuclei in this process are small transient aggregates of atoms or molecules which spontaneously form in the melt. Heterogeneous nucleation is also caused by configurational fluctuations in a liquid but in this case the fluctuations occur at a surface.

The theories on nucleation generally answer two separate questions: 1) what is the size of the critical nucleus and what is the probability of occurrence or 2) the rate of formation?

During the nucleation process, nuclei grow by adding single atoms to a growing cluster (embryo) of atoms having the configuration of the solid. This may happen homogeneously somewhere in the volume of the liquid or heterogeneously on the surface of a foreign solid. Since the latter usually occurs in practice and due to the fact that homogeneous nucleation can be approximated as one extreme of heterogeneous nucleation one explanation can serve for both examples.

Pound (4) described the nucleation process as a cap-shaped embryo forming on a perfect substrate. Figure I. It exists at a temperature T below the melting temperature T_m. Assuming an equilibrium distribution exists among

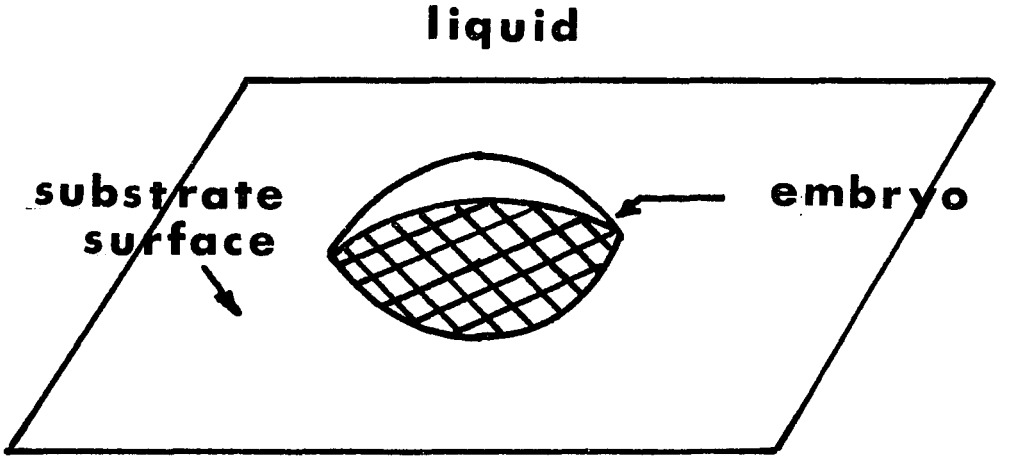

Figure I

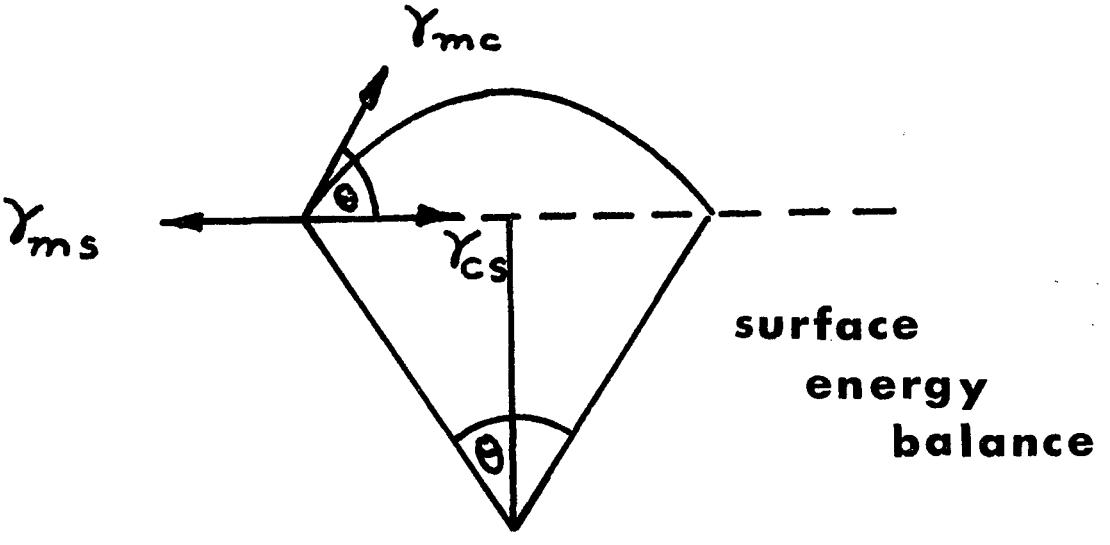

Figure II

embryos containing i atoms and those consisting of one atom, the familiar relationship between the concentration n(i) of embryos of size i and Gibbs Free Energy of Formation ΔG_i is given as

$$n(i) = n(1)\, e^{-\Delta G_i / kT} \qquad 1\text{-}5$$

where n (1) is the number of single atoms of the supersaturated phase in contact with 1 cm of substrate surface.

Both the volume free energy change

$$\Delta G_v = \Delta H \left(1 - T/T_E\right) \qquad 1\text{-}6$$

and the specific interfacial free energies γ contribute to ΔG_i; ΔH is the enthalpy of fusion and Θ is the equilibrium contact angle of the crystal C on the substrate S (Fig II) so that

$$\gamma_{ms} = \gamma_{cs} + \gamma_{mc} \cos\Theta \qquad 1\text{-}7$$

The ΔG_i = Δ Free Energy of the droplet surfaces

\+ Δ Free Energy of the droplet volume 1-8

He expressed The Free Energy of droplet surfaces as:

$$\Delta G_s = G_{fs} - G_{is}$$

$$= \pi R^2 \sin^2\Theta\, \gamma_{cs} + 2\pi R^2 (1 - \cos\Theta)\gamma_{mc} - \pi R^2 \sin^2\Theta\, \gamma_{ms} \qquad 1\text{-}9$$

The Free energy change due to the volume is

$$\Delta G_v = G_{vf} - G_{vi}$$

$$= \frac{\pi R^3}{3} \left(2 - 3\cos\Theta + \cos^3\Theta\right) \Delta G_v \qquad 1\text{-}10$$

Finally

$$\Delta G_i = \Delta G_s + \Delta G_v$$

$$= \left[\gamma_{mc}\, \pi R^2 + \frac{\pi R^3}{3} \Delta G_v\right](2 - 3\cos\Theta + \cos^3\Theta) \qquad 1\text{-}11$$

which exhibits a maximum when

$$\frac{\partial \Delta G_i}{\partial r} = 0 \qquad 1\text{-}12$$

The radius corresponding to this maximum is

$$r^* = \frac{2\gamma_{mc}}{\Delta G_v} \qquad 1\text{-}13$$

Substituting in 1 - 7

$$\Delta G^* = \frac{16\pi\gamma_{mc}^3}{3\Delta G_v^2}(2+\cos\theta)\left(\frac{1-\cos\theta}{4}\right)^2 \qquad 1\text{-}14$$

and

$$n(i)^* = n(1)\, e^{-\Delta G^*/kT} \qquad 1\text{-}15$$

Note that when $\theta = 0$ there will be complete wetting of the solid by the crystal and $\Delta G^* = 0$. At the other extreme when $\theta = 180$ there is no wetting and the system is a case of "homogeneous" nucleation. Then

$$\Delta G^* = \frac{16\pi\gamma_{mc}^3}{3\Delta G_v^2} \qquad 1\text{-}16$$

If the change in free energy of the surface (1-9) and the volume of the drop (1-10) were plotted as a function of r, the total ΔG_i, could simply be determined as the sum of the individual free energies. At the point where ΔG_i is a maximum (point B) the derivative of free energy with respect to r is zero. Decreasing or increasing the radius from this point causes a decrease in the ΔG_i of the system (Figure III).

The rate of nucleation of new crystals I per cm^2/sec on

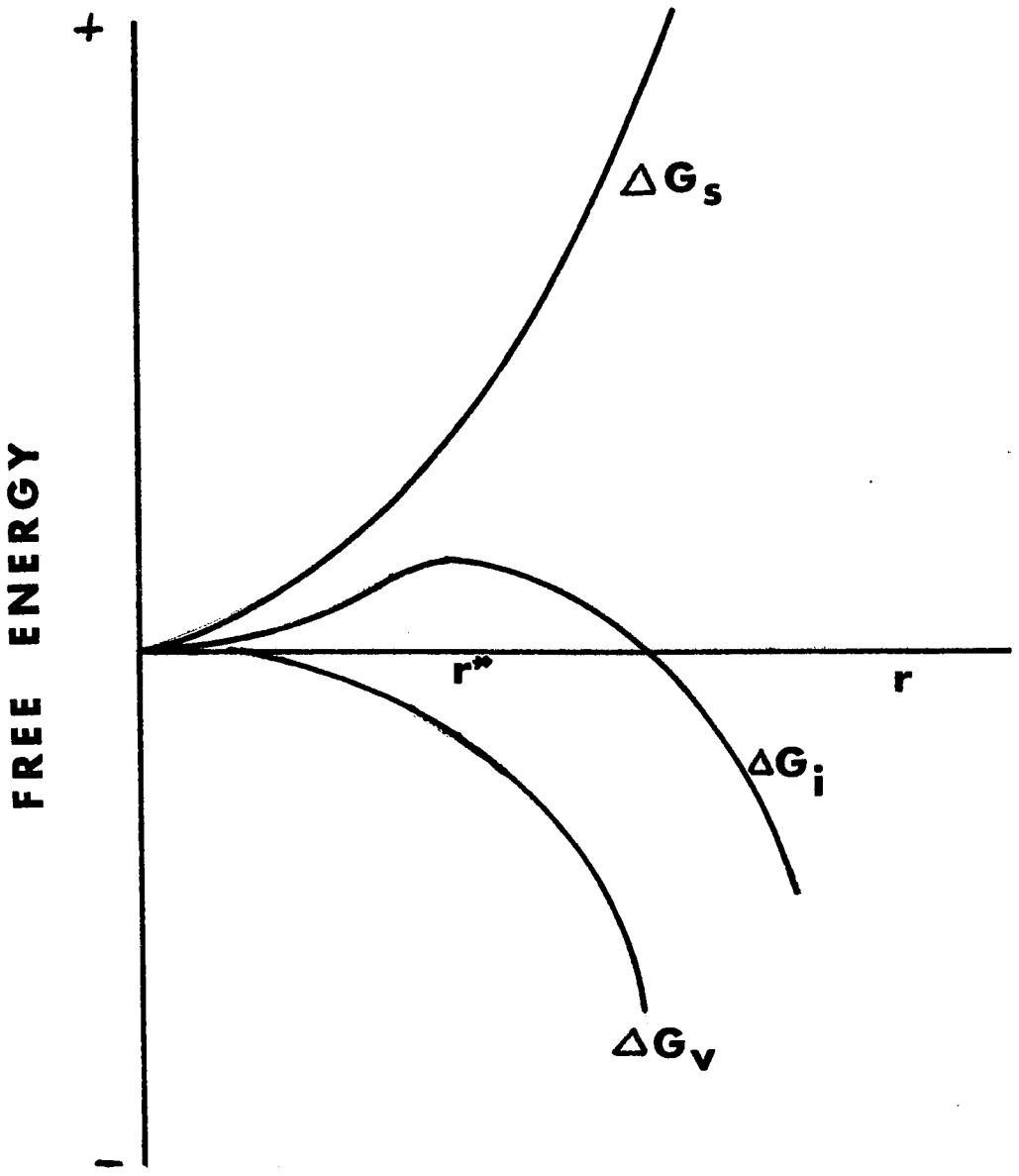

Figure III

the substrate is given as

$$I = \nu\, n(i^*) \qquad 1\text{-}17$$

ν is the frequency at which a single atom from the liquid joins a critical nucleus to form a stable crystal. ν has been formulated by Pound to be

$$\nu = n_s^* \varepsilon \nu_l e^{-\Delta G_i^*/kT} \qquad 1\text{-}18$$

n_s^* is the number of atoms of liquid in contact with the surface of the critical nucleus.

ε = probability of a given atomic jump direction $(\sim 1/6)$

ν_l = lattice vibration frequency $(\sim 10^{13}\ sec^{-1})$

ΔG_D^* free energy of activation for diffusion $(\sim kT)$

$$I = n_s^* \varepsilon \nu_l n(1) e^{-(\Delta G_D^* + \Delta G^*)/kT} \qquad 1\text{-}19$$

A qualitative variation of the nucleation rate of new crystals I as a function of T is given in figure IV.

The implications of this theory on nucleation is that the driving force in crystallization is the difference between the free energies of the liquid and solid state. At equilibrium, the rate of crystallization is zero.

Experimental evidence (5) indicates that the liquid phase most often supercools before crystallization. The magnitude of supercooling is determined by the energy absorbed in producing a crystallite nucleus by random fluctuation. A crystallite in equilibrium with the supercooled liquid will be termed the nucleus. If a

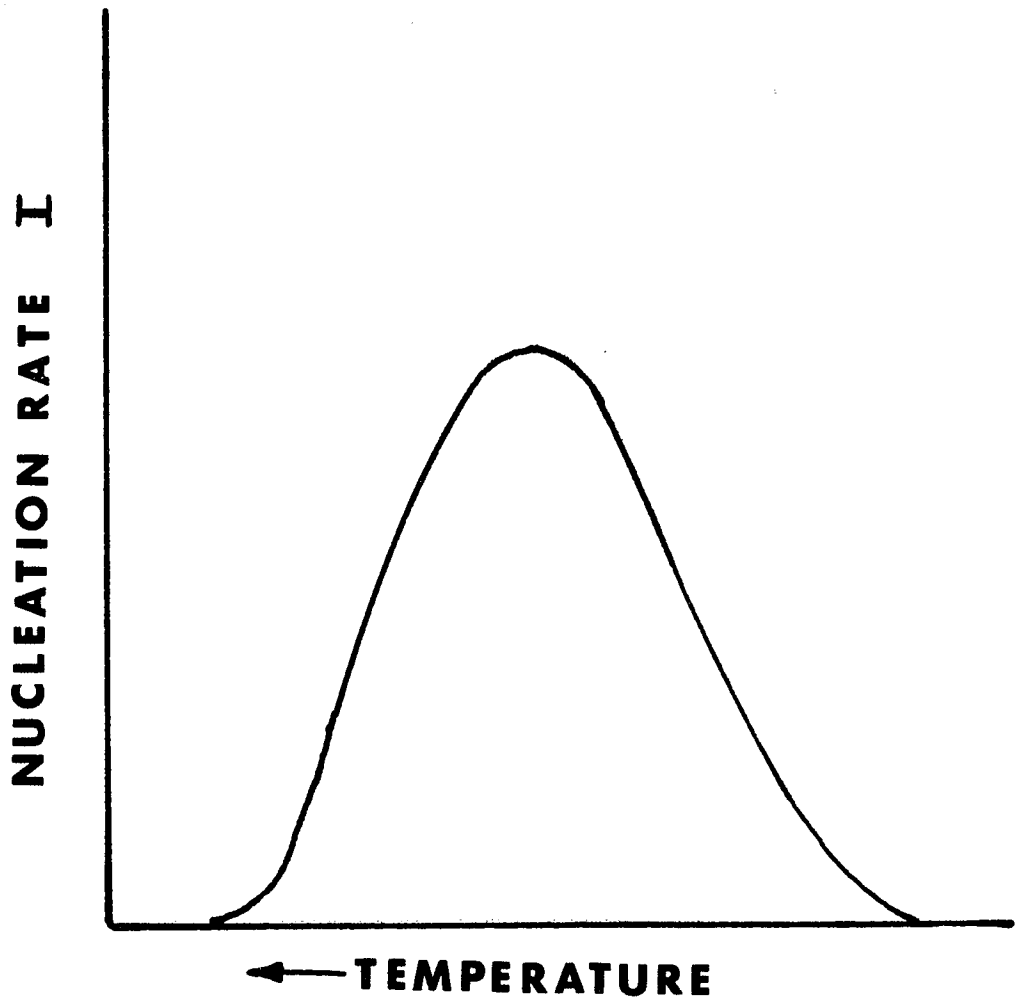

Figure IV

crystallite is larger than a nucleus it grows. This is called a crystallization center.

The above equations state that the number of centers forming and their growth, therefore structure depend on the liquid (γ, E) and the external conditions (T). Removal of heat from the liquid is the external factor which provides the conditions for crystallite formation and growth.

For pure materials the supercooling is usually far greater than normal materials (contain impurities) because the impurities can serve as nucleating sources for crystallization.

Once the Liquid-solid interface is established the growth rate may be explained in terms of other theories based on various physico chemical properties.

In order to define a solid-liquid interface it is necessary to have a criterion which differentiates between an atom in the liquid and in the solid phases. Jackson (6) suggests that when a metallic atom leaves the liquid and adds itself to the interface, its amplitude of vibration is less than 15% of the interatomic distance.

1.4 The Solid Liquid Interface

For a crystalline solid undistorted right up to its surface, all the bonds have the same energy within the crystal. An atom at the surface however, may have any number of nearest neighbors thus the energies of these

surface atoms will therefore be higher than the atoms in the interior. Knowing the surface arrangement of atoms allows one to estimate the magnitude of energy in the surface.

The interface is defined in this work as the surface which separates all those atoms that occupy lattice sites from those that do not. This general definition implies the interface need not be atomically smooth.

A smooth interface involves only one or two atomic layers and has a small specific area, whereas a rough interface involves several atomic layers and has a much larger specific area.

The degree of smoothness of a solid-liquid interface can be evaluated by deriving the changes in interfacial free energy as atoms are added to an initially planar interface. The change is great if the surface is rough and zero if the surface is perfectly smooth.

Solids in equilibrium with their supersaturated vapors are usually considered as having smooth interfaces. (7) However, solid-liquid interfaces may either be rough or smooth, and differences in growth patterns can to a large extent be accounted for by differences in smoothness; for example there is a striking difference between the growth patterns of metals (rough interfaces) and those of non-metals (rather smooth interfaces.)

Rough interfaces have been studied by Burton and Cabrera (8) and by Mullins (9). The next section will discuss in more detail the most widely accepted way of

correlating interface smoothness and crystal growth.

1.5 Solid/Liquid Interface Kinetics

The degree of smoothness of the interface is related to the magnitude of solidification entropy(small for rough interfaces, large for smooth interfaces.) as has been shown by Jackson. (6,10,11)

In his statistical mechanical treatment, atoms randomly added to an initially smooth interface give rise to a change in free energy ΔF_s such that:

$$\Delta F_s = -\Delta E_o - \Delta E_1 + T\Delta S_o - T\Delta S_1 - PdV \qquad 1\text{-}20$$

The term PdV arises from the change in volume and is negligible with respect to other terms in the liquid-solid transformation, at atmospheric pressure.

To derive the different terms of this expression two assumptions are made:

1. It is assumed that the N_A atoms will add themselves to the solid phase as part of a single atomic layer. This layer will be completed before the next layer can be started. This is referred to as the "single layer rough interface."

2. It is furthermore assumed that the difference in bond energy of an atom in the liquid and the same atom in the solid is equal to $\frac{2L}{V}$, where L is the energy required to take the atom from the solid and put it in the liquid (i.e. latent heat of melting per atom), V is the total number or nearest neighbors. The number two is used because every bond energy is shared by two atoms.

The total number of nearest neighbors of an atom in the solid, V, is equal to the sum of the number of atoms in its crystal plane (N_1) in the crystal plane above it (N_0), and in the crystal plane below it (N_0). Thus V=N, + $2N_0$.

ΔE_o is the energy gained by adding N_A atoms to the interface. According to the above assumptions:

$$\Delta E_o = \frac{2L}{V} N_A N_o \qquad 1\text{-}21$$

ΔE_1 is the energy gained by the bonding of some of the N atoms between themselves. If N is the number of surface sites available $\frac{N_A}{N}$ is the proportion of occupied sites adjacent to the added atoms.

$$\Delta E_1 = \frac{2L}{V} \cdot \frac{N_A}{N} \cdot N_A \cdot \frac{N_1}{2} \qquad 1\text{-}22$$

(here again $\frac{N}{2}$ is used instead of N because each bond energy is equally shared by the two adjacent atoms.)

ΔS_o is the entropy change corresponding to the liquid-solid transformation of N_A atoms.

$$\Delta S_o = N_A \cdot \frac{L}{T_E} \qquad 1\text{-}23$$

ΔS_i is the entropy gained by the random arrangement of the N atoms among the N available sites. If P is the number of such arrangements.

$$\Delta S_1 = K \ln P \qquad 1\text{-}24$$

With $V = N_1 + 2N_0$ and with $X = \frac{N_0}{V}$ = fraction of sites filled. (Appendix II)

$$\frac{\Delta F_S}{N K T_E} = \frac{L N_A N_i}{N V K T_E}(1-X) + X \ln n + (1-X)\ln(1-X) \qquad 1\text{-}25$$

The quantity $\frac{L}{KT_E} \cdot \frac{N_i}{V}$ is α (in which $\frac{N_i}{V} < 1$)

The final expression is therefore:

$$\frac{\Delta F_S}{N R T_E} = \alpha X (1-X) + X \ln n + (1-X)\ln(1-X) \qquad 1\text{-}26$$

These expressions represent the change in free energy of a planar interface having N available sites when N_A atoms are added to it. Figure V is the graphical interpretation.

This function of x becomes zero when x becomes either zero or one. The plot of the function has the straight line $x=\frac{1}{2}$ as its axis of symmetry.

The number of minima on the plot depends on the position of α with respect to two.

A minimum of change in the surface free energy (ΔF_S) corresponds to a stable form of the interface.

When $\alpha < 2$ the curve has two minima , one close to x=0, and one close to x=1, i.e. when the interface has most of its sites either vacant or filled; either case implies a smooth interface. Therefore, the stable interface is smooth.

When $\alpha > 2$, the curve has only one minimum, obtained when $x=\frac{1}{2}$, i.e. when half of the sites are filled. Therefore, the stable interface is rough.

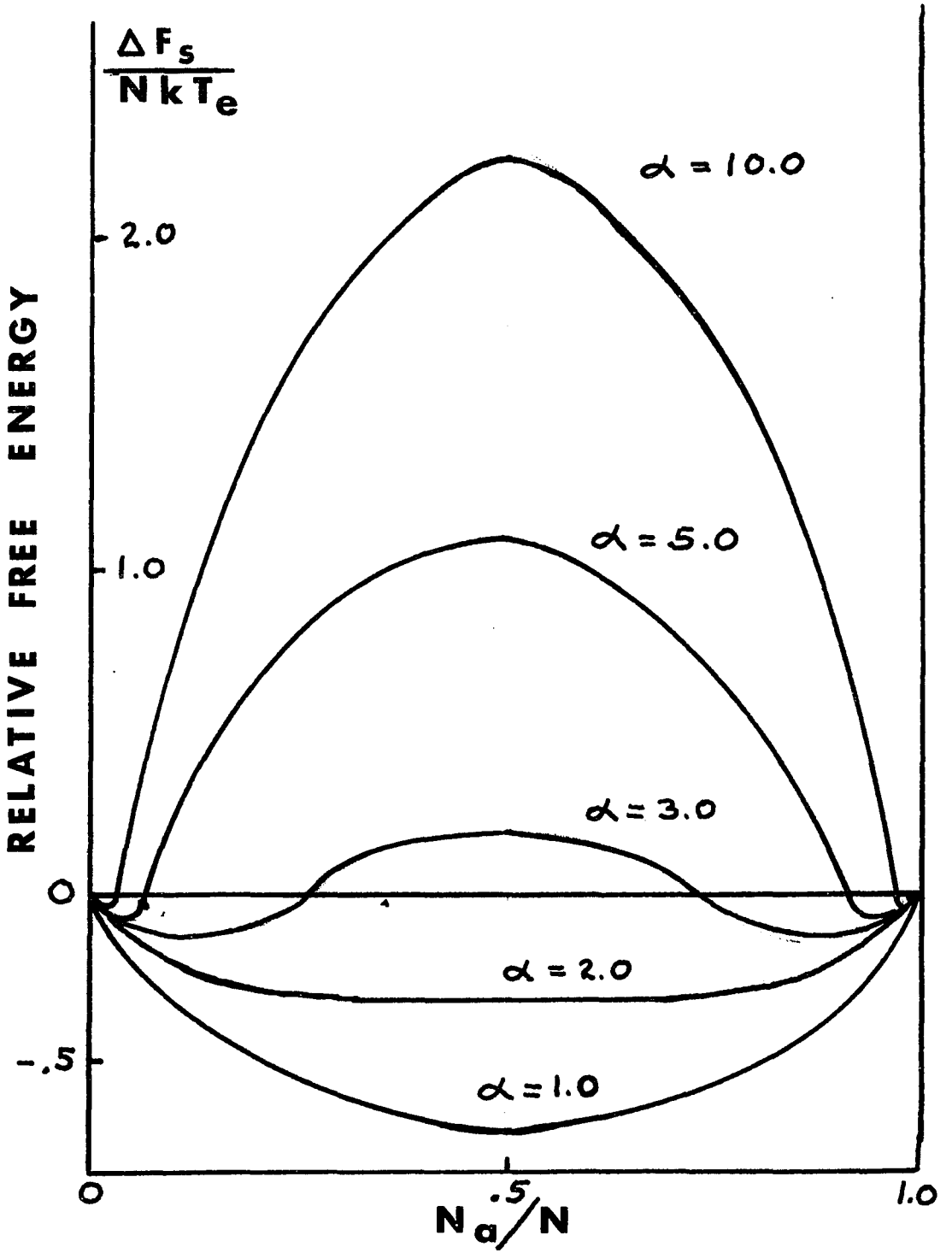
ΔF_s / NkT_e
RELATIVE FREE ENERGY
α = 10.0
α = 5.0
α = 3.0
α = 2.0
α = 1.0
2.0
1.0
0
-.5
0
.5
1.0
N_a/N

Figure V

As the quantity of α increases the initiation of new layers becomes more important until, for large α 's, the kinetics of growth applies.

In the term $\alpha = \frac{L}{KT_E} \cdot \frac{N_1}{V} \cdot \frac{N_1}{V}$ is less than but close to one. Therefore a small α implies a small L and a large α implies a large L. This treatment correlates the nature of the interface (smooth or rough) with the quantity α , i.e. with the entropy L; interfaces are rough where L is small (metals); smooth where L is large (organic compounds.)

As the quantity α increases, the growth becomes less isotropic and the interface becomes more faceted. For example, the tetrabromure of carbon grows very isotropically and has a value of α =0.8. For very high α 's the growth tends to be spherulic. This type of growth is characterized by autonucleation processes and frequent changes in the direction of growth.

This treatment holds for one component systems with the "single layer" assumptions. Work has been done on alloys and growth from solutions. Cahn considers that the interface extends a large number of layers and emphasizes that there is a continuous range of intermediate possibilities between smooth and rough, whereas for Jackson an interface is either rough or smooth.

As an application of this theory the particular case of ice is of some interest. For ice, the quantity α has different values depending upon the crystallographic direction. This is due to a distortion of the ice lattice from its ideal

lattice. Thus α is greater than two in the basal plane. As a result large sheets of ice dendrite form parallel to the "smooth" basal plane and move along the "rough" direction perpendicular to the basal plane.

1.6 Normal Growth Rate

The normal growth theory assumes that growth can take place at any site on the interface (i.e. the interface is ideally rough). Turnbull (12) derives one net rate of freezing, whereas Wilson (13) and Frenkel (14) assume that the rate R is the result of a dynamic equilibrium between freezing and melting. The Jackson-Chalmers treatment of this theory will be outlined here:

If R_F is the rate of freezing and R_M the rate of melting, the net rate is $R = R_F - R_M$.

Let the cohesive energy per atom in the solid be E_S and the energy of the activated state (minimum energy required to make the transition from solid to liquid) E_A.

The fraction of atoms at the interface at temperature T possessing an energy equal to or greater than E_A is $\exp -(E_A-E_S)/kT$ where (E_A-E_S) is the thermal energy required per atom. The $(E_A - E_S)$ term is simply the activation energy for melting in molar units. Similarly Q_F is the activation energy for freezing.

According to this theory, the rate of freezing and melting also depends on the number of atoms per unit area N, a geometric coefficient G and an accommodation factor A.

A. These terms for simplicity will be grouped together as R^{o}. The net rate can therefor be rewritten as:

$$R = R_F - R_M = R^{o}F \exp(-Q_F/kT) - R^{o}_M \exp(-Q_M/kT) \quad 1\text{-}27$$

If L is the latent heat of fusion,

$$L = Q_M - Q_F \quad 1\text{-}28$$

So:

$$R = R^{o}_F \exp(-Q_F/kT)\left[1 - \frac{R_m^{o}}{R_F^{o}} \exp\left(-\frac{L}{kT}\right)\right] \quad 1\text{-}29$$

At equilibrium $R_F = R_M$ i.e.

$$\frac{R_M^{o}}{R_F^{o}} = \exp\left(\frac{L}{kT_E}\right) \quad 1\text{-}30$$

and the expression of the rate becomes:

$$R = R^{o}_F \exp\left(-\frac{Q_F}{kT}\right)\left[1 - \exp\left(\frac{L}{kT_E} - \frac{L}{kT}\right)\right] \quad 1\text{-}31$$

with $\Delta T = (T_E - T)$

In the case where $\frac{L\Delta T}{kTT_E} \ll 1$ (small under-coolings) the exponential can be expanded and the equation becomes:

$$R = R^{o}_F \frac{L\Delta T}{kTT_E} \exp(-Q_F/kT) \quad 1\text{-}32$$

Expressing R^{o}_f in terms of R^{o}_M taken as a ν (interatomic distance times atomic vibration frequency);

$$R = a\nu \frac{L\Delta T}{kTT_E} \exp\left(-\frac{Q_F}{kT} - \frac{L}{kT_E}\right) \quad 1\text{-}33$$

The rate is proportional to the undercooling.

1.7 Heat Transfer at the Interface

An important factor which must be taken into account for crystal growth is the manner in which heat is removed

from the system.

For a flat interface, the temperature at which neither solidification nor melting takes place is the equilibrium temperature (T_E). If the interface is curved with radius r, the equilibrium temperature will be different than T_E. Equation (12) can be applied to determine this new equilibrium temperature since $\Delta T = \frac{2\gamma T_E}{r L}$. In any event, the latent heat of fusion must be removed from the interface to maintain the crystallization process. If the latent heat is not removed (by conduction etc.) it eliminates the supercooling and suppresses the process. Therefore the local rate of growth at any point on the surface depends on thermal conditions and the orientation of the surface since this influences the relationship between temperature and the rate of growth. For anisotropic materials a very complicated morphology can develop as a result of different heat flows in different crystal directions.

If the latent heat is conducted away from the interface through the crystal the solid liquid interface will remain planar. The temperature distribution in the solid and liquid can simply be described by using Fourier Law of Conduction. The temperature gradient in the crystal is that required to carry H + L, where H is the heat reaching the interface by conduction in the liquid and L is the latent heat.

$$\therefore \left.\frac{dT}{dx}\right|_{CRYSTAL} = \frac{H + L}{K_c}$$ where K_c is the thermal conductively 1-34

For the liquid

$$\left.\frac{dT}{dx}\right|_{LIQUID} = \frac{H}{K_L}$$

1-35

From this, one can determine the temperature profile in the liquid and solid.

If the latent heat is conducted into the liquid (i.e. the liquid is at a lower temperature than the interface) dentritic growth is observed. This is logical since the crystal will grow more rapidly as the solid/melt interface increases in area. The exact shape of the dendrite (long spikes or short protrusions) depends on how rapidly the heat is conducted away from the interface and immediate area.

1.8 The Growing Interface

A) Some Models. The simplest model of interface is a planar isotropic interface, the stability of which is in Figure VI.

A "heat sink" HH is assumed parallel to the interface. If a protuberance forms, as in A, the tip of A is farther from HH than the rest of the interface. Therefore, the flux of heat at the tip is smaller. A grows more slowly than the interface and vanishes.

In reality such an interface is affected by the proximity of the walls of the container or by the proximity of grain boundaries. Furthermore, a solid phase in contact

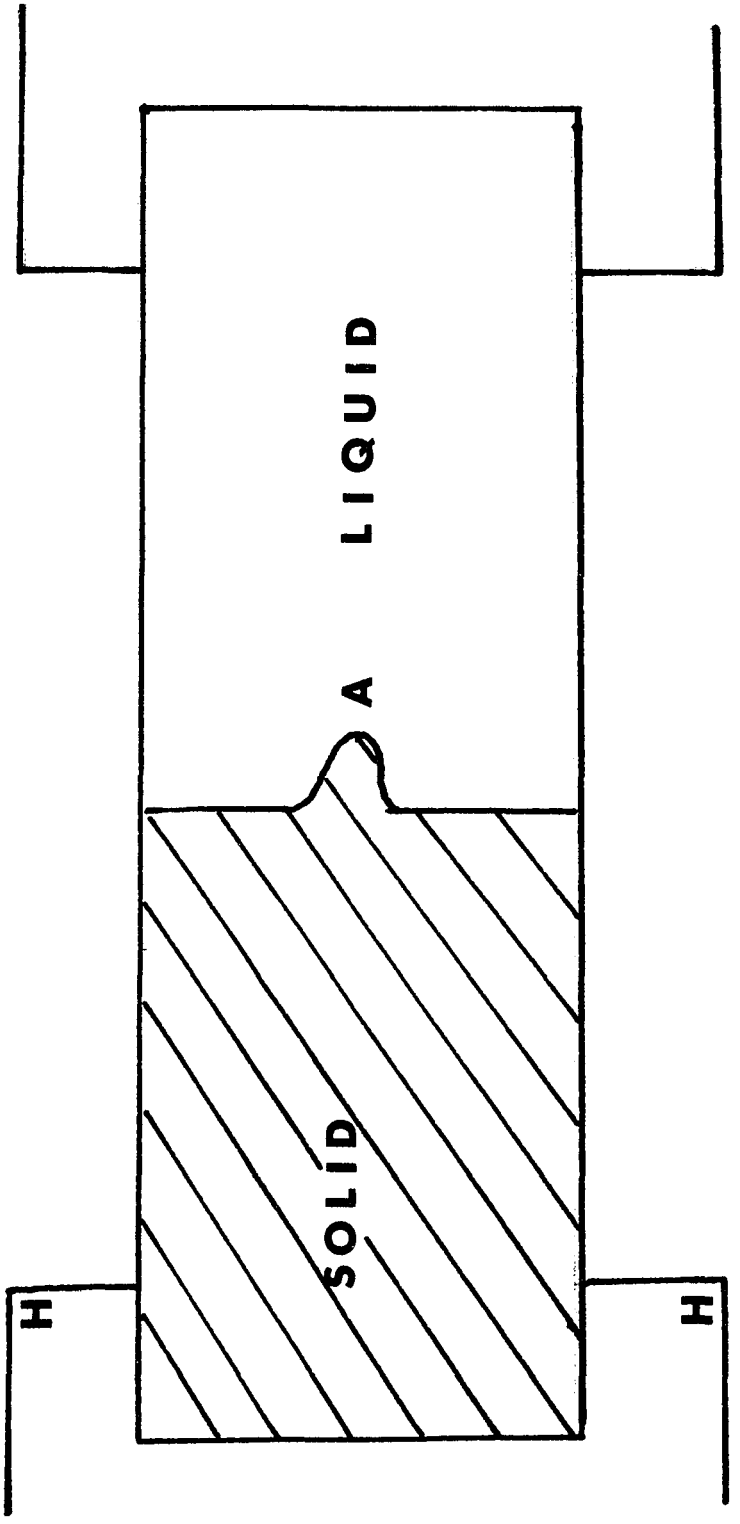

Figure VI

with the melt has a stable liquid-solid interface if the melt is an infinite liquid phase at a uniform temperature. These conditions will not be fulfilled in the presence of solute.

1.9 Redistribution of Solute During Solidification

Solute redistribution is an involved and complicated area of study. Metallurgists in particular have been studying this process for over a century. Textbooks in this field by Frenkel (3) and Pfann (16) discuss the various types of solidification processes.

For the solidification processes studied in this work diffusion plays the major role of mixing in the liquid. A review of the problem is given below.

Classically, equilibrium between a crystalline solid and a liquid is conveniently represented on a binary phase diagram by two lines; the liquidus line above which the liquid is stable and the solidus below which the solid is stable. The phase rule for a N component system states that there will be N degrees of freedom for this two component system.

The salient features of the solid liquid equilibrium relationship is expressed in terms of: concentration, c ; equilibrium distribution coefficient, k_o, which is the equilibrium concentrations of the solid and liquid (C_S/C_L) and the effective distribution coefficient k_E which is given by C_S/C_o where C_S is the solid concentration and C_o

is average liquid concentration.

Figure VII depicts the distribution of solute during uniaxial solidification. The initial composition of the liquid is C_o and $k_E = C_S / C_O$. The solute rejected at the interface diffuses into the liquid and its distribution is represented by curve D.

Under steady state conditions, the amount of solute rejected at the interface is just balanced by the amount that diffuses away from it; the diffusion coefficient for the solute is D cm^2/sec. The steady state distribution of solute ahead of the interface was found by Tiller (17). For a small element of the distribution curve a net flow of solute, D $(d^2c/d\ x^2)$, per unit volume diffuses into a volume element. If the solid liquid interface is taken as the origin, and solidification is represented by moving the solute distribution at a rate of R cm/sec then the net flow out of the same element is R (dc/dx).

Hence:

$$D \frac{d^2c}{dx^2} + R \frac{dc}{dx} = 0 \qquad 1\text{-}37$$

The solution of Tiller is:

$$C_L = C_a \exp\left(- \frac{R}{D} X' \right) + C_o \qquad 1\text{-}38$$

C_a = interface concentration

X' = distance from the interface to the point where the concentration is C_L

If the composition of the solid is C_o then C_a must be

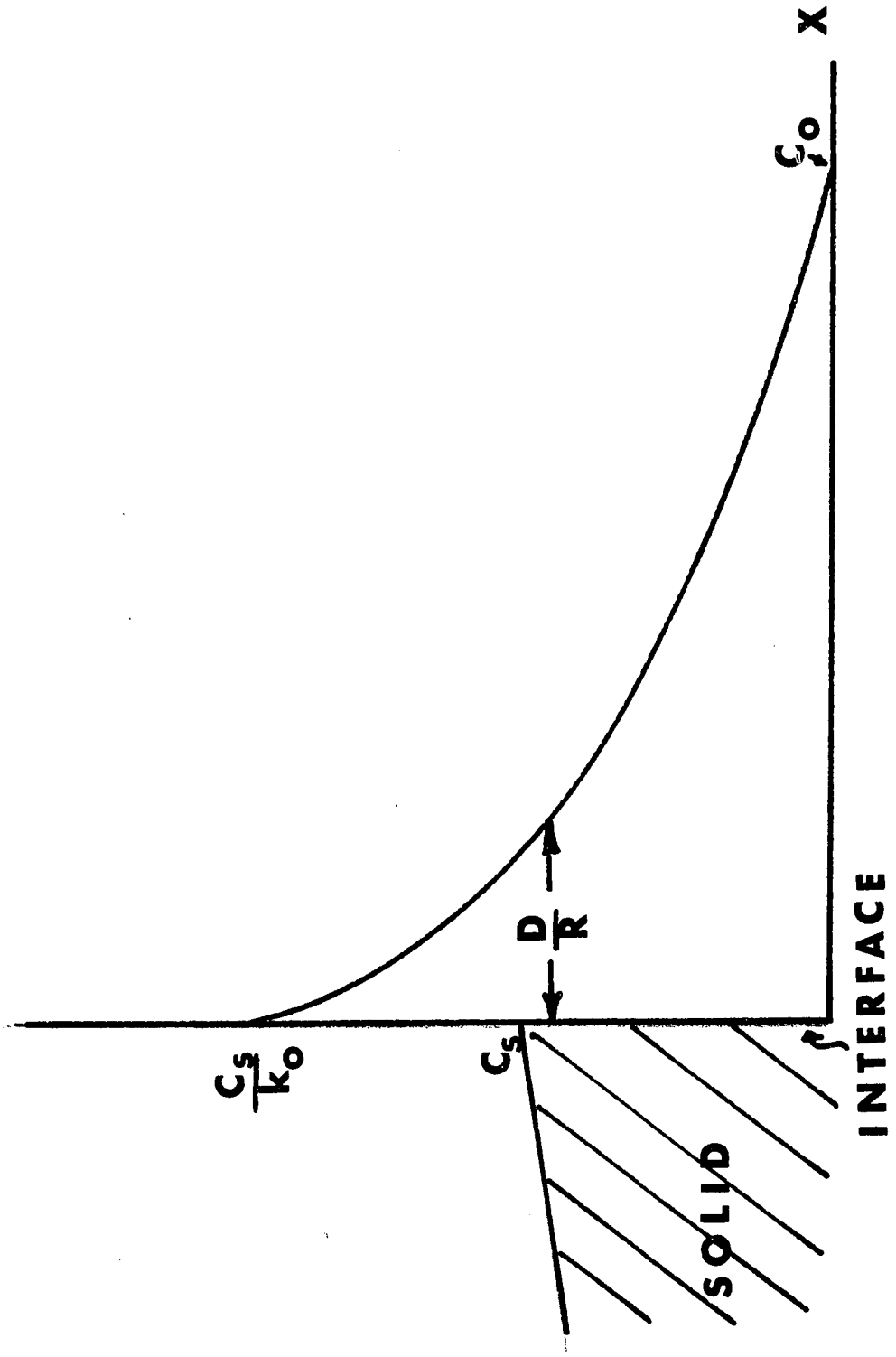

Figure VII

C_o / k_o and the expression for C_L becomes

$$C_L = C_o \left[1 + \frac{1-K_o}{K_o} \cdot \exp\left(- \frac{R}{D} X' \right) \right] \qquad 1\text{-}39$$

In actuality the problem of solute redistribution is more involved because a liquid in which temperature gradients exist is likely to be subject to convection. The effect of mixing by fluid motion has been examined by Wagner (66) who assumed that the solute moves purely by diffusion through a layer of liquid of thickness d beyond which there is sufficient convection to insure uniformity. The diffusion layer is the region close to the interface. In his study Wagner shows that the thickness of the stagnant layer is sufficient to include nearly the whole diffusion layer when the liquid motion is due to convection. When the motion of the liquid is more violent, the stagnant layer is not thick enough to accommodate the whole diffusion zone.

As a result of this diffusion the liquid in contact with the advancing solid liquid interface will in general have a composition that differs from that of the bulk. Theoretically, this implies that the liquid ahead of the advancing interface can be constitutionally supercooled with large Δ T'S. However before this occurs thermal and concentration instabilities along the interface result, which leads to a departure from steady state conditions. As a result the smooth interface breaks up and dendrite growth takes place.

It was shown by Rutter and Chalmers (18) that a planar interface would be unstable when exposed to a gradient of supercooling because the growth rate would be increased in any localized region that advanced ahead of the general interface. The theory of solute redistribution of Tiller, Jackson, Rutter and Chalmers (18) quantitatively predicts the conditions that determine whether constitutional supercooling exists ahead of a planar interface.

Chapter II

Freezing and the Solid/Liquid Interface of Aqueous Systems

2.1 Temperature Gradient Microscope Stage

In the past, the majority of work on freezing organic materials under the microscope has been carried out using an isothermal microscope stage. Walton and Judd (19), Harrison and Tiller (20), Macklin and Ryan (21), MacKenzie (22), and Chauffard (23) have designed many of the notable isothermal stages used in research today.

Although this type of stage is suitable for nucleation and phase identification experiments, it is of little use for the investigation of kinetic and dynamic processes. When an isothermal stage is used growth rates are often difficult to control and temperature gradients must essentially be zero. Nevertheless, it is known that both the growth rate and temperature gradients in a sample are important factors in determining how a material solidifies. With this in mind, Hunt, Jackson and Brown (24) at the Bell Telephone Laboratories, Murray Hill, New Jersey, developed a temperature gradient microscope stage for the study of pure systems and the effect of trace amounts of impurities on the solidification process. The stage is pictorially described in Figure VII. The specimen cell consists of two thin glass slides (22 x 22 x 0.2 mm) sandwiching a thin film of the sample to be studied. One end of the cell rests on a cold plate while the opposite edge serves as a heat reservoir or heat sink. The thin film of solution is essentially in a two dimensional heat transfer plane

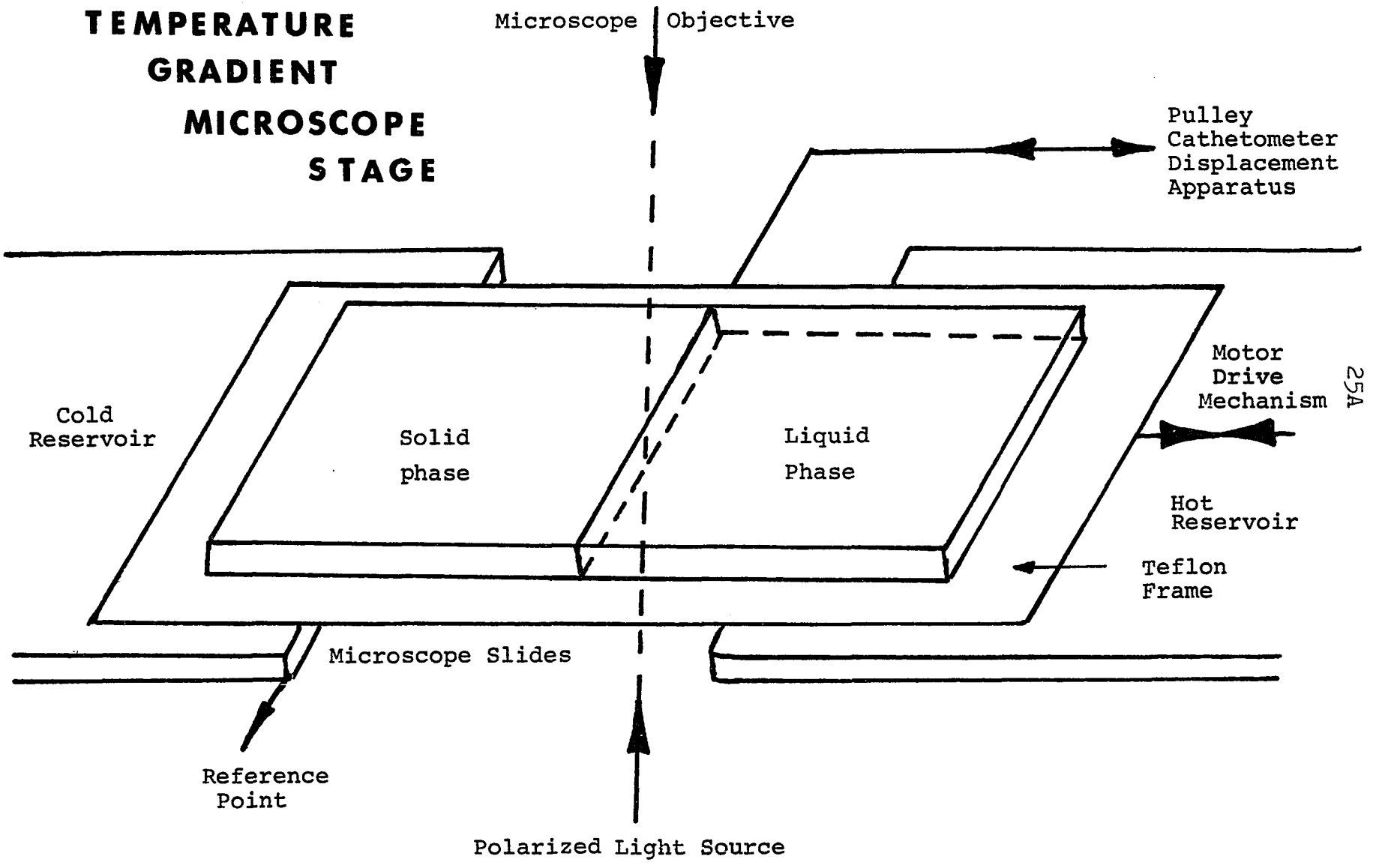
TEMPERATURE
GRADIENT
MICROSCOPE
STAGE
Microscope Objective
Pulley
Cathetometer
Displacement
Apparatus
Motor
Drive
Mechanism
Cold
Reservoir
Solid
phase
Liquid
Phase
Hot
Reservoir
Teflon
Frame
Microscope Slides
Reference
Point
Polarized Light Source

and a unidirectional temperature gradient. This arrangement eliminates many of the three dimensional heat transfer problems. A controlled flow of dry air is flushed through the system in order to prevent frost formation on the cell and cold plate.

For the present work on pure and complex systems such as emulsions, a number of modifications were necessary. Since we are interested in both solidification and melting or freezing and thawing, the present stage is equipped with a reversible and variable D.C. motor to move the cell at any rate between .01 mm/sec and .05 mm/sec. This allows the study of the individual processes or as a combination of freezing and thawing cycles. Freeze-thaw cycles appear to be important when the stability of a system is being examined (25). In addition both the hot plate and cold plate have been modified to individually control the plate temperature above the reservoir temperature. This allows for a wide choice of temperature gradients.

For the present work, it is important that the temperature profile be known at every point on the cell. The use of a fine thermocouple is impractical for accurate work especially when the gradient is of the order of $10^{o}C/mm$. In addition, if the thermocouple is placed in the sample it serves as a site for heterogeneous nucleation which may influence the experimental results.

To alleviate this problem, the temperature profile of this cell was calibrated by using various salt solutions

which form well defined eutectic compositions and freezing points. (Table I). When equilibrium is attained the distance from the tip of the cold plate to the eutectic liquid interface is recorded for each solution. Correlation of the distance vs eutectic temperature will then yield the temperature profile of the cell. Above $0^{o}C$ pure solids which have well defined melting points and did not exhibit polymorphism were used to give data points. These solids were initially melted and spread on the glass slides to produce a thin film. Then they were solidified by rapidly cooling and then placed on the gradient stage. At equilibrium, the solid above the equilibrium temperature on the gradient had melted leaving the well defined solid/liquid interface. (Figure "IX). Once the cell has been calibrated for a given gradient, the temperature is known at every position of the cell at equilibrium. A cathetometer is used to measure the cell position within $\pm$ .01 mm. The unique feature of this microscope stage allows the observation of a growing interface to be observed at all times at a particular temperature and with a defined temperature gradient. The microscope used is a Reichert "Zetopan" research microscope equipped with a photographic set up. This simple and exact method was found to be superior to the use of thin thermocouples.

Figure X is a series of calibration curves at equilibrium and at different rates of melting and solidification.

Table I

Salt Eutectic	Interface Temperature
	C
KCl	-10.7
NH_4Cl	-15.3
NH_4NO_3	-16.7
NaCl	-21.0
Organic Solids	Melting Point
	C
Laurophenone	+46.5
Cetyl Alcohol	+50
p-Dichlorobenzene	+53
Docosanol	+62

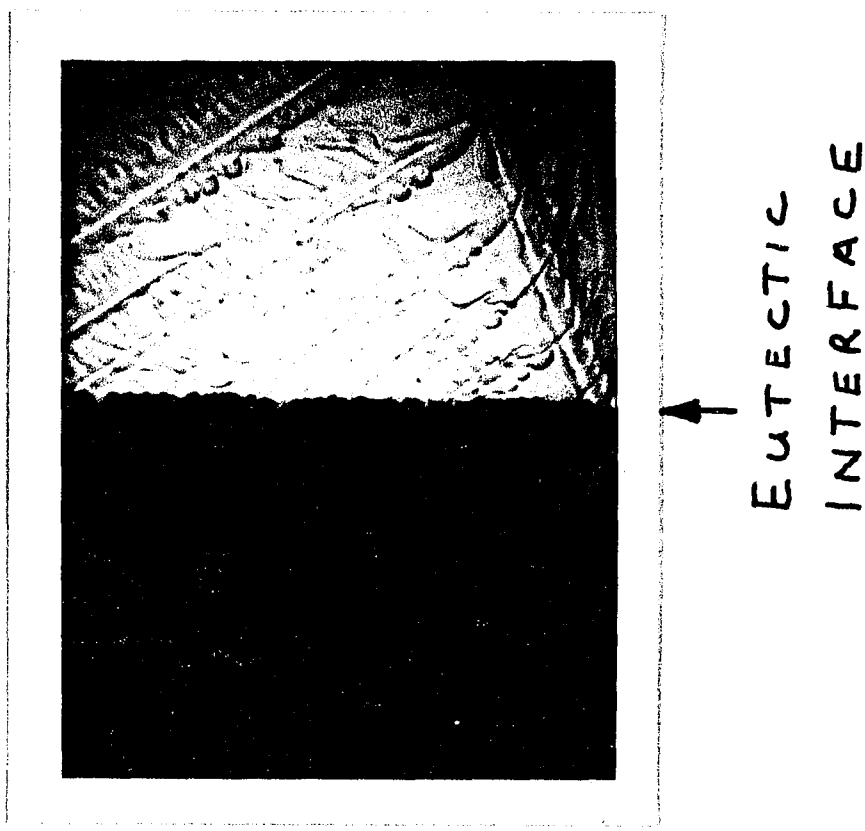
EUTECTIC
INTERFACE

Since the rate of heat transfer also changes with the rate at which the stage is moved, the calibration curves shifts to the right of the equilibrium curve when the rate of melting increases and to the left of the curve when the rate of freezing increases. The slope of the calibration curves remains essentially constant.

2.2 Temperature Gradient Freeze-Drying Microscope Stage

Like freezing, the process of freeze drying is not a new one. For the past twenty-five years it has assumed a role in the laboratory for the removal of water. Only recently, however, has extensive development of the theory behind freeze drying and its application to large commercial fields such as the food and drug industry been undertaken as major research projects.

To understand this process it is of extreme importance to physically observe structural changes under actual conditions. With this in mind a stage was designed by Rosano etal (26) to study this process under the microscope.

The stage is essentially composed of 1) a completely wettable slide inserted into 2) a circular cold plate and connected to 3) a vacuum chamber. The stage is shown in Figure XI. It has a distinct advantage over the conventional isothermal stages in that a radial temperature gradient exists perpendicular to the observer. This allows the viewer to examine the freezing front as it starts at

FREEZE DRYING CELL

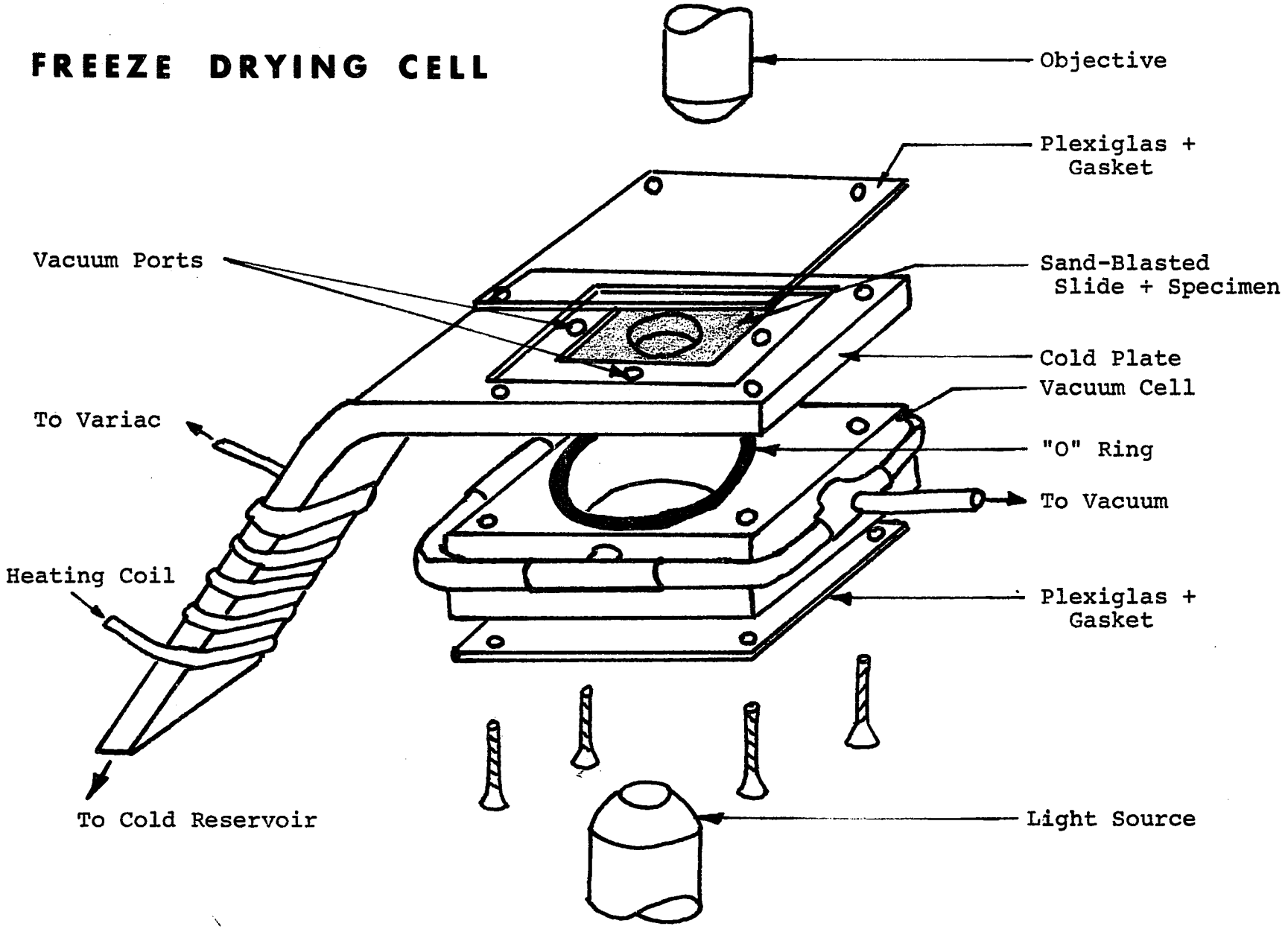

the circumference of the viewing area and propagates in a radial direction to the center of the sand blasted slide.

A sand blasted glass slide is used since the liquid solution will easily spread on its surface to produce a thin transparent film of uniform thickness. No cover slip is used to cover the specimen surface.

The sand blasted slide fits into a recess on the copper slab which serves as the cooling medium. One end of the copper slab is placed into a cold reservior (i.e., dry ice-aceton mixture or liquid nitrogen). Attached to the cold plate is a heating coil which regulates the temperature.

The cold plate rests on the top of the vacuum chamber. Holes in the cold plate serve as vacuum ports which connect the vacuum chamber and the specimen surface.

Plexiglas plates are used to seal the top of the cold plate and the bottom of the vacuum chamber while still allowing light to be transmitted to the specimen or the sand blasted slide. Only the copper plate surrounds, supports and conducts heat away from the slide.

To prevent condensation on the windows dry nitrogen is gently flushed across the top of the cell.

Procedure for the Stage Calibration

1) A microscope sand blasted glass slide is placed on the cold plate. The plexiglas top is placed on the cell to prevent condensation between the cold plate and glass

slide. The system is allowed to come to equilibrium.

2) One drop of the salt solution is spread on the slide. Care must be taken to prevent any liquid from seeping between the cold plate and the sand blasted slide thus altering the heat transfer.

3) When the system reaches equilibrium, the distance between the cold edge and solid eutectic front is measured.

4) Results are graphed on polar coordinate paper.

Using a dry ice-acetone mixture for the cold reservoir and eutectic solutions of NaCl, KI, NH_4CNS, NaBr and Zn (NO_3) a calibration was made. The positions of the solid eutectic fronts when plotted on polar coordinate paper produced a series of isotherms shown in Figure XII. It is evident that the isotherms are circular on the cold sink side while being egg shaped on the O.D. axis. This is primarily due to the environmental conditions and its effect on the shorter side of the cold plate. The ambient temperature during this experiment was 21 C.

Good reproducibility exists for this calibration and similar ones at different cold plate temperatures provided the slide sits evenly in its recess and no liquid exists between the cold plate and slide. The ambient conditions can vary as much as $4^{o}C$ without any serious error.

The overall cell dimensions are relative to the microscope being used. The only two dimensions which should be of greatest concern are 1) the diameter of the hole in the cold plate and 2) the working distance of the

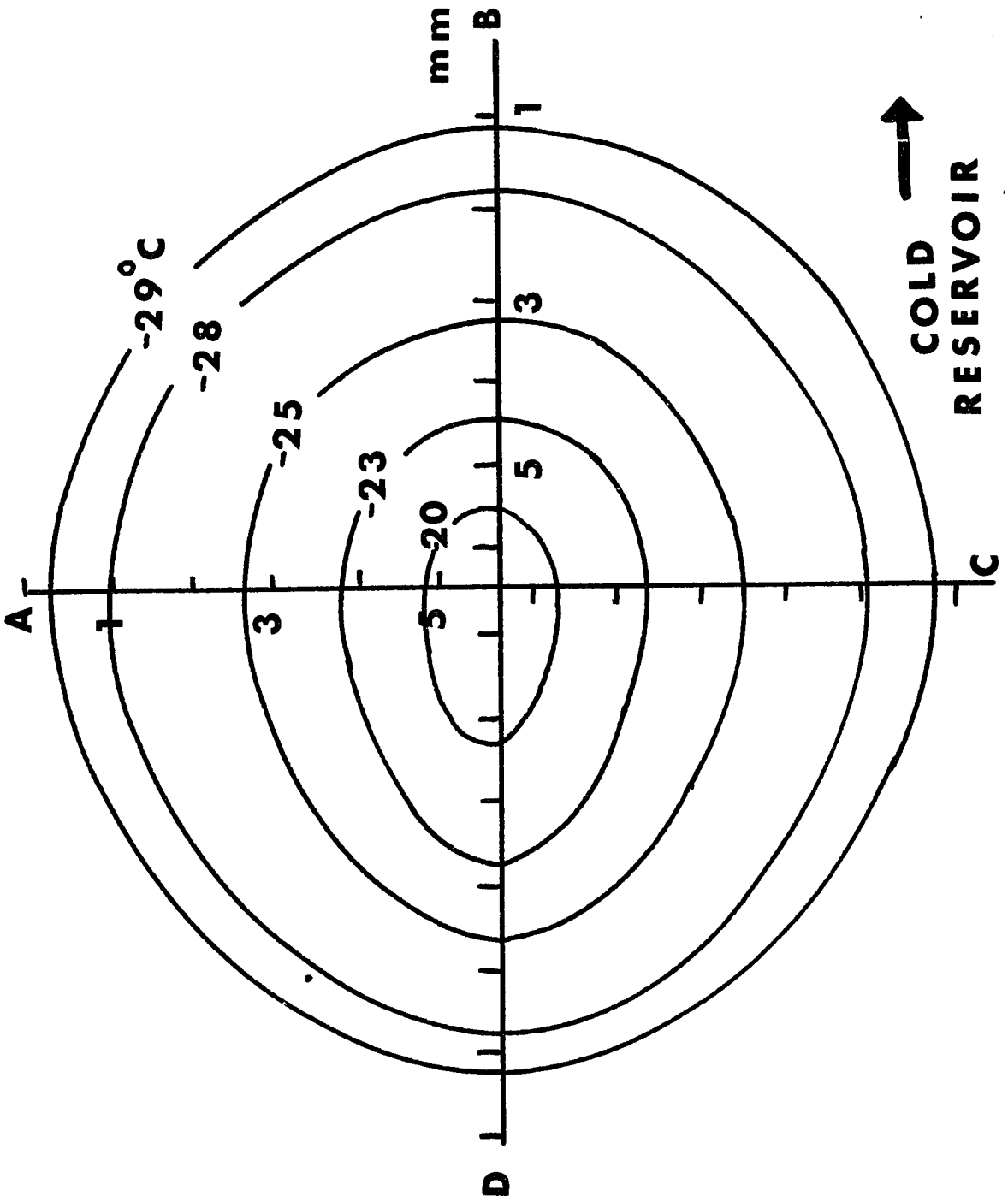

Figure XII

microscope objective. The cold plate hole is important since it will regulate the size of the temperature gradient. In our case a 13 mm diameter hole produced a 10°C gradient from the cold plate edge to the center of the viewing area.

Our experiments are conducted using a Reichert "Zetopan" research microscope. An upper plexiglas cover 3 mm thick and a 0.5 mm rubber gasket allows us a 7.5 mm working distance from the objective to the plate top at 40 X magnification. At a magnification of 30 X the working distance is 21 mm.

It has been found that the nature of freezing plays a determinant role on the final structure of the freeze dried product. Systems have been studied using freezing rates as fast as 5 mm per minute and as slow as 5 mm per 60 minutes. These rates of freezing are manipulated by the type of cold reservoir and the use of the heating coil.

The high ratio surface/mass of the frozen film when combined with a vacuum of 50 microns of mercury produces systems which are freeze dried in approximately thirty minutes (this generally refers to salts solutions which will freeze-dry markedly faster than sugar solutions). The rate of freeze drying may also be varied by changing the vacuum readings until the desired condition is attained.

2.3 Freezing of Various Aqueous Systems

A. Experimental

Solutions of KCl (0.05 M - 3.3 M), NaCl (0.05 M -5.2 M),

Sucrose (0.03 M -2.0 M), PVP General Aniline and Film Corp., N. Y., N. Y.; Avg. H.W. 40,000 (1 gm/50cc -12 gms/50cc) and silica suspensions (0.2 gms/50cc - 5.0 gms/50cc) were studied.

The T.G.M.S. cold plate was cooled by a dry ice/acetone mixture and the hot plate was maintained at 21 $\pm$ 0.5° C. The temperature gradient was determined from the slope of the calibration curve to be 4 °C/mm. In this experiment, the time in seconds for the ice front to pass between two fixed points in the temperature gradient (at - 28° C and - 25° C respectively) was measured.

B Results

The average rate of freezing ($\bar{V}$) was determined between the two fixed points on the cell. These results (Figure XII) indicate that the rate of freezing decreased as the concentration of KCl and NaCl increased. As the salt solutions became more dilute the rate of freezing approached that of pure water: 0.27 mm/sec for this cell.

The results obtained with PVP and sucrose solutions were markedly different from the KCl and NaCl solutions. It was observed that for the entire range of concentrations studied, the rate of movement of the ice front remained equal to that of pure water. For the silica suspensions the rate of freezing remained equal to pure water and independent of the concentration. In addition, it was observed that the shape of the interface of the suspension was greatly different from KCl, NaCl, PVP or sucrose.

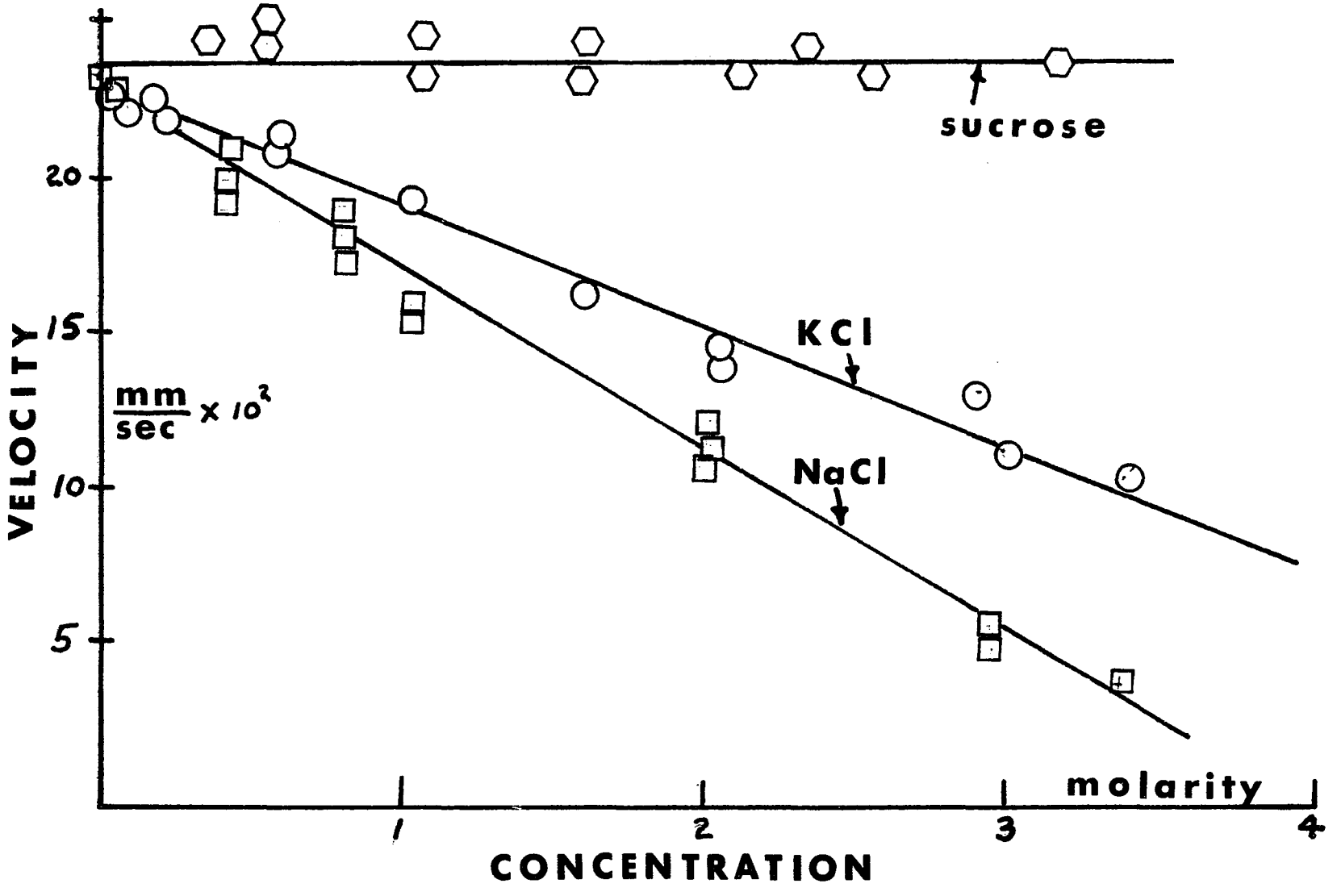
sucrose
KCl
NaCl
VELOCITY
mm/sec x 10²
20
15
10
5
molarity
1
2
3
4
CONCENTRATION

C. Discussion

The growth of dendrites in aqueous solutions and suspensions is a complicated phenomenon. Among the variables which must be accounted for are:

1. diffusion of the solute
2. concentration buildup at the Solid/liquid interface
3. heat of crystallization
4. associated or bound water

The diffusivity constants of NaCl and KCl are 20°C are 3×10^{-5} cm^2/sec and 1.6×10^{-5} cm^2/sec (33) respectively while that of sucrose, PVP and glycerol are almost an order of magnitude lower ($\sim .5 \times 10^{-6}$ cm^2/sec). According to Fick's Law of Diffusion and equation 1-38 the smaller the diffusivity the greater the solute buildup at the S/L interface. In turn, this greater solute buildup for the glycerol, PVP and sucrose interfaces should depress the freezing point to a greater degree thus slowing down the velocity of dendrite growth. Note that even when the Van't Hoff factor is included in the freezing point depression formula, $\Delta T = Kmi$, to correct for the dissociation of the salts one would expect an equivalent undercooling and therefore slower propagation velocity for the non salts at higher concentrations. This was not observed.

A more likely explanation is that during the freezing of PVP and sucrose solutions and silica suspensions there is no significant heat evolved or absorbed to affect the rate of freezing of these aqueous systems. On the contrary

significant amounts of heat are produced during salting out of KCl and NaCl, thereby decreasing the rate of freezing. Heats of dilution given in the International Critical Tables (26) for 1 mole of a solute /25 moles of water upon the addition of 25 moles of water at $20^{o}c$ for salts are of the order of 500-800 joules while glycerol and PVP are considerably lower ($\sim$ 50 joules). The negative of this value is used to indicate the heat of crystallization.

Since heat is being withdrawn to the cold plate, production of heat of crystallization in the area behind the interface prevents the latent heat given off at the interface from being withdrawn as readily. In the case of silica, the rate of ice formation is independent of the silica concentration because the latent heat is rapidly withdrawn to the cold sink;the silica particles themselves playing no part in the freezing process.

An additional contrast between PVP, sucrose solutions, silica suspensions and NaCl and KCl solutions is the number of water molecules associated with solute compared to the total number of water molecules in the system. The nature of the ionic atmosphere in a polar solvent is described by Brescia etal (27) as "an ion surrounded by a sheath of solvent molecules." The coulombic forces holding this complex together is made of strong ion-dipole interactions. In the case of the other solutes the forces are much weaker since it is essentially dipole-dipole interaction. The

more water bound to the solute and the stronger the bond the more difficult it will be to crystallize or freeze the ice. The exception of course is when the solute orients the water molecules to form the crystalline ice structure.

2.4 Interface Configuration

A. Experimental

The dendrite structure of aqueous solutions of NaCl, KCl glycerol, ethylene chloride and PVP were studied. The PVP was provided by General Aniline and Film Corp. N. Y., N.Y. and had an average molecular weight of 40,000. All other reagents were manufactured by Fisher Scientific Company, FairLawn, New Jersey and were of certified A.C.S quality. The water was distilled in a Stokes Still to remove any impurities. 0.2 -3.0 molal solutions were prepared except for PVP solutions in which the weight per cent was varied between 5 and 15%. This range was comparable to the molal solutions. The temperature gradient microscope stage with the same conditions as in section 2. 3A was used. The rates of freezing were varied from .01 - .04 mm/sec which corresponds to freezing rates between 2.4 and 9.6 ^{o}c/min.

B. Results

In this series of experiments the peak to peak distance and the width of the dendrites (0.6 mm from the dendrite tip) were measured. The results are tabulated in Table II and III and plotted in Figure XIV - XVII.

Legend

Weight %	NaCl	Glycerol	PVP
5	○	△	□
10	◒	▲	▬
15	●	▲	■

Figure XIV

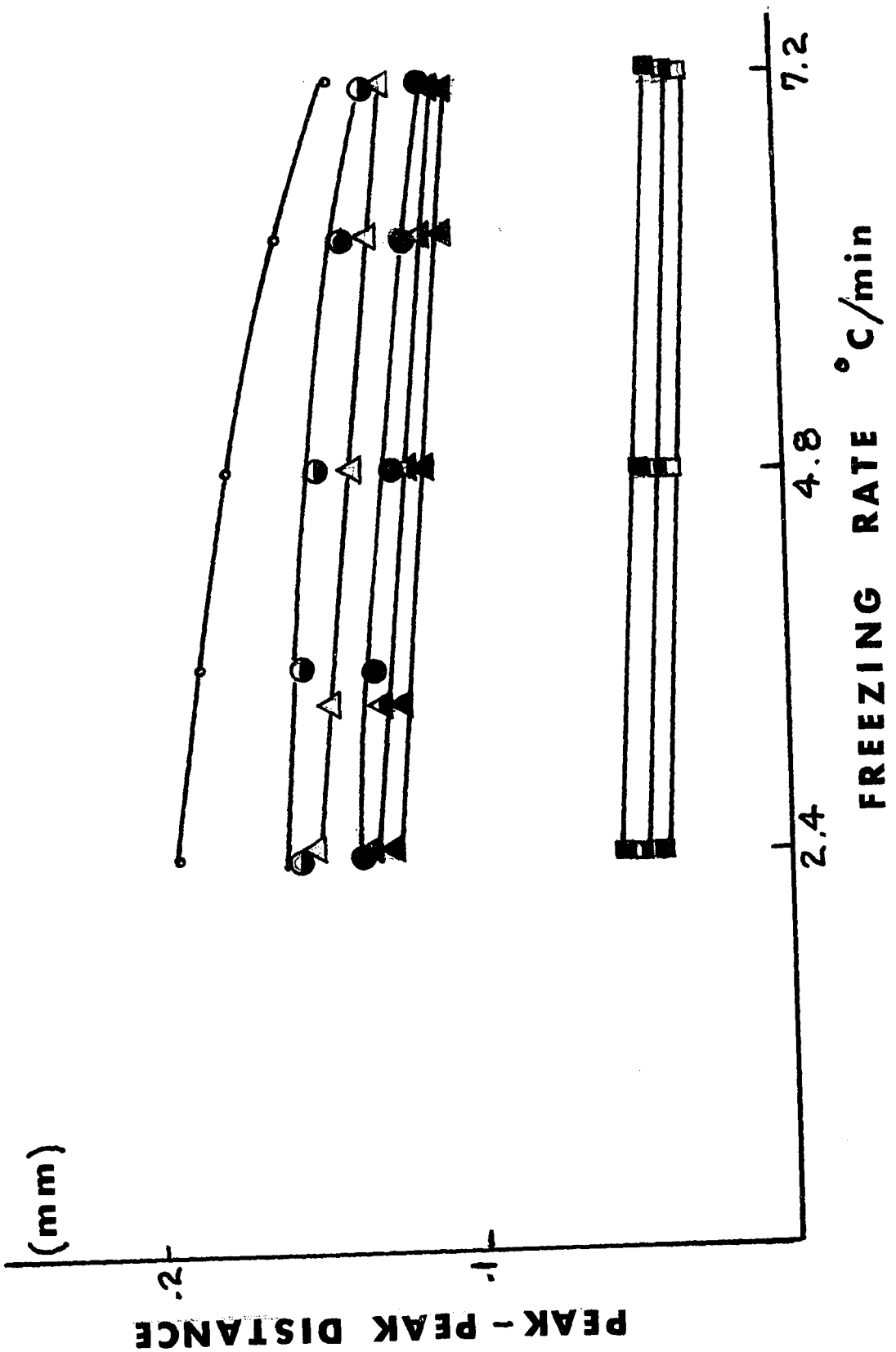
PEAK - PEAK DISTANCE
(mm)
.2
.1
FREEZING RATE °C/min
2.4
4.8
7.2

Legend

Freezing Rate C/min.	NaCl	Glycerol	PVP
2.4	○	△	□
4.8	◒	◭	◨
7.2	●	▲	■

Figure XV

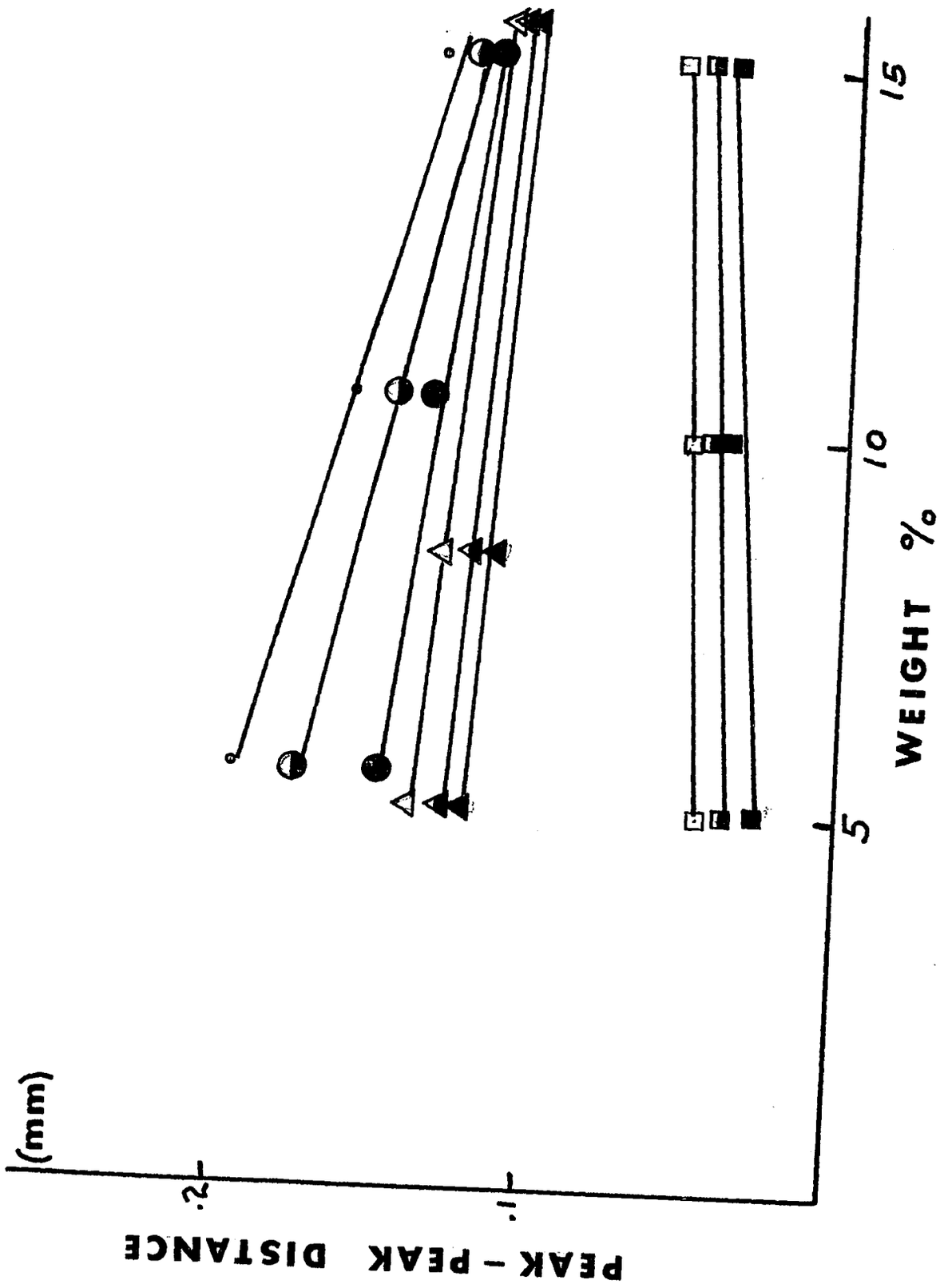
PEAK - PEAK DISTANCE
(mm)
.2
.1
WEIGHT %
5
10
15

Legend

Weight %	NaCl	Glycerol	PVP
5	○	△	□
10	◒	▲	▬
15	●	▲	■

Figure XVI

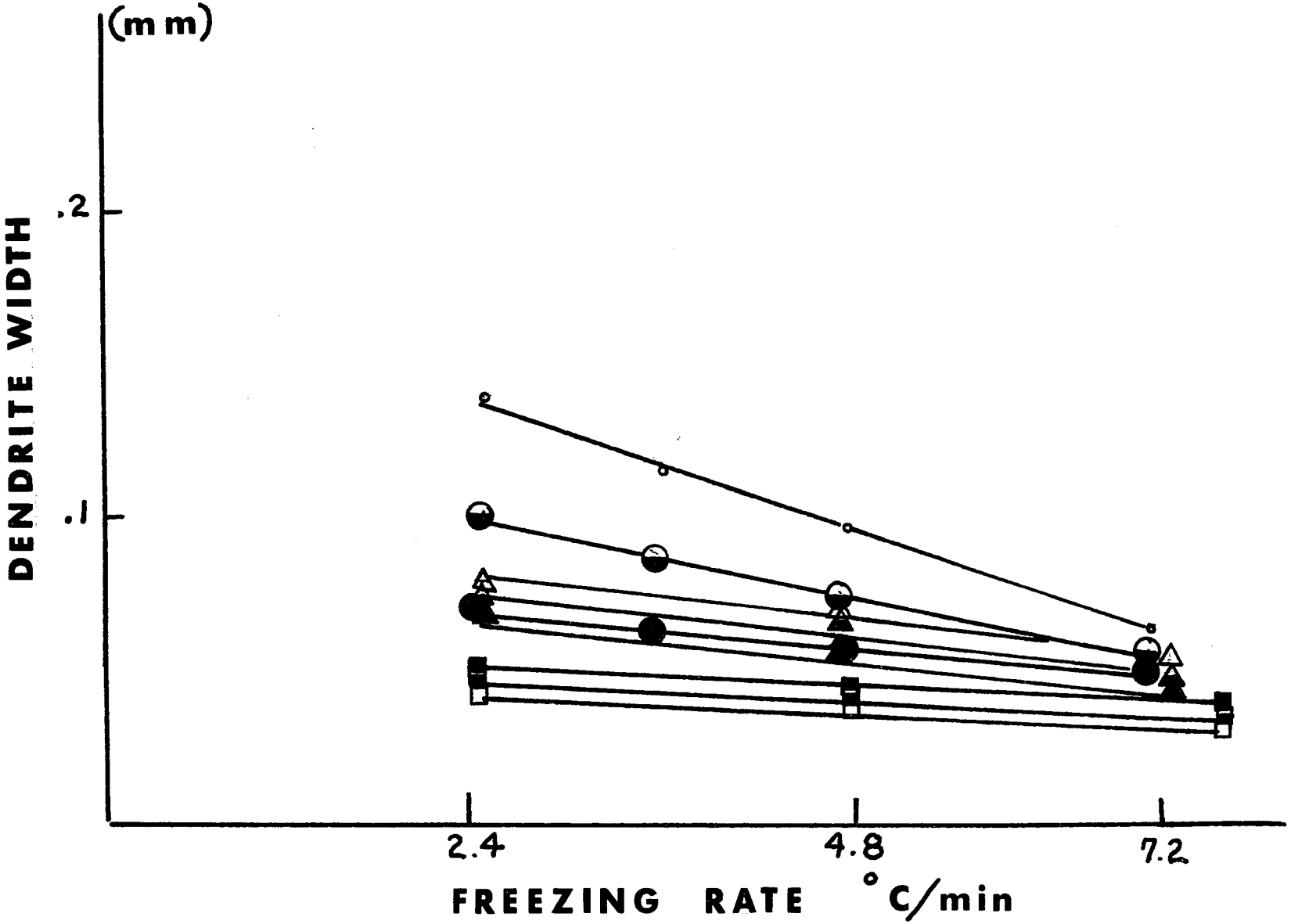
(mm)
.2
.1
DENDRITE WIDTH
2.4
4.8
7.2
FREEZING RATE °C/min

Legend

Freezing Rate C/min	NaCl	Glycerol	PVP
2.4	○	△	□
4.8	◒	▲	▬
7.2	●	▲	■

Figure XVII

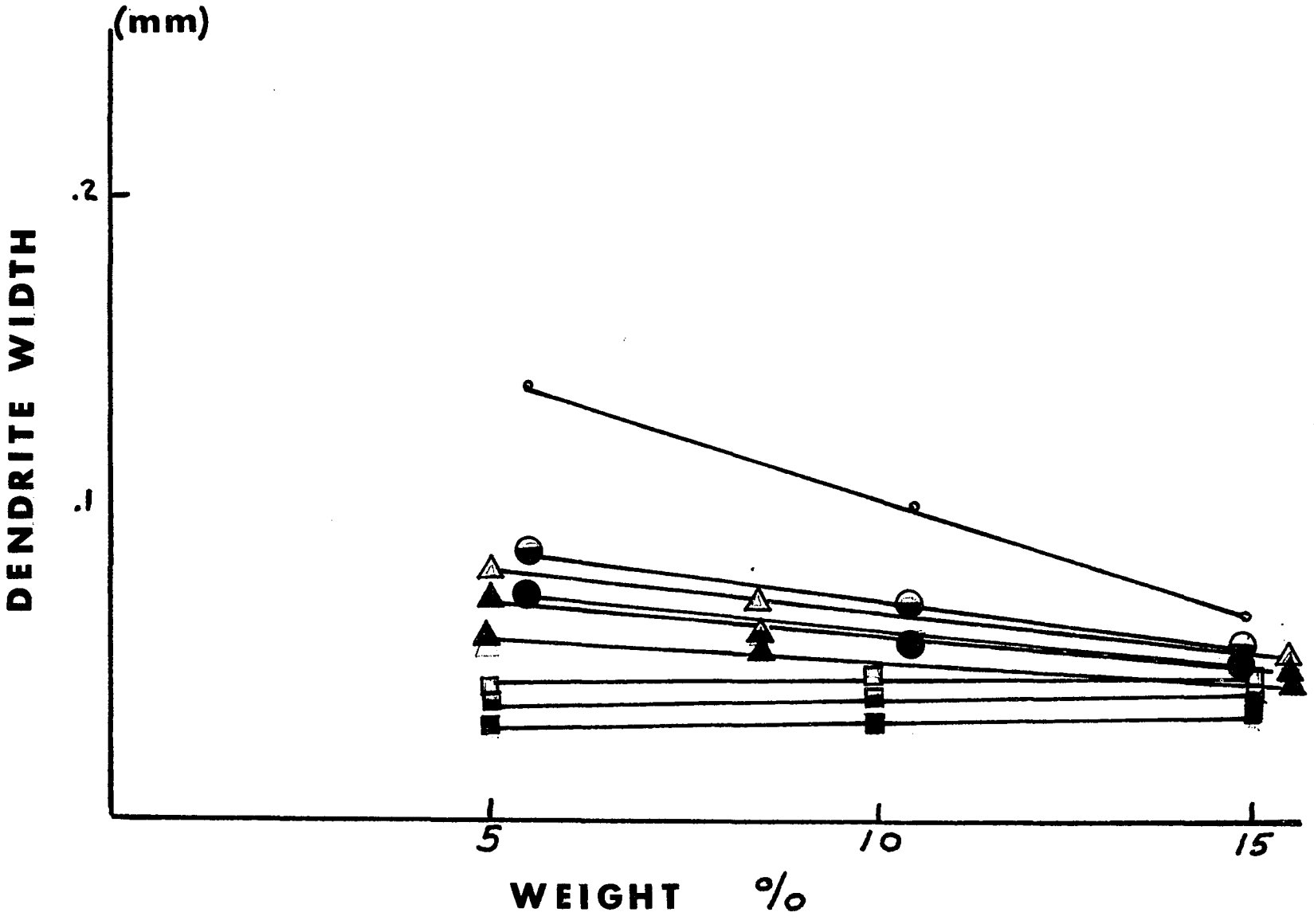
(mm)
.2
.1
DENDRITE WIDTH
5
10
15
WEIGHT %

TABLE II PEAK PEAK DISTANCE OF ICE DENDRITES

	NaCl			KCl			Ethylene Glycol			Glycerol			PVP		
Wt. %	5.5	10.4	14.8	6.9	12.9	18.2	5.8	11	15.7	5	8.4	15.5	5	10	15
Modality	1	2	3	1	2	3	1	2	3	.58	1	2	-	-	-
Rate						Width	(microns)								
2.4	193	155	134	155	125	115	129	114	108	121	124	125	42	47	52
4.8	175	148	123	135	120	110	110	106	108	118	120	120	39	40	41
7.2	143	135	115	130	112	105	106	105	106	100	102	105	28	30	35

TABLE III ICE DENDRITE WIDTH

	NaCl			KCl			Ethylene Glycol			Glycerol			PVP		
Wt. %	5.5	10.4	14.8	6.9	12.9	18.2	5.8	11	15.7	5	8.4	15.5	5	10	15
Modality	1	2	3	1	2	3	1	2	3	.58	1	2	-	-	-
Rate						Width (microns)									
2.4	141	102	70	105	64	60	102	95	94	79	70	68	42	47	52
4.8	87.5	70	52.5	70	43	39	68	64	62	72	62	62	39	40	41
7.2	69	53	51	48	39	36	64	63	64	56	54	53	28	30	35

Except for PVP the dendrites become more needle like as the rate of freezing increases. For PVP the dendrites do become sharper as the freezing rate increases, but they are extremely close to one another with little solution in between them.

In general the peak to peak distance decreases as the rate increases. The dendrite width also appears to decrease as the rate increases. In the case of the salts NaCl and KCl the dendrite spacing appears to be inversely proportional to the square root of the freezing rate. For the nonionic solutes the distance decreases linearly with increasing rate. The peak to peak width also decreases linearly with increasing rate. In the systems where the freezing rate is constant the peak to peak distance decreases linearly with increasing concentration of salt solutions (NaCl and KCl). A much smaller decrease is seen with ethylene glycol and glycerol. The PVP peak to peak distance on the other hand, appears to increase with increasing concentration. The dendrite width also follows this order.

It was also found that the greatest changes in peak to peak distances and dendrite width is seen in dilute solutions. As the solutions become more concentrated (2-3m) the changes become less pronounced. The salt solutions in all cases show the greatest change in dendrite size.

C. Discussion

In reality, the "heat sink" postulated in section 1.8

does not exist. A protuberance created by a perturbation in the heat flow develops because the tip of the protuberance meets a higher supercooling and becomes a spike, which in turn grows and becomes less stable. The radius of curvature of the tip decreases and the spike divides. The difference in aspects of the branching on both sides of the dendrite is very likely due to changes in crystallographic orientations.

Dendrites grow preferentially in certain crystallographic directions (100 in f.c.c. and b.c.c., for example) and changes in orientation give rise to dramatic changes in the growth pattern. In a large vessel, ice dendrites are free to grow in the preferred crystallographic orientation. But in this experiment the sample is very thin. The walls of the cell containing the water interact with the directions of growth.

A basic study of dendrite growth was done by Papatreau (28) who foresaw the stability shape of the tip of a dendrite. The stability theory deals with the stable shape of the tip of the dendrites, using as models isothermal surfaces which grow without deformation. Its method consists of solving the diffusion equation for a pre-assumed shape of interface, then applying a perturbation and calculating whether or not the perturbation is stable. (29)

A spherical tip was to be excluded because such a shape loses heat uniformly, and tends to increase its radius of curvature.

Ivantsov (30) shows that the correct solution for the shape of the tip in an isothermal freezing process was a paraboloid of revolution, the rate of growth being proportional to $\frac{(\Delta T)^n}{r}$

ΔT: undercooling

r: radius of curvature of the tip

$n > 1$: for usual undercoolings

Horvay and Cahn (31) proved that a paraboloid of elliptical cross-section was also a correct solution.

Bolling and Tiller (32) slightly modified the approach by introducting heterogeneities of temperature on the surface of the dendrites.

Although numerous theories exist there is still no one theory which may explain all the aspects of dendrite growth. However the quantity D/R (as seen in section 1.9 equation 1-3) seems to be a good indication of interface structure.

For a very small thermal driving force for solidification the freezing rate will be slow enough to allow solute rejected at the solid/liquid interface to diffuse completely into the melt. In practice, however true equilibrium solidification is seldom approached and the solute rejected at the advancing interface cannot undergo infinite diffusion into the bulk melt. A solute rich region in the liquid phase thus develops adjacent to the interface.

As described by Rutter and Chalmers (18), "any system with a temperature gradient imposed on a growing liquid/solid interface in the presence of a solute may constitutionally

supercool." That is the presence of the solute results in the boundary layer depressing the interface temperature so that liquid far from the interface is below its freezing temperature. Depending on how steep the concentration gradient is at the interface, the solidification temperature of the solution theoretically should increase sharply from a value corresponding to the interface concentration C_i as compared to the bulk concentration C_∞ In actuality the temperature distribution in that small interface region probably cannot change that quickly therefore the temperature profile in the neighborhood of the interface is below the solidification profile. This accounts for the supercooling.

During constitutional supercooling part of the interface advances ahead of the rest of interface into a region of greater supercooling where it experiences a greater driving force for faster growth. Tiller et al (17) believes that the planar interface takes on a cellular mophology in an attempt to eliminate constitional supercooling. If the supercooling becomes too extensive dendrites appear in a further attempt to eliminate the supercooling.

In a study by Tiller and Rutter (35) they found the interface morphology of tin lead mixtures to be influenced by the D/R ratio.

The quantity $\frac{D}{R}$ is the distance at which the concentration in solute (C_1) falls to $\frac{1}{e}$ of its value at the interface. (Figure VII) If $D = 5 \times 10^{-5}$ cm^2 /sec. and $R = 0.1$ cm./ sec., then $\frac{D}{R}$ is five microns. This means that

the solute does not diffuse away from the interface as the solid rejects it. The solute forms a ripple parallel to the interface. The large $^{D}/_{R}$ the more stable the interface. In this present study, the interface also appears to become more dendritic for a given system as R, the rate of freezing increases. However, the concentration profile cannot explain the entire effect. From the experiments in Section 2.3 the amount of heat liberated at the interface is an important factor. For this reason the greatest changes in peak to peak width and dendrite width is seen for the salt solutions.

In a study by Rohatgi and Adams (36) on dilute salt solutions frozen as droplets and in Tygon tubing, they found the dendrite spacing of the frozen solutions appears to be inversely proportional to the square root of the freezing rate. This study on the peak to peak distance of the ice dendrites at the interface also follows the relation

$$P.P. = -K \cdot R^{-\frac{1}{2}} + C \qquad 2\text{-}1$$

however for the non electrolytes

$$P.P. = -K' \cdot R + C \qquad 2\text{-}2$$

In the study of Rohatgi and Adams (36) the brine layer was frozen (i.e. below the eutectic temperature). The peak to peak distance was measured at the ice interface therefore the brine layer was still liquid.

The effect of solute concentration shows a linear change in the peak to peak and dendrite width. Assuming the effects of concentration and rate are additive (as

it appears from the crossplots of Figures XII -XV) the following relation is obtained:

$$P.P._{Salts} = K \cdot R^{-\frac{1}{2}} + K_2 C + C \qquad (3)$$

$$P.P._{non\ electrolytes} = K' \cdot R + K_2 C + C' \qquad (4)$$

The dendrite width seems to follow equation 4 for all systems studied.

The fact that PVP has slightly positive slopes does not invalidate our previous explanation but has to be treated as a completely different system since the number of kinetic units are few due to the high molecular weight of P.V.P. Also, entangling of the molecules can produce artifacts due to viscosity.

This work also concludes that while heat transfer is assumed to occur much more readily than mass transfer (i.e. diffusion coefficients of NaCl in water is of the order of 10^{-5} cm ^{2}/sec) while thermal diffusivities of ice and water are of the order of 10^{-2} and 10^{-3} cm^2/sec respectively) the overall freezing rate is governed by the rate and amount of heat extraction. To solidify at the rate required by the heat flow, ice crystals grow as arrays of parallel plates or dendrites.

Chapter III

Solid/Liquid Phase Transformations and Its Relation on Enzyme Activity

3.1 Introduction

A. Enzymes

When enzyme solutions are frozen, heated or subjected to various conditions, they are found to undergo a partial or complete loss of enzymatic activity. As stated by Melnick (37), "enzymes are chemically active protein molecules that depend on a precise structure for their specific activity. This structure is complementary to the structure of the substrate on which they act". Denaturation of an enzyme can therefore be interpreted as a change in the enzyme structures active sites even though the protein molecule is chemically intact. This definition is some what different then that of Neurath etal (38) who defined denaturation as "any non proteolytic modification of the structure." A proteolytic change occurs when hydrolytic degradation takes place: $-CO - NH - + H_2O \quad COOH + H_2N-$

The main factors that bring about protein denaturation and inactivation (if the protein is an enzyme) are 1) heat 2) high pressure 3) freezing and thawing 4) radiation 5) ultrasonic waves and 6) chemical reactions. This thesis will only be concerned with the freeze-thaw changes.

Generally when biological systems are cooled above 0^oC, the physical chemical properties generally remain reversible. However below 0^oC two main consequences occur:

1. Mechanical injury due to volume change.

This occurs when water freezes to form ice. Its density changes from o.999 g/cc to 0.917 g/cc on overall 8% increase in volume.

2. Biochemical injury due to dehydration

This injury may develop in the following ways.

a) When a protein is in solution a certain number of solvent molecules contribute to the free energy involved in the stabilization of the protein structure. When ice is formed during the freezing process, some of these "bound" solvent molecules can actually be removed and consequently the protein is irreversibly damaged. (Bruce etal) (39)

b) Dehydration can cause injury to enzyme systems as a result of changes in pH. Finn (40) investigated the denaturation of ox muscle juice caused by freezing. He observed that the maximum rate of denaturation (measured by loss of solubility), occurred at $-3^{o}C$ and that a further lowering of temperature resulted in a reduction rather than an increase in this rate. pH measurements of the unfrozen liquid remaining in frozen samples showed a correlation between loss of solubility and pH which fell to less than 6 at $-3^{o}C$ and rose again at lower temperatures. In order to confirm that the loss of solubility is due to pH changes and not due to a lowering of the temperature, the protein was shown to be denatured at temperatures above freezing when exposed to electrolyte concentrations at a pH below 6.

c) Protein-protein interaction which can come about as a result of dehydration also may cause injury to biological systems. Lovelock, (41) using β-lipoprotein

(extracted from human plasma) found that for this particular system there was no relationship between denaturation and pH or denaturation and the concentration of salt in the suspending medium. Samples of lipoprotein were frozen in various salt solutions which had eutectic temperatures ranging from -4^{o} to $-86^{o}C$. More denaturation was observed the higher the eutectic temperature. It was concluded that the denaturing factor in this experiment was the progressive removal of water which concentrated the lipoprotein molecules until they will interact with each other. The denaturation of the protein coincided with the removal of the last traces of water from the suspending medium as the eutectic solutions crystallized. It was shown that very low concentration of methanol and glycerol were enough to protect the protein from freezing injury. This small amount of additive is necessary to prevent an amount of water from freezing which is close to the minimum amount necessary to maintain the protein in fluid suspension. The reason why the molecular contact causes denaturation is that it permits formation of undersirable cross linkages between molecules leading to distortion or rupture of the protein on rehydration. According to this reasoning, the protective effect of these additives is simply to fill the space between structures and prevent contact between molecules and active groups during freezing.

d) Dehydration can cause denaturation by breaking stabilizing hydrogen bonds in a protein that prevent inter-

action between molecules. The fact that urea is often found to imitate the effects of freezing lends support to the hypothesis that disruption of hydrogen bonds in a protein is a frequent mechanism for freezing injury. Urea forms strong hydrogen bonds and might be expected to break hydrogen bonds on a competitive basis as much as perhaps dehydration does. Kloth (42) has proposed that the denaturing effect of urea may be due to its ability to dissolve the structured water which gives stability to certain amino acid sidechains. This type of denaturation could also presumably result from dehydration.

Chilson (43) etal,suggests that the effects of freezing on certain enzymes (e.g. lactic dehydrogenase-LDH) are primarily the result of dissociation of subunits. The enzyme is found in heart tissue (H-type) and muscle tissue (M-type) and each type contains 4 identical subunits - (M_4, H_4). Enzymes which consist of subunits have been found to be considerably less stable on freezing when compared with enzymes which consist of only one polypeptide chain.

The lowering of pH and the concentration of salts may induce this dissociation. The reassociation of subunits is a slow and incomplete process and the loss of enzyme activity may be a failure of normal reassociation. The subunits may interact in the wrong position forming abnormal polymers which do not have catalytic potential (enzymatic activity). In order to minimize this detrimental effect of

pH and high salt concentration, quick freezing and quick thawing do not allow the enzyme to be exposed to critical pH and salt concentrations long enough for this dissociation to occur.

B. Cryoprotection

To prevent damage to enzymes or biological cells due to solid/liquid phase transformations cryoprotective agents are often used. This concept was recognized as far back as 1913 when Keith (44) reported the improved survival of microorganisms frozen at -20°C in milk, glucose, sucrose, or glycerol. The theory of cryoprotection will depend on the theory of freezing injury to which one subscribes. Since several theories for the latter have been advanced, one could expect at least as many theories for the mechanism of cryoprotection. First, however, in order to understand the behavior of aqueous solutions, it must be realized that water is a highly associated liquid containing a large number of hydrogen bonds. (45). According to Frank and his associates, (46) a solute will go into this hydrogen bonded solvent in essentially one of three ways: by increasing the structuring, decreasing the structuring or more or less not changing the structuring of the water system. The last can occur by breaking some hydrogen bonds between water and replacing them by nearly equivalent new hydrogen bonds between water and replacing them by nearly equivalent new hydrogen bonds between solute and water. From the studies of Nash,(47) it is likely that hydrogen bond capacity is

most important. The more hydrogen bonding sites per molecule the greater the protective capacity. Ionic groups bind water molecules in a near layer but break down water structure further away, while nonpolar groups orientate water molecules and probably interfere with adjacent hydrogen bonding. Both types of groups, in an otherwise cryoprotective molecule reduce protective activity. (48).

Among H-bonding solutes one may further distinguish several subclasses (49,50). Rowlinson (51) using excess thermodynamic functions has interpreted the behavior in solution of these different kinds of H-bonding solutes. Formation of few or weak hydrogen bonds fail to provide cryoprotective activity. As more numerous or stronger hydrogen bonds become possible in a molecular structure, excess enthalpy of mixing for water-solute becomes increasingly negative. Excess entropy becomes less negative thus the excess free energy becomes negative. This implies that the more numerous and stronger are the solute hydrogen bonds with water, the more soluble the compound and the more stable the solution at any temperature (i.e. complete miscibility).

Cryoprotective activity is also attributed to colligative properties and water binding. Although all solutes will depress the freezing point of water, some are more effective than others. The colligative properties of a solute will vary depending upon its concentration according to Rauolt's Law in which the mole fraction of solute is equal to the

proportional reduction of solution vapor pressure compared to pure solvent. In its simplest form the relationship is expressed as $n_1/(n_1 + n_2) = (p^0 - p)/po$ in which $n_1 + n_2$ are the number of moles of solvent and solute and p^0 and p are the vapor pressures of solvent and solution, respectively. This simple relationship rarely exists in practice because of interactions between solute and solvent molecules which tend to increase or decrease the fluidity (vapor pressure) of the solvent. (52) With most solutes, the actual reduction in vapor pressure exceeds that which would be predicted on the basis of Raoult's law and when one calculates the amount of water necessary to produce the experimental vapor pressure depression, one finds that it is less than the amount of water actually present. The excess water which is apparently making no contribution to vaper pressure, has been termed "bound water". An example is rarely found in which only a specific portion of the water present makes no contribution whatsoever to the vapor pressure. It should be realized that in most biological solutions, all water molecules are probably being ordered to a greater or lesser degree. To say that 10% of the water is bound should be viewed only as a figure of speech. The fact is that many or most water molecules have been restrained to varying degrees by imposed forces resulting in a mean reduction in vapor pressure by 10%.

Regardless of the above limitation, it is of interest to determine the ability of a solute to influence its solvent

environment. In a study by Meryman (53), it was found that the water binding ability of trimethylamine acetate (TMAA) and ammonium acetate was extraordinarily high compared to other materials studied (e.g.glycerol, ethylene glycol, methanol). The manner in which the "water binding capacity" is reflected in conventional melting point curves of these substances was also studied. Meryman's findings conclude: 1) methanol approximates an ideal solute, 2) Both ethylene glycol and ethanol are exceptional up to concentrations of 20 molar. Above this concentration ethylene glycol becomes too viscous to freeze further during a short term experiment. The ethanol simply becomes ineffective. 3) Glycerol and DMSO are both more effective than an ideal solute indicating some water structuring or "binding" capacity. Trimethylamine acetate again showed the greatest departure from ideality, reaching a limiting viscosity at -35°C.

From this data it is evident that there are two important ways in which colligative characteristics of a compound can make it more or less desirable as a cryoprotective agent: 1) Its water binding capacity can make it possible to achieve cryoprotection with both a smaller intial and final concentration. The water binding capacity for ethanol becomes so poor at lower temperatures and high concentrations that it essentially has no protective effect at all. 2) The development of elevated viscosity with concentration and reduced temperature can effectively reduce the final concentration actually achieved on freezing even though further concentration might theoretically be expected.

3.2 Effects of the Freeze Thaw Process on α Amylase

It is common knowledge that the freezing and thawing of an enzyme may affect its activity. The question is not only to know how great an activity change will take place but even more important, can the freeze thaw effect be controlled to produce a minimum of damage. Heber (54) has stated that most soluble enzymes frozen at a neutral pH, moderate rate and in presence of soluble substances show little change in activity even in the absence of protective substances such as sugars. On the other hand, "purified" enzymes such as catalase (55), lactate dehydrogenase (56-58) glutamate dehydrogenase and glyceraldehyde, phosphate dehydrogenase (59) lose some of their activity during the freeze-thaw process. In this study the effects of the rate of freezing, rate of thawing, enzyme concentration, and the effects of additives on "purified" amylase have been undertaken.

3.2 A Experimental

α Amylase is an enzyme which occurs in nearly all plants, animals, and microorganisms. Its molecular weight is 45,000. Crystalline amylase (swine pancreas) suspensions in sodium-calcium chloride were purchased from Worthington Biochemical Company (Freehold, New Jersey) and used as the starting material.

Concentrations of 0.25 and 0.50 ml of the suspension were diluted in 1 liter of buffer solution pH 6.9 (buffer composition 0.06 m NaCl and 0.02 m sodium phosphate). Mea-

surement of activities was based on the changes of optical density of a buffered 1% soluble starch and 3.5 dinitro-salicyclic acid at 540 mm and a controlled temperature of 25° C. A unit of activity is that liberating 1 mole of reducing groups calculated as maltose per minute at 25° C. The prepared 2-ml samples were frozen in Nalgene test tubes (115 x 16 mm). The low temperature baths were maintained at temperatures of -20 and -70° C. The frozen suspensions were thawed by one of three ways: 1) 30°C water bath (2) 25° C air cooler, (3) series of water baths from 60 to 30° C with constant agitation.

3.2 B Results

The activity of α amylase solutions frozen in an aqueous buffer was significantly higher (86 vs 76% activity) for the fast freeze process over the slow freeze process. For the fast freeze, the temperature time profile (not shown) from 25° C until complete solidification took approximately 2 minutes while the slow freeze monitored over the same conditions lasted approximately 15 minutes. The thawing process was accomplished by placing the specimen tubes in a 30° C thermostated water bath for 10 minutes. To demonstrate the effects of some widely used additives Figure XVIIIA,B was plotted as percentage of activity vs concentration of additive for both the fast freeze-thaw (A) and slow freeze-thaw (B) processes.

A minimum activity for some solutions with an additive has been observed. This minimum is below the activity of the

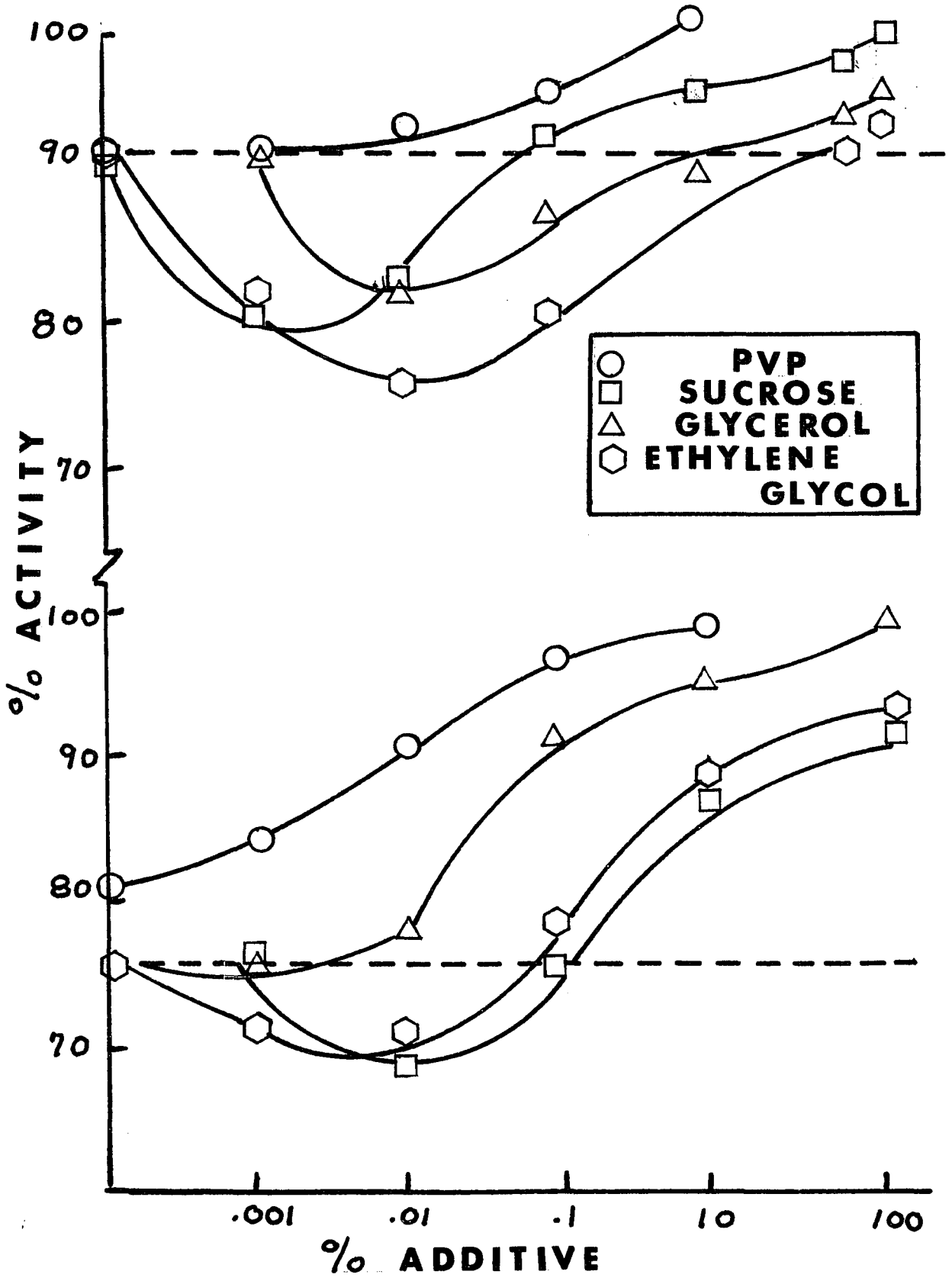

Figure XVIII

enzyme water system. In each case this phenomenon observed when the additive concentration is approximately 0.01%. For the slow freeze (~15 min)-thaw processes glycerol and plyvinylpyrolidone (PVP) additives produce no minimum but ethylene glycol and sucrose yield minimum points below the observed enzyme water activities. Protection occurred for the enzyme when ethylene glycol and sucrose were added in excess of 0.1%. Glycerol protected when the concentration was greater than 0.01% and PVP appeared to protect for concentration as low as 0.0001%.

In the case of the fast freeze-thaw process, PVP was the only additive to produce no minimum. The other three additives produced minima which were well below the activity of an enzyme water solution experiencing a comparable freeze-thaw cycle. It should also be noted that ethylene glycol did not produce any protection for concentrations up to 20%.

Figure XIX describes the effect of the rate of thaw on an enzyme system with sucrose protection. Each of the specimens were frozen slowly to -20° C. Thawing was conducted at three rates: 1) rapidly by a series of water baths from 60 to 30° C with constant agitation over a period of 2 minutes 2) thaw at 30° C in a water bath for for 10 minutes. 3) thaw at 25° C air cooler for 45 minutes. Rapid thawing produced the best results for protection with sucrose while the air cooled thaw drastically reduced the enzyme protection. The minimum point appeared in each

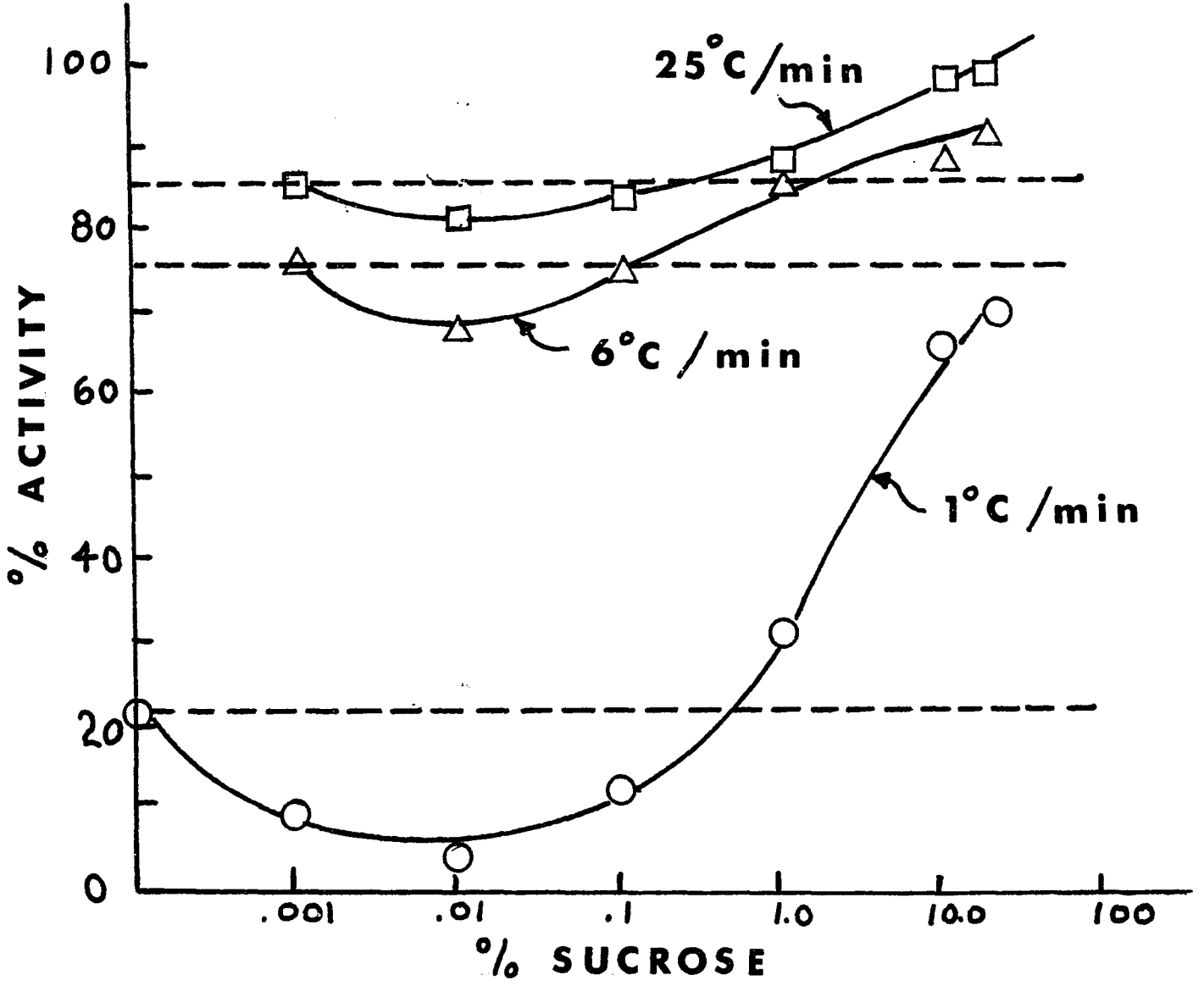
100
80
60
40
20
0
% ACTIVITY
25°C/min
6°C /min
1°C /min
.001
.01
.1
1.0
10.0
100
% SUCROSE

of the experiments and was most noticeable in the case of the air thaw. The thawing rates were determined over the temperature range from $-20^{o}C$ to $0^{o}C$.

3.2 C. Discussion

The effect of additives on the stability of biological materials is constantly being studied. Ashwood-Smith and Warby (60) studied freezing and thawing of catalase in the presence of PVP, dextran and glycerol. They found that PVP worked most effectively. Doebbler (61), Lovelock etal (62) and Luyet (63) also summarize some of the aspects of cryoprotective compounds. Generally the role of the additive is to prevent ice crystallization (especially in the case of cellular materials) and to prevent salt concentration effects. However, the phenomenon of an additive protecting the enzyme at high concentrations while harming it at lower concentrations appears to be a rarity.

As discussed by the review articles on enzyme activity (61-65) the exact mechanism which governs enzyme properties is still uncertain. Whether all enzymes are affected in the same manner appears doubtful. For this reason alone no one cryoprotective agent is used universally. Often mixtures of these agents (cryoprotective cocktail) are added to an enzyme system in hope of minimizing activity loss. However, as mentioned before most evidence for enzyme denaturation after freeze thaw cycles is related to solute concentration.

From the results of this section the following hypothesis is suggested. At low concentrations of "protective agent" the aqueous solution that forms in between the ice crystals.

is rich in solute (mainly salts) which will destroy active sites on the enzyme. The more concentrated the solution is and the longer the time of interaction, the greater the loss of activity. In addition, this small amount of "protective agent" (~.01%) possibly may act to flocculate the enzyme molecules together increasing enzyme-enzyme and solute-enzyme interactions which result in a greater loss of activity than an enzyme water system. For example, at low sugar concentration more amylase molecules will compete to interact with sugar molecules thus favoring enzyme sugar enzyme flocculation. At higher sugar concentration α amylase will be sugar saturated minimizing enzyme-enzyme interaction. At high concentrations of "protective agent" the solution that now forms between the ice crystals is a water in solute (i.e., water in sucrose) system. Since the majority of solute is the protective agent (not salt), activity loss is much less than in the enzyme water system.

The loss of activity with increasing thawing time is not as an uncommon a phenomena. Mazur (65) also sites examples where slow thaw rates may be more damaging to cell survival than a faster rate of thaw. In our case it appears that the slower the enzyme is thawed, the longer it is subjected to solute-enzyme and enzyme-enzyme interactions which will permanently destroy the activity. Addition of "protective agents" at high enough concentrations serves to dilute the solute effects and protect the enzyme activity.

Chapter IV

Polymorphic Phase Transformations on Saturated Monoacid Triglycerides

4.1 Introduction

An important class of organic materials where the processes of solidification and melting assumes a significant role in determining their physical properties are fats, fatty acids and their natural derivatives, the glycerides.

Glycerides in general serve as the principle constituent of fat. Their presence is found in most living matter from plants to human beings. The functions of these lipids especially in the case of shortenings, confectionary products and biological membranes depend on their crystalline structure or more appropriately, their polymorphic form. Because of their importance, glycerides and triglycerides in particular have been studied for over a century to determine the various polymorphic forms which exist. However few people have been concerned with the kinetics of transformation from one solid to another (or more simply aging) and the solidification of the melt to the various crystalline forms. Yet these dynamic processes have great technological consequences such as the mouthfeel properties and stability on everyday products.

In addition, it is also important to determine the degree of stability that each form exhibits. Some forms seem to be thermodynamically stable over a given temperature and pressure range while others are never thermodynamically stable but exist as a result of the kinetics of formation and transformation.

Obviously this presents a problem since a product could be prepared in one form with the desired properties but as a function of storage, temperature and pressure (Physical Aging Process) a transformation may take place from an unstable polymorph to one of greater stability. The end result is the deterioration of the product quality and its original properties. For this reason, it is of interest to understand the laws involved in the kinetics of transformations or more simply aging.

4.2 Background

The polymorphic behavior of fatty materials was first observed over a century ago when Heintz (67) observed that tristearin when rapidly solidified would melt at 52°C then resolidify and exhibit a second higher melting point at 65°C. In 1853 Duffy (68) reported that tristearin could have three melting points. In the following years, numerous scientists (69-72) disputed the various melting points and forms of the triglyceride. In one report tristearin was found to have seven transformation temperatures (72) at which time it was speculated that the multiple melting points were due to some form of isomeris. It was really Malkin and Clarkson (73) who used X-ray diffraction patterns to demonstrate that the multiple melting was due to different crystalline forms of a single compound (polymorphism). In their work (74) they claimed however that four polymorphs of tristearin existed including a "glassy" form first

observed by Ravich (75). The period between 1945 and 1955 was open to many debates by Malkin and his supporters and a group lead by Lutton (76) and Bailey (77) who only accounted for three forms. Today it is accepted that saturated mono acid triglycerides exhibit, with rare exception, only three cross sectional structures (α_L, B'_L, B_L) which refer to the packing of the hydrocarbon chain. The subscript L refers to Lutton's convention. These forms can be observed using techniques such as differential thermal analysis, x-ray single crystal studies, infra red spectroscopy and nuclear magnetic resonance. A summary of the various physical constants used to differentiate the polymorphs appears in Table IV. The transformation or melting points for the saturated monoacid triglycerides is given in Table V.

4.3 Experimental Techniques for Studying the Phase Transformations of Triglycerides

A. Microscopy

The temperature gradient microscope stage as described in section 2.1 was used for all visual observations. A temperature gradient of $10^{o}C$/mm was used. The temperature varied over the range of $-20^{o}C$ to $+90^{o}C$. Observations were made through cross polars to differentiate the various polymorphs. The magnification unless otherwise specified is 80X. Approximately 4 mgms of the sample was placed between the microscope slides. This small amount produced a thin film when melted and then solidified to cover the

Polymorphic Forms of Saturated Mono Acid Triglycerides

	α	β'	β
Sub Cell Packing	Hexagonal $a = b \neq c$ $a = B = 90°$ $Y = 120$	Orthorhombic $a \neq b \neq c$ $a = B = Y = 90°$	Triclinic $a \neq B \neq Y$ $a \neq b \neq c$
X-ray Short[18] Spacing	4.15 s 2.40	4.2 vs 3.8 s 2.53 m 2.26 m	4.6 vs 3.84 s 3.68 s 5.24 m 2.85 m
I.R.[15] Spectrum	Single band at 720 cm^{-1}	doublet 719 at 727 cm^{-1}	singlet band 717
NMR[16] Line Width	6.8 gauss	———	13
Second Moment	11.1	-----	22
Micrscope Data[12]	spherulite (-) elongation	spherulite(+) or (-) elongation extinction	no spherulites oblique extinction crystals

TABLE V

Melting Points (84) (± .5°C)

Trilaurin	15	34	46.4
Trimyristin	32.8	45	58.0
Tripalmitin	45	56.6	66
Tristearin	54.7	63	73.5
Triarachidin	61.8	69	78
Tribehenin	68.2	75	82.5

entire specimen cell. The film was thin enough to allow optical identification of the crystalline material and also produce good reproducibility.

B. X-Ray Diffraction Patterns

X-Ray studies still serve as the foundation for determining different polymorphic forms. The complete structure of a particular polymorphic form can also in principle be obtained. The latter however, depends on the production of large enough single crystals. As of this date only one single crystal study has been made. (83) This gave information on the β form of trilaurin grown from a solution of benzene by evaporation at room temperature.

From the diffraction patterns of long chain molecules essentially two sets of data may be obtained. The long spacing data relates the distance between planes formed by methyl or polar groups. The long spacing is usually a linear function of the number of carbon atoms. The short spacing data relates the cross sectional arrangement of the crystal and is practically independent of chain length. Polymorphism is therefore, indicated by this short spacing information.

The short spacing dimensions for each form are those of Lutton and are summarized in Table IV. The system to be studied was placed in a fine capillary tube (.7 mm dia, wall thickness $\frac{1}{100}$ mm. General Rand Corp. Edison, N.J. 08817) which was then heated above the triglyceride melting point and

rapidly quenched to form the α phase. The tube was then placed in a thermostated bath at the desired aging temperature for a given interval. After the aging interval the sample temperature was kept some 20^{o} below the α transition temperature and an x-ray diffraction pattern was taken in a temperature controlled camera to determine if a phase change occurred.

C. Differential Thermal Analysis

The method of determining a particular phase using the DuPont DTA 900 was most convenient since the test could be conducted quite rapidly (heating rate 15^{o}C/Min.) and sample preparation was minimal. The starting temperature for each of the sample was approximately 20^{o}C below the α transition.

D. Infra Red Spectroscopy

Chapman (78) was one of the first scientists to use IR to classify the forms of the triglyceride. His results are summarized in Table IV. The region of interest has to do with the CH_2 -CH_2 rocking motion. The spectra of these molecules was found to vary according to the polymorphic form in which they occur. Among other spectral differences a single band occurs at 13.9 μ (720 cm $^{-1}$) in the spectrum of the α form; a doublet at 719 and 727 cm^{-1} in the spectrum of the B^{γ} form and a singlet band at 717 cm^{-1} for

The sample to be studied was placed between two NaCl salt plates and melted using a temperature controlled IR

cell. Rapid cooling was obtained by placing the cell in a refrigerated system. Precautions must be taken to prevent water from condensing on the cold plates and ultimately fogging them. Also care must be taken in cooling the plates since rapid cooling will crack the plates. Once the triglyceride was in the α form the system was aged at the desired temperature while continuously scanning the I.R. spectrum. The tests were conducted on a Perkin Elmer 621 High Resolution Spectrophotometer.

This technique was only used to confirm the experiments conducted on the instruments mentioned above since the aging temperature could not be controlled accurately and due to the size of the I-R cell a temperature gradient always existed.

E. Light Scattering

The detection of crystal structure changes may be observed by examining the light scattering properties of the various crystals. This technique has been used by Santoro and Esposito (79) to detect liquid crystal samples in the bulk. Barrall and Guffy (80) have also used a similar technique using a polarized light source.

Our instrument combines the advantages of the above authors in addition to having the ability to measure the absorption of ultraviolet and visible light on thin film samples.

The quartz microspectrophotometer is illustrated in Figure XX . The instruments basic design was originally

MICROSPECTROPHOTOMETER

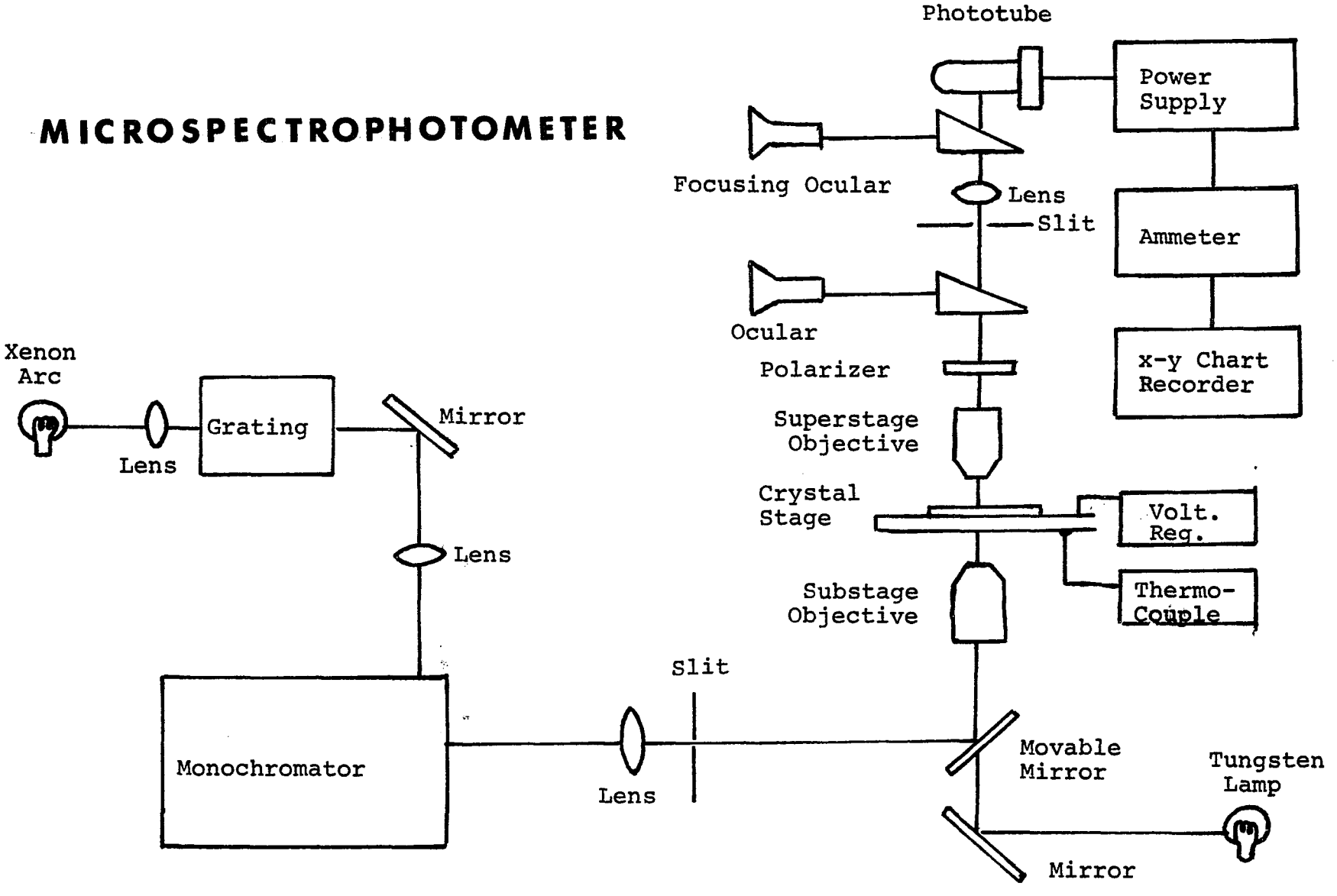

constructed at the National Institute of Health under the direction of Dr. W. Eaton and Dr. T. Lewis of the City College of New York. The main virtue of the instrument is its ability to measure high optical densities on very small crystals. It is built around a Leitz Ortholux Pol polarizing microscope. Monochromatic light is obtained by passing light from an Osram 150w Xenon arc source through a Jarrell Ash grating monochromator (model 82-410 16.5A/mm dispersion, 1mm slits). The monochromatic light is plane polarized at the exit slit of the prism monochromator with a Glan prism (Karl Lambrecht Crystal Optics, Chicago Illinois.) Another Glan prism may be inserted in the microscope tube in order to align crystals by extinction on the rotary microscope stage. The light detection system consists of a RCA 1P28 photomultiplier tube, Fluke power supply and Keithley Model 4145 picoameter. The stage contains a silicon oxide coating which acts as a heat resistor when a voltage is put across it. This allows the temperature of the thin film to be regulated. A thermocouple is used to determine the temperature of the isothermal stage.

Crystal thicknesses may be determined form refractive index measurements using oil immersion methods and from measurements of relative retardation. A Leitz Brace Koehler compensator is used to measure the retardation effect.

F.N.M.R.

Wide line N.M.R. can be used to define some of the polymorphic forms of glycerides. Chapman, Richards and York

(81) determined line widths for tristearin and tripalmitin. The alpha form measuring 7 gauss and the beta form 13 gauss. The line width for the beta prime form was not determined for these systems.

In our study, a Jelco Wide Line NMR (40 Hz) was used to study aging. A derivative curved was periodically taken and the line width measured to determine if aging had taken place. The samples were originally prepared in the α forms by melting the triglyceride and then quenching the sample. Once again the main problem with this technique is due to heat transfer within the sample since the sample tube has a diameter of 15 mm. It must be realized that any bulk sample will therefore have a temperature gradient existing from the tube walls into the center of the sample. This temperature gradient was minimized by placing a hollow glass rod evenly spaced in the tube to form an annulus. The sample was placed in the annulus and a thermocouple used to determine the temperature.

Reagents

Essentially pure (99%) monoacid (even) triglycerides were purchased from Applied Science Laboratories Inc., State College Pa. with the exception of triarachidin, C_{20}, which was purchased from Hormel Institute Minneapolis, Minn. The purity was judged by gas chromatography on a Hewlett Packard 5750 Chromatograph with area analysis. 20mg samples dissolved in chloroform were injected (as /5 µl plugs) into a 10'-1/8

column containing 4-5% OV-1 on a chronosore Q support. Triglycerides, purchased from Eastman Chemicals, Rochester, N. Y. of slightly less impurity (95%) were also used.

4.4 Formation of Polymorphic Forms and the Effect of Thermal History

A material which may form more than one kind of crystal, each having different physical and thermodynamic properties is said to be polymorphic. In general the polymorphic forms of a substance are distinguished by a) orientation of molecules at lattice sites b) crystal structure or arrangement of molecules in a lattice. Either or both of these factors may give rise to polymorphism.

The transition from one polymorph to another may be thermodynamically described. At the transition point the Gibbs Free Energy of the phases in equilibrium are equal and the free energy curves at constant pressure intersect. The transitions which occur are either enantrotropic or monotropic. In the former case each phase is stable within a given region of temperature and pressure while the other phases are unstable. For this case the usual thermodynamic relation are valid i.e. G= H-TS

$$\left(\frac{\partial G}{\partial T}\right)_P = -S \text{ and } \left(\frac{\partial G}{\partial P}\right)_T = V$$

In addition the change from low temperature to high temperature form takes place with the absorption of latent heat.

From this it follows that the pressure on the transition temperature is determined by the Clapeyron equation:

$$\frac{dp}{dT} = \frac{\Delta S}{V_{II} - V_I}$$

In the latter case one or more forms are unstable under all conditions. The phase diagram is pictured in Figure XXI. For this system the validity of the above thermodynamic equations is questioned.

The transitions for the triglyceride are considered monotropic or as a combination of monotropic and enantrotropic transitions. The observations in the forthcoming sections quantitatively indicate that the α and β' polymorphs are unstable. Only the β form appears to be stable below the solid liquid transformation temperature. In addition, solvent recrystallization only yields β triglyceride crystals. In no case are the transitions from one solid to another reversible. However it is possible to go from the melt to any form (this may take considerable time. See Nucleation section.) From the data obtained the following relation between the phases is proposed:

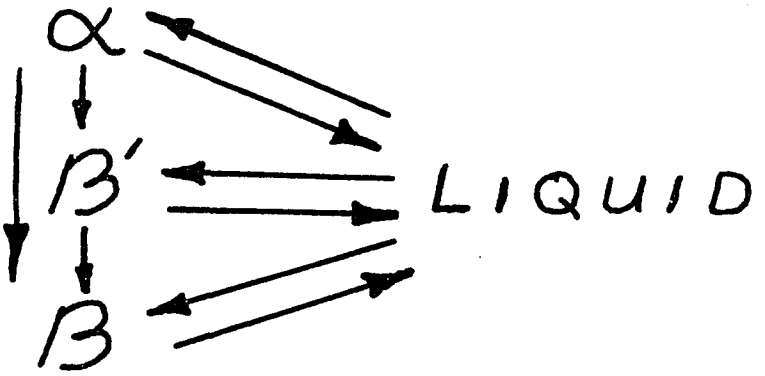

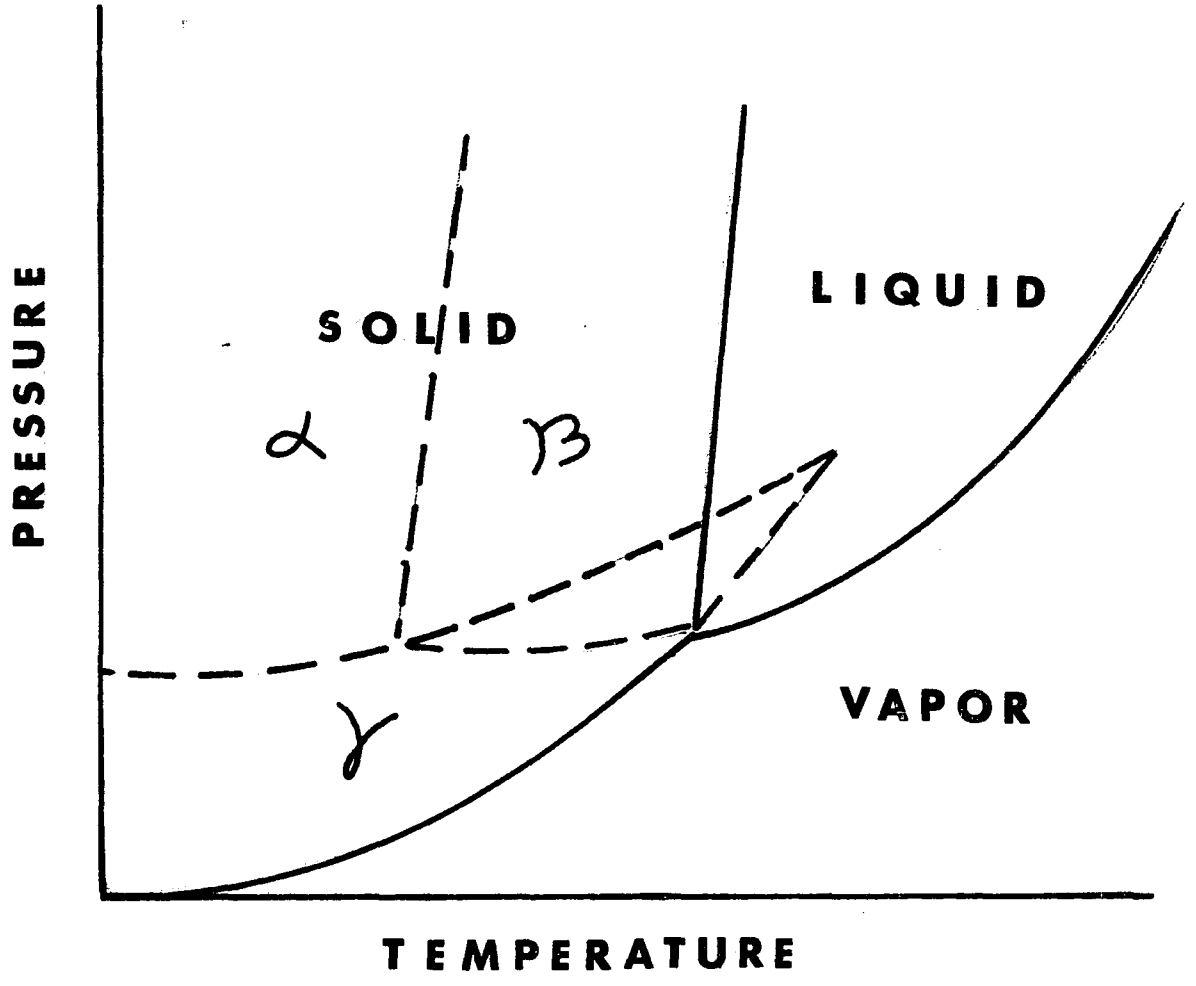
PRESSURE
SOLID
LIQUID
α
β
γ
VAPOR
TEMPERATURE

4.5 Results of the Microscope Examination

A. Generation of a Phase Diagram

A phase diagram of the monoacid triglycerides showing the various initial crystalline forms and the temperatures that they form at can be produced on the same microscope slide. The tripalmitin phase diagram is shown in Figure XXII. The sample was initially melted on the slide and then pressed to form a thin liquid film free of air bubbles. The glass sandwich was then quenched rapidly to $0^{o}C$ producing the α phase sphrulites. This was detected by observing the system through cross polars. Differential thermal analysis and x-rays were used to verify the α phase by this method of solidification. The sample was then placed on the microscope stage where the cold reservoir contained dry ice/acetone mixture and the hot plate was maintained at + $20^{o}C$. The hot reservoir was then increased to produce the desired temperature gradient mentioned above. As the gradient changed, the α spherulites melted receding toward the cold plate in a uniform melting front leaving behind the liquid (Section D), β phase (Section C) β' phase (Section B) in the appropriate temperature region. The melting front stopped at the α-β' equilibrium temperature ($45^{o}C$.) If the sample is heated to melt all the crystals and immediately placed on the same temperature gradient spherulites form and propagate into the warmer region as a continuous freezing front. The interest-

TRIPALMITIN

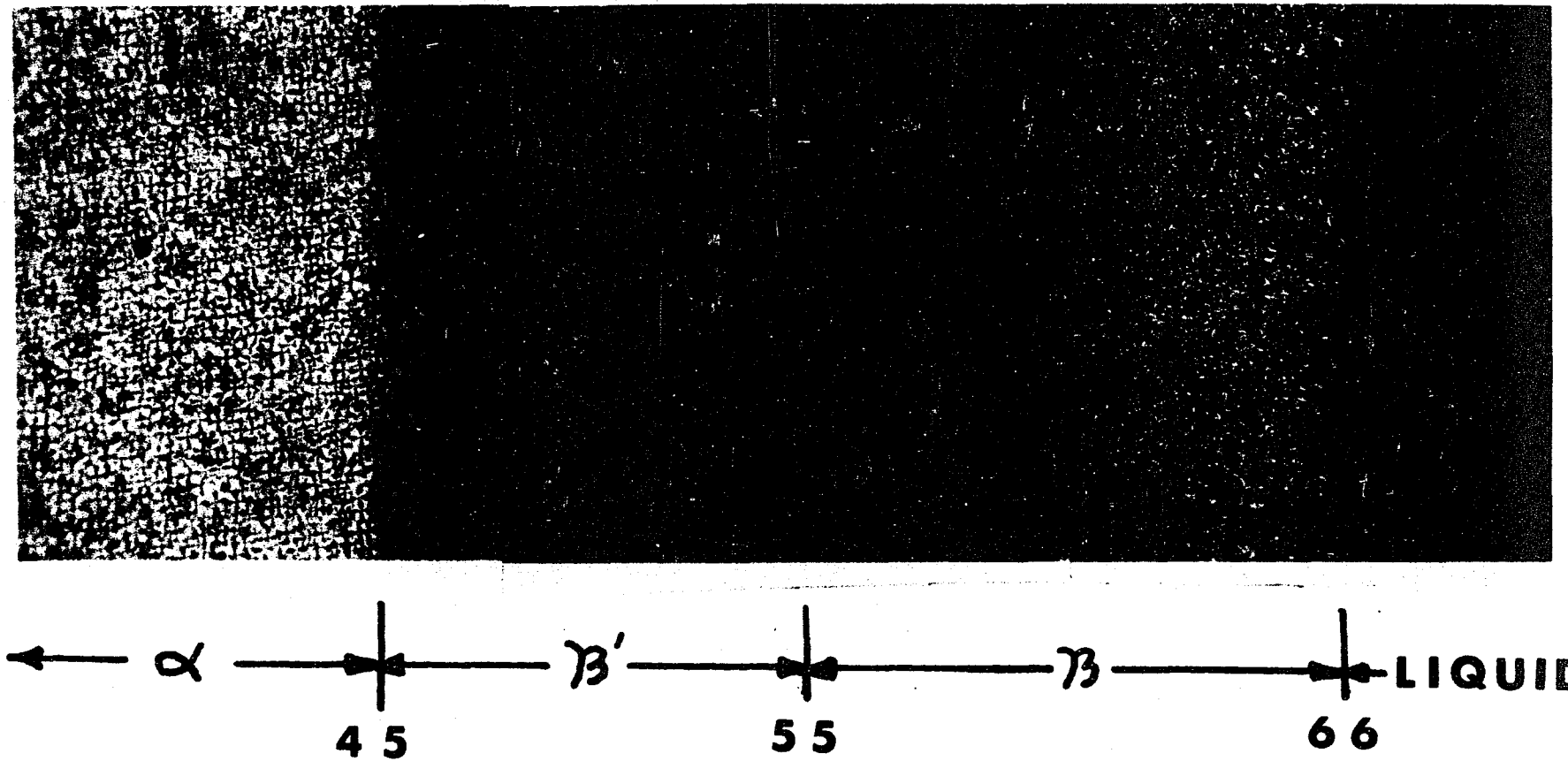

Figure XXII

ing feature of this experiment is that the spherulite freezing front stops below the expected α-β' equilibrium temperature. In the case of tripalmitin the α-β' equilibrium temperature given in the literature and as seen in the first experiment is 45°C. In this experiment the α-β' front stopped at 38.5°C. A liquid section is next observed in the temperature region from 38.5°C to 52°C but is followed by a second crystal region which is optically defined as a β region. Immediately following this region is the liquid phase. The liquid section in the 38.5-52°C slowly solidifies (after ~480 sections) in the form of large colored and featherlike spherulites. A photomicrograph of this solidification process for tripalmitin is given in Figure XXIII.

B. Aging

Figure XXIV is an aging curve of the triglycerides. This is obtained in a manner similar to that described in Section A. The triglyceride to be studied is initially solidified in a α form. It is then placed on the temperature gradient stage and melting of front rapidly takes place as the cell approaches equilibrium. When the resolidification front reaches the α-β' equilibrium temperature the velocity of the front appears to be zero. However accurate measurements with the cathetometer over a period of time indicate movement of the α-β' front beyond the equilibrium temperature. The aging curve can therefore

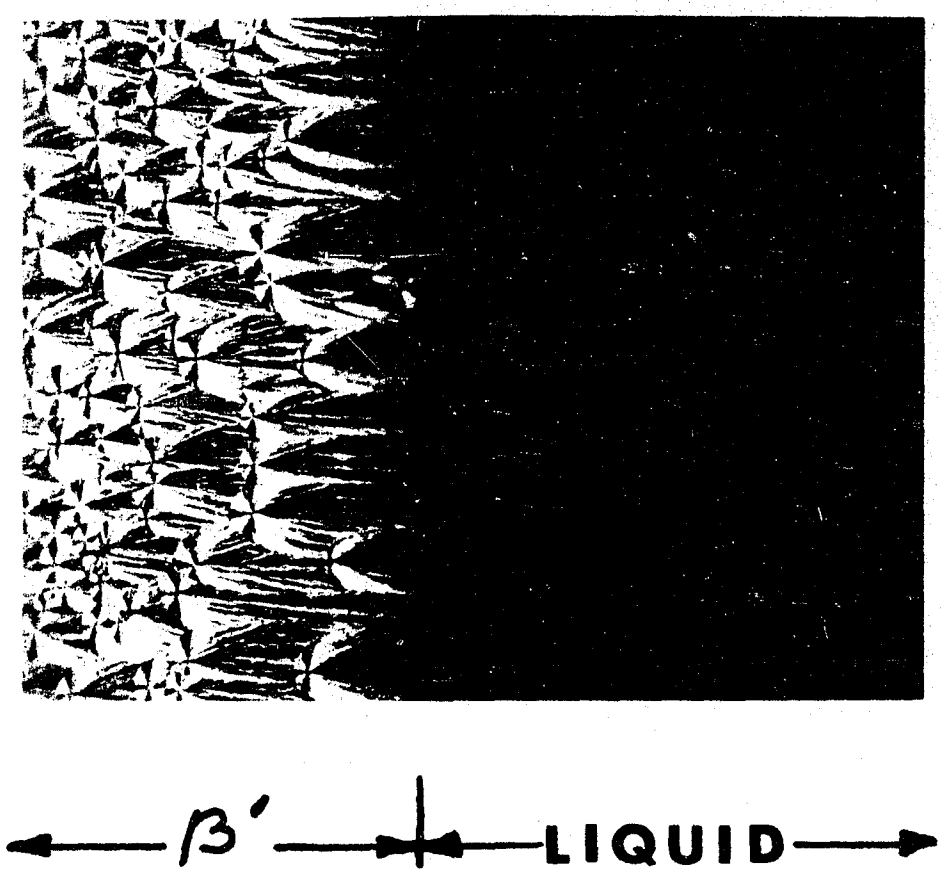

Figure XXIII

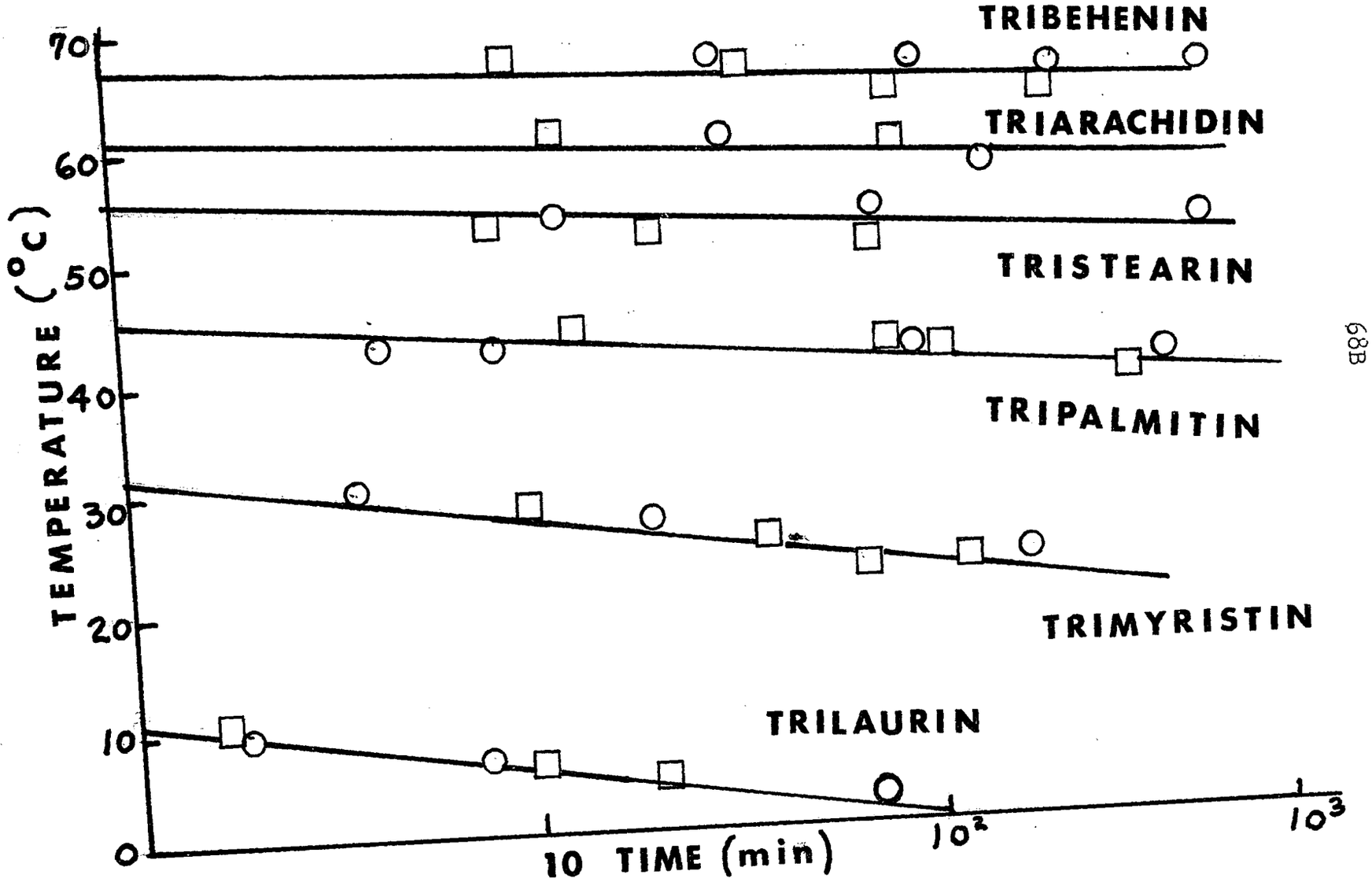
TRIBEHENIN
TRIARACHIDIN
TRISTEARIN
TRIPALMITIN
TRIMYRISTIN
TRILAURIN
TEMPERATURE (°C)
70
60
50
40
30
20
10
0
10
TIME (min)
10²
10³

68B

be made by determining the temperature of the α-β' front as a function of time.

Our optical identification of the various phases and the phase diagrams produced correlate quite well with the results of Quinby (12). The α phase contains "bright spherulites" having (-) elongation and are not colored when viewed between cross polars with a halogen lamp. The isogyres are perpendicular to one another and quite sharp. This pattern is sometimes referred to as a "Maltese Cross".

The + or - birefringence character is determined by using a tilting compensator. The triglyceride crystals are uniaxial which is determined by the Maltese Cross pattern. The position of this axis determines the crystal optical axis . The cross is also surrounded by faint interference rings.

When the compensator plate is tilted the rings in two opposite quadrants of the cross move either toward the center or the periphery of the crystal. The optical character is deduced from this movement.

The most difficult distinction to make is that between the α sperulite and the β' spherulites. The β' is distinguished by a colored and featherlike spherulite. The two isogyres are not as well defined as those in the α phase. The β phase is easiest to distinguish since it lacks the spherulitic pattern with the Maltese Cross Figure XXVII.

The phase diagram is most easily produced by first forming α spherulites over the entire slide and then introducing the temperature gradient. The reason for this becomes evident when experiments are conducted using the reversible motor to study interface solidification. The a phase forms quite readily from the liquid once the temperature is below the observed α-β' equilibrium temperature. Currently experiments are being conducted to relate the degree of super-cooling to the rate of freezing and the temperature gradient. These results will be discussed at a future date. β' and β phases, on the other hand take a much longer time to solidify from the melt. However the transformations from α-β' and α-β and β'-β takes place almost the instant the temperature reaches the equilibrium transformation temperature.

The aging phenomena described in section B appears to be quite significant since it really questions the true meaning of the α-β' and α-β transition temperature from one phase to another as given in the literature.

4.6 Additional Techniques for Observing the Physical Aging of Triglycerides

A. D.T.A.

Figure XXIX describes the effect of temperature on the time required for the triglyceride to transform from the α form to either β' or β. This method was most convenient for long range storage since the sample could be

prepared and stored in an externally controlled temperature bath and then tested at given intervals.

To determine if the system had aged it is necessary to know the thermogram of the various triglycerides in the α form. A typical series of aging curves is given in Figure XXV for trimyristin.

B. X-ray, I.R. and N.M. R. techniques can be used to reaffirm the aging curves and to determine which phase the sample transforms to ie $\alpha \rightarrow \beta'$ or $\alpha \rightarrow \beta$. Wide line NMR data is seen in Figure XXVI.

C. Microspectrophotometer

This instrument also provides quantitative information on the α transformation. It is especially convenient since the output signal can be recorded on an x-y recorder. The results agree with those of figure XXIV.

4.7 Physical Aging vs Storage Temperature

The influence of temperature on the aging time is presented in Figure XXIV. The results obtained from D.T.A. studies and the TGMS technique show good correlation especially with aging times greater than ten minutes. D.T.A. results tend to be somewhat scattered for aging times under ten minutes. This is most likely due to heat transfer in the sample and the time lost ($\sim$ 5 minutes) in obtaining the thermogram.

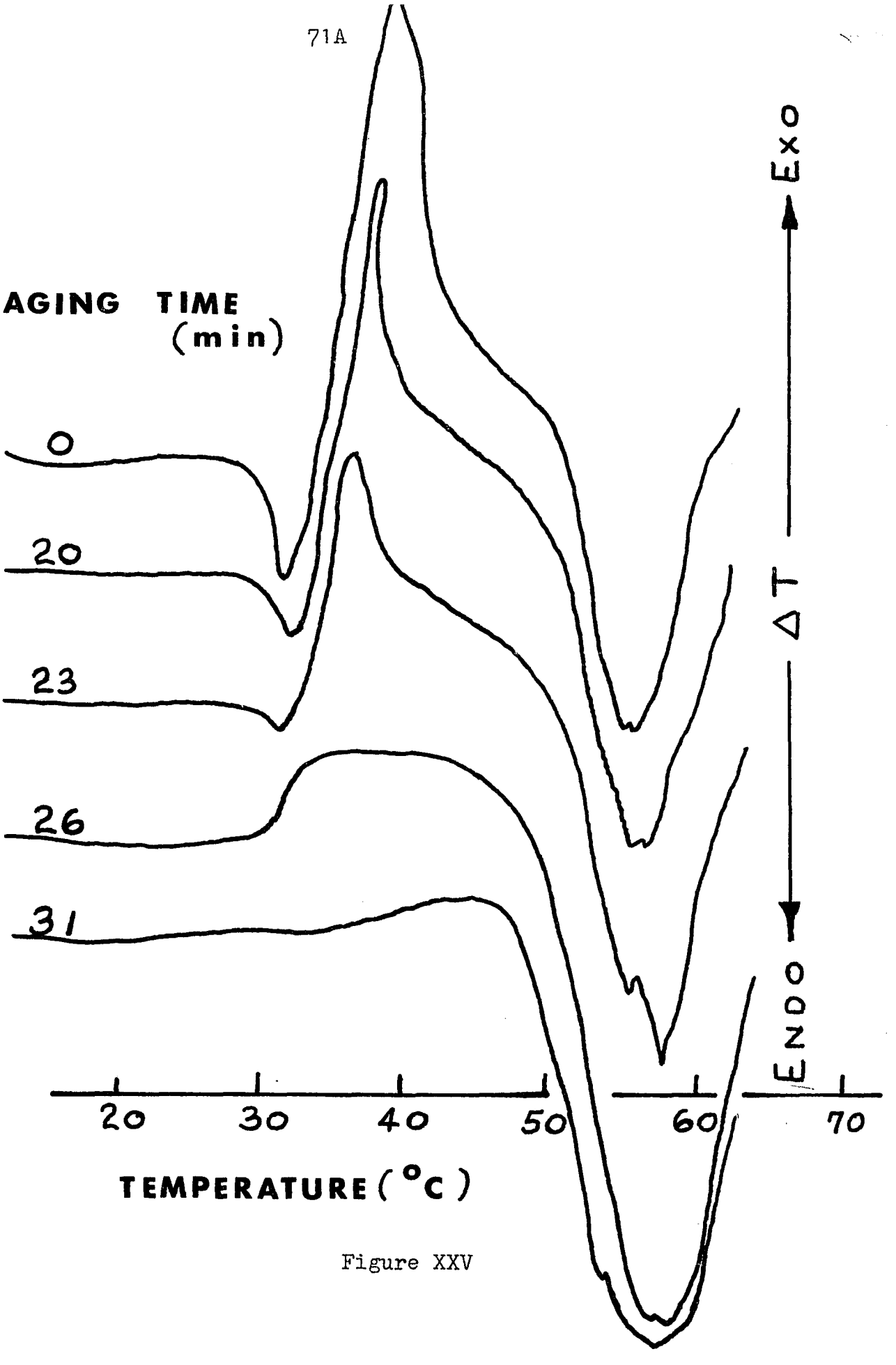
AGING TIME
(min)
0
20
23
26
31
EXO
ΔT
ENDO
20
30
40
50
60
70
TEMPERATURE (°C)

Figure XXV

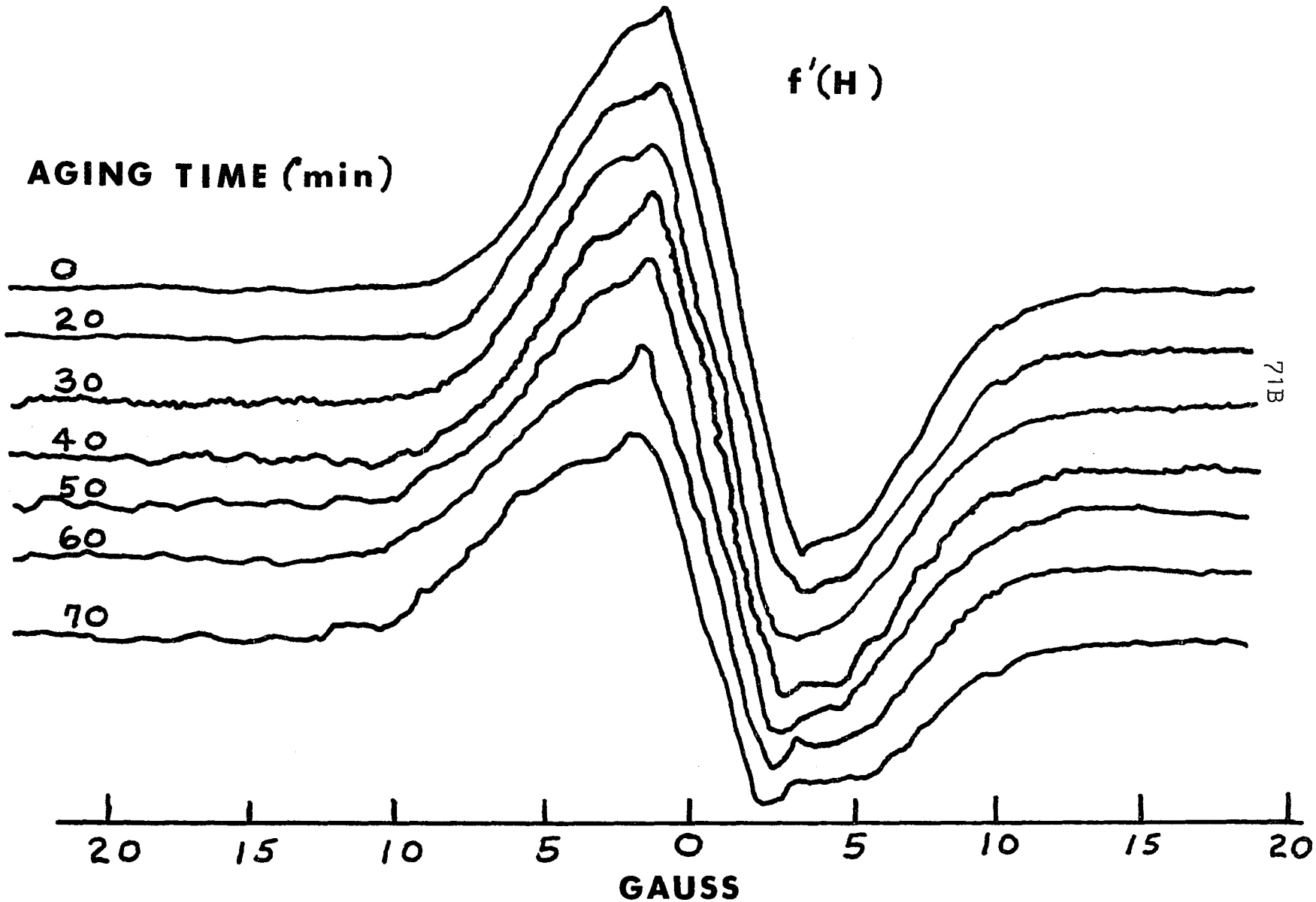
f'(H)
AGING TIME (min)
0
20
30
40
50
60
70
20
15
10
5
0
5
10
15
20
GAUSS
71B

A series of aging curves for trimyristin stored at 26°C are shown in Figure XXX. The heating rate was programmed at 15° C/min and the starting temperature was set at least 10°C below the alpha transition temperature. It should be noted that the heating rate is an important factor in determining the thermogram for triglycerides. Although slower heating rates will yield sharper endo or exotherms and can locate an equilibrium transformation temperature more accurately, the alpha transition is not a thermodynamic equilibrium transition. Therefore a high heating rate must be used to determine these metastable states. If a heating rate of 1°C/min was used, the trimyristin would automatically have aged in the DTA regardless of the previous thermal history. This can be predicted from Figure XXIX which indicates that the storage temperature of trimyristin at 31°C ($\Delta T_E = 1$) for approximately one minute will cause the alpha phase to transform.

Physical aging as noted earlier can also be observed using wide line N.M.R. Figure XXXI is an example of tripalmitin aging at 40.5°C. The field strength was set at 10^4 guass with a modulation frequency of 280 cps and a modulation width of 4 gauss. The α-form has a line width of 6.8g as first observed by Chapman et al (81). In a similar manner as seen with the D.T.A. work (Figure XXX) the triglyceride changes from the α-polymorph over a period of time to the more stable phase. The rate is

dependent on ΔT_E. In this case the line width continuously widens until the β width is obtained. It is also interesting to notice the development of the narrow line component as the system ages.

The second moment of the proton resonance is primarily due to the long chain hydrocarbon. The C-H group of the glycerol and the terminal CH_3 group are assumed to make a rather small contribution to the wide line spectra and will be mainly predominant in the narrow line. The smaller the second moment or line width (peak to peak width of the derivative curve) for the alpha form indicates that the hexagonal structure allows a considerable amount of molecular motion and would be less stable than the β polymorph.

4.8 Relation of Chain Length and the Stability of the α Hexagonal Polymorphic Phase

The results indicate that the alpha form is most stable for the higher chain triglycerides (C_{22}, C_{20}) when the temperature is kept at an equivalent number of degrees below the alpha transition temperature. Curve fitting the data produces the general formula:

$$T = e^{K\Delta T_E} - 1 \qquad 4\text{-}1$$

where $$\Delta T_E = (T_{Equiv\ a} - T) \qquad 4\text{-}2$$

The values of K are given in Table VI.

The fact that the stability of the α form increases at a given ΔT with increasing chain length can be explained

Table VI

	$K(deg^{-1})$	H^I (kcal/mole)
Trilaurin	.45	42
Trimyristin	.46	76
Tripalmitin	.672	152
Tristearin	.92	175
Triarachidin	.95	182
Tribehenin	2.30	228

by the energy diagram in Figure XXVII. The alpha form exists in a higher energy level than the more stable β form. Charbonnet and Singletown (81) have confirmed this experimentally by determining heat of transitions from α → β for trimyristin (9.1°K cal/mole), tripalmitin (10.7 Kcal/mole) and tristearin (12.2 Kcal/mole) to be exothermic. However Δ H of transition is not a measure of the stability of the system but $H^{\ddagger}$ or the energy of activation is. Classically the rate can be expressed as follows:

$$\frac{\alpha \rightarrow \beta \text{ Transition}}{\text{Time}} = A\, e^{S^{\ddagger}/R}\, e^{-H^{\ddagger}/RT} \qquad 4\text{-}3$$

For a given triglyceride let us assume that the entropy factor, $e^{S/R}$, is approximately constant and the data in Figure XXIV is used to determine the energy of activation. These results (Table VI) indicate that the energy of activation is highest for the most stable alpha phase (tribehenin). The magnitude of the energy of activation (10-228 kcal/mole) is reasonable since it is assumed that to break CH_2-CH_2 interaction requires 250 to 300 cal/mole. For trilaurin (C_{12} chain) in the unsymmetric tuning fork orientation, we estimate $H^{\ddagger}$ necessary to break all Van der Waal's attraction is ~20 kcal/mole. As the chains increase in carbon content it is reasonable to assume that not only should the energy of activation increase due to the additional carbons but also because the chains become more entangled in the crystal structure (therefore, greater Van der Waal's interactions). The absolute entropy in the

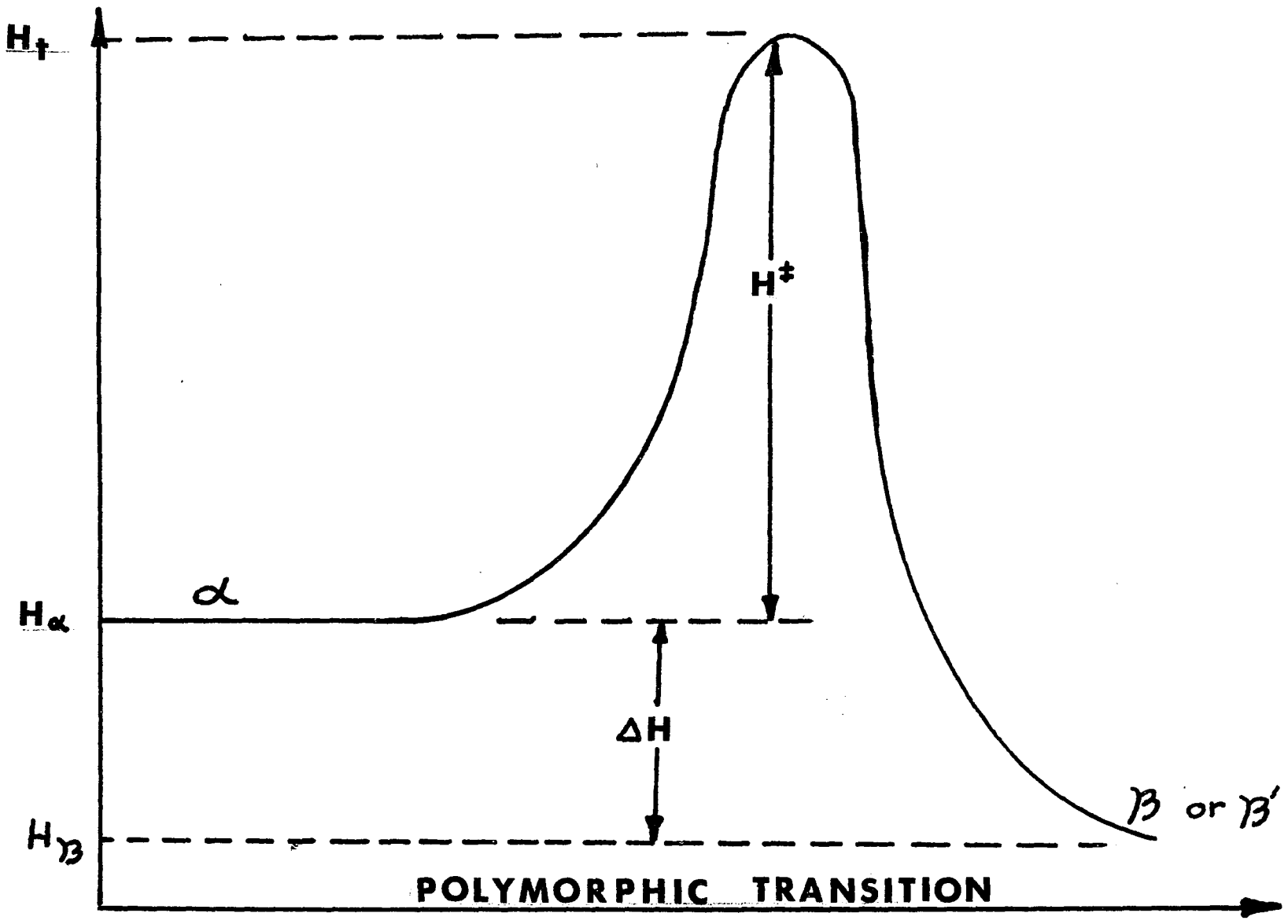
H_t
$H^{\ddagger}$
H_α
α
ΔH
H_β
β or β'
POLYMORPHIC TRANSITION

α or β state will be larger as the carbon content increases but the entropy term ($S^{\ddagger}$) in the activated state will be lowered since it is assumed that the chains are ordered and untangled in this high energy state.

In light of the above information it must be concluded that the a transition temperature does not represent thermodynamic equilibrium transitions but rather non equilibrium kinetically controlled transition. The aging time has been quantitatively described by the equation $t=e^{K\Delta T_{\epsilon}-1}$. The greater stability of the higher chain triglyceride polymorphs can be attributed to the greater energy of activation needed for the transition to occur. Simply stated when the chains of the triglyceride are longer than 12 carbons chain entangling slows down the transformation to more stable crystalline structures.

4.9 Mixed Triglycerides

Mixtures of two monoacid triglycerides were studied to see the effect of impurities on the aging process and phase properties of the base triglyceride. Essentially two categories are considered here.

1) HMTGI - high melting triglyceride impurities added to a lower melting triglyceride.
2) LMTGI - low melting triglyceride impurities added to a higher melting triglyceride.

The choice or combination of triglycerides is somewhat

limited since D.T.A. studies are difficult to analyze if the melting and transition temperatures of the individual triglycerides overlap. For example, tripalmitin has an α transition at 45°C, a β' transition at 55°C and a β transition at 66°C. Tristearin on the otherhand has an α transition at 55°C, a β' transition at 65°C and a β transition at 72°C. Obviously the α form of tristearin and the β' form of tripalmitin have the same transition temperatures and will therefore have similar thermograms in that area. The same is true for the β form of tripalmitin and the β' form of tristearin. This makes it extremely difficult to detect what triglyceride the thermogram peak belongs to. Secondly because of the mixtures, the transition temperatures and melting points tend to decrease or become broader on the thermogram making it even more difficult to differentiate two or more close peaks. (ie $\pm$ 4°C).

Another problem which occurs when studying mixtures in the solid state is how to produce and maintain a homogeneous mixture throughout the experiment. In many cases it could be observed that when the triglycerides were dissolved in a solvent which was later evaporated two distinct types of crystals would precipitate. Slow solidification of the mixture melt also produced samples which yielded inconsistent data. The general procedure was to form a melt some 20°C above the highest melting triglyceride phase (this insured that no nucleating sites would be left) and then rapidly chill.

Inconsistences were seen with the DTA and TGMS techniques after repeated freeze thaw cycles. This is most likely due to solute redistribution. An example of this is seen in Figure XXVIII where a 20% tribehenin in Tripalmitin mixture was subjected to ten freeze-thaw cycles. (+30 ⟷ + 85°C) Gradually at the solid/liquid interface the "impurity" accumulated establishing a definite "line of demarcation" between the two triglycerides. Magnification is 80 x.

a) Microscopy

In addition to the observations made during the freeze thaw cycles, increasing the impurity content also produced a definite effect on the triglyceride texture. Figure XXIX illustrates the texture of pure tubehenin and 25% trimyristin in a tribehenin mixture. In each case the material was solidified at a rate of 15°C/min. At this rate of freezing only the α form of tribehenin forms.

b) D.T.A.

These observations were made on the following mixed triglyceride systems:

1) trimyristin in tribehenin
2) trilaurin in tribehenin
3) trilaurin in tristearin
4) tribehenin in trimyristin
5) triarachidin in trimyristin

Figures XXX-XXXIII are typical thermograms for these

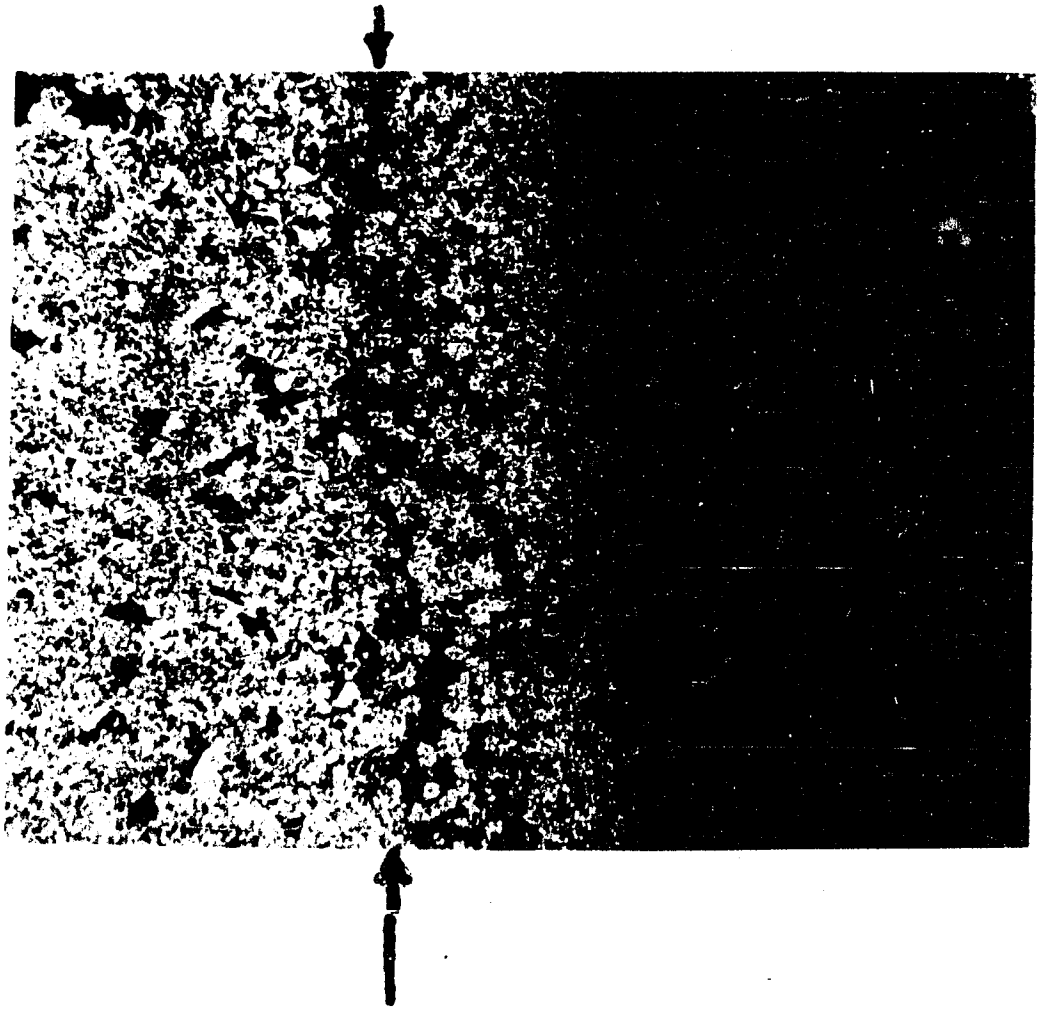

IMPURITY

INTERFACE

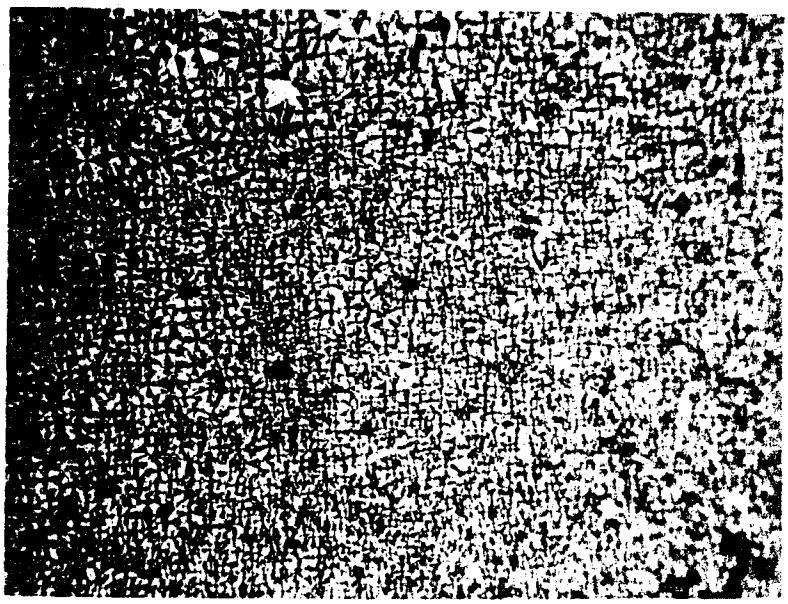

PURE α TRIBEHENIN

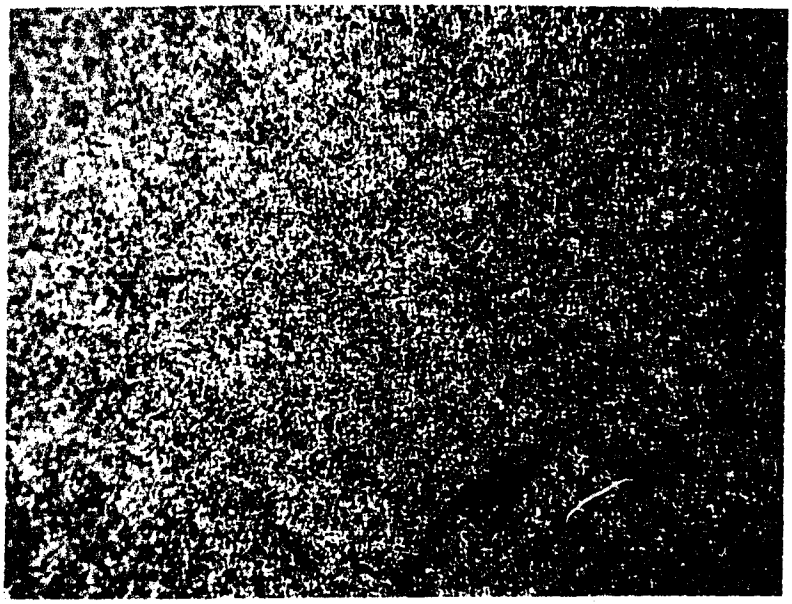

25% TRIMYRISTIN IN TRIBEHENIN

Figure XXIX

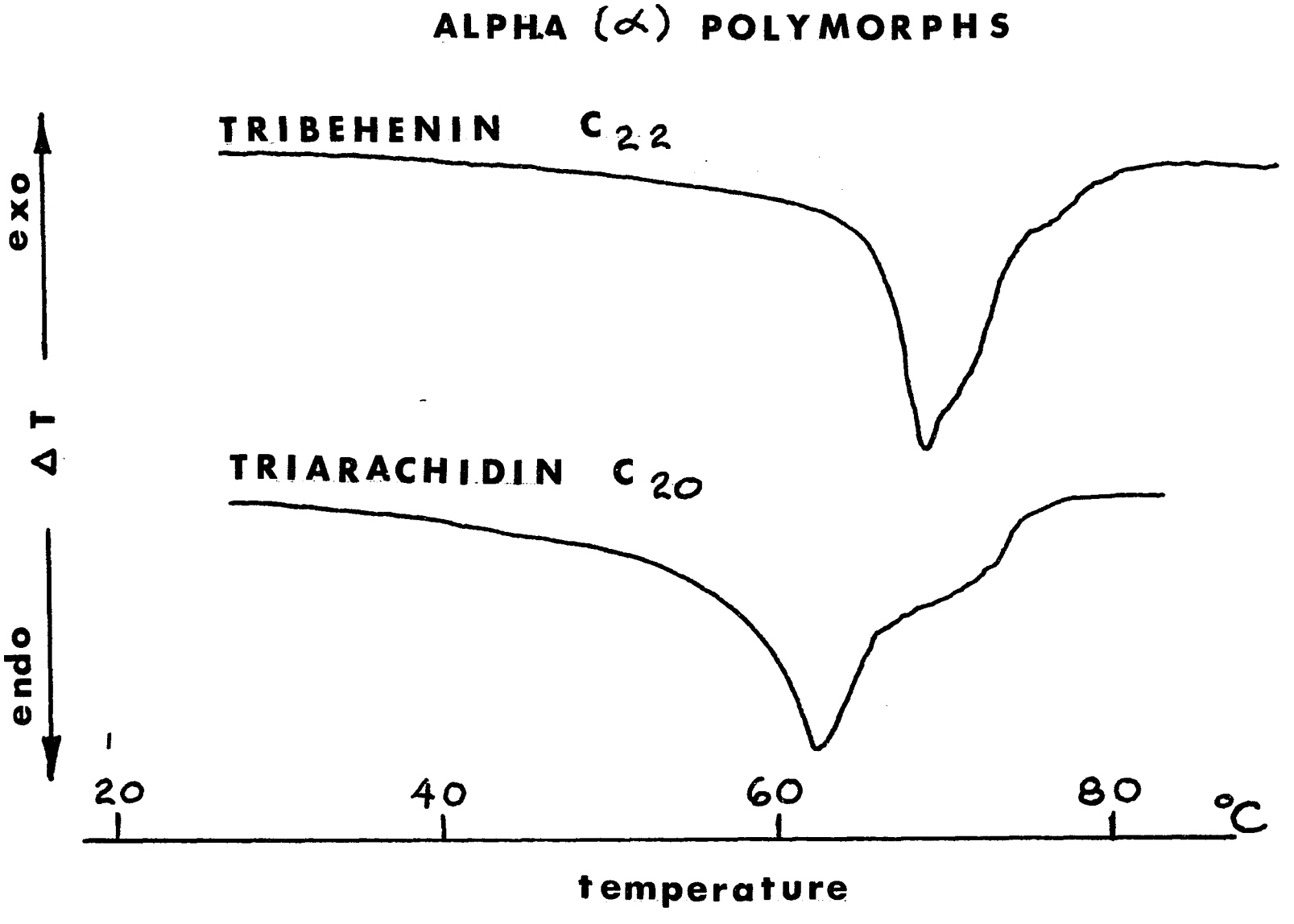
ALPHA (α) POLYMORPHS
TRIBEHENIN C22
TRIARACHIDIN C20
exo
endo
ΔT
20
40
60
80
°C
temperature

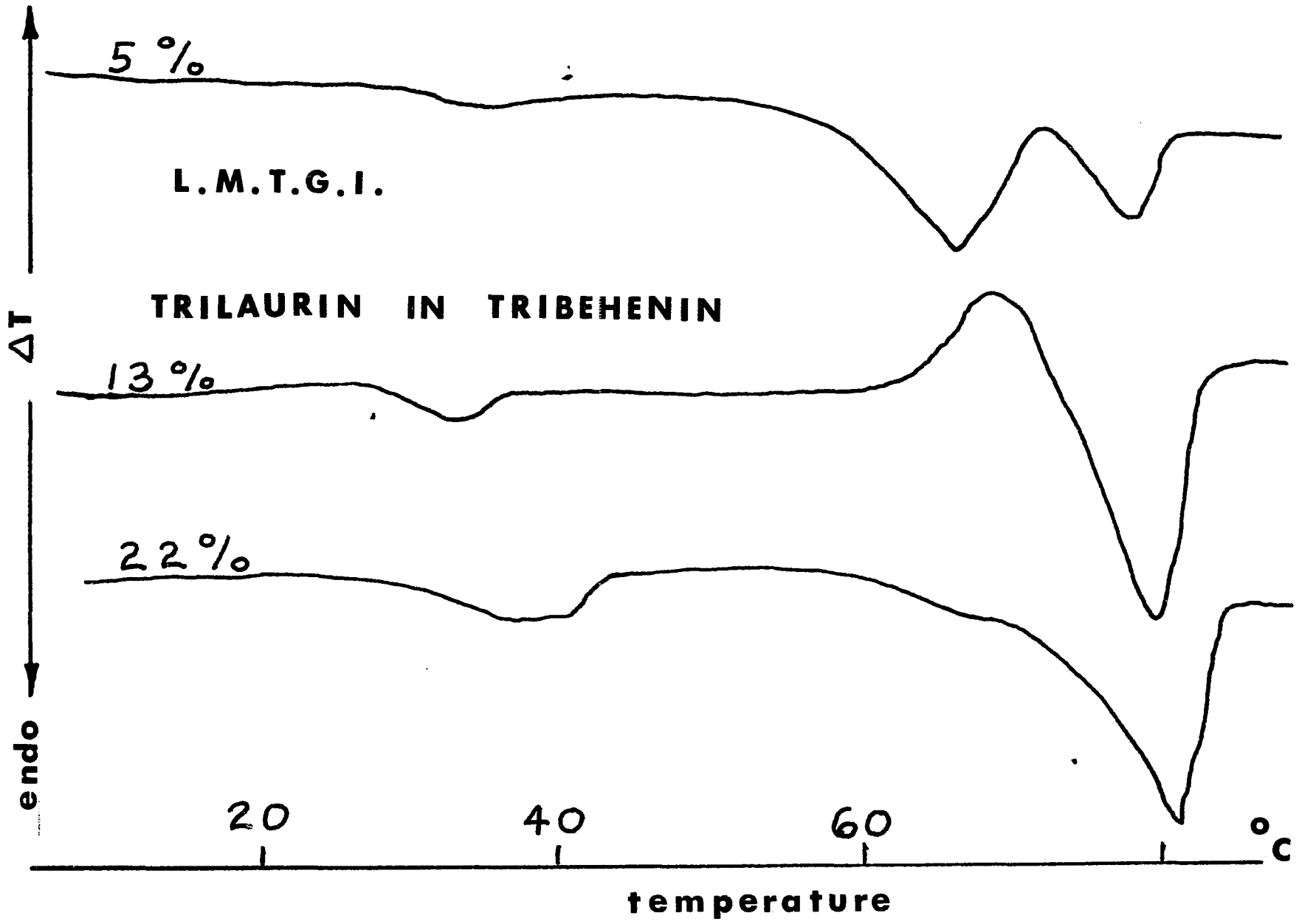
5 %
L.M.T.G.I.
TRILAURIN IN TRIBEHENIN
ΔT
13 %
22 %
endo
20
40
60
°C
temperature

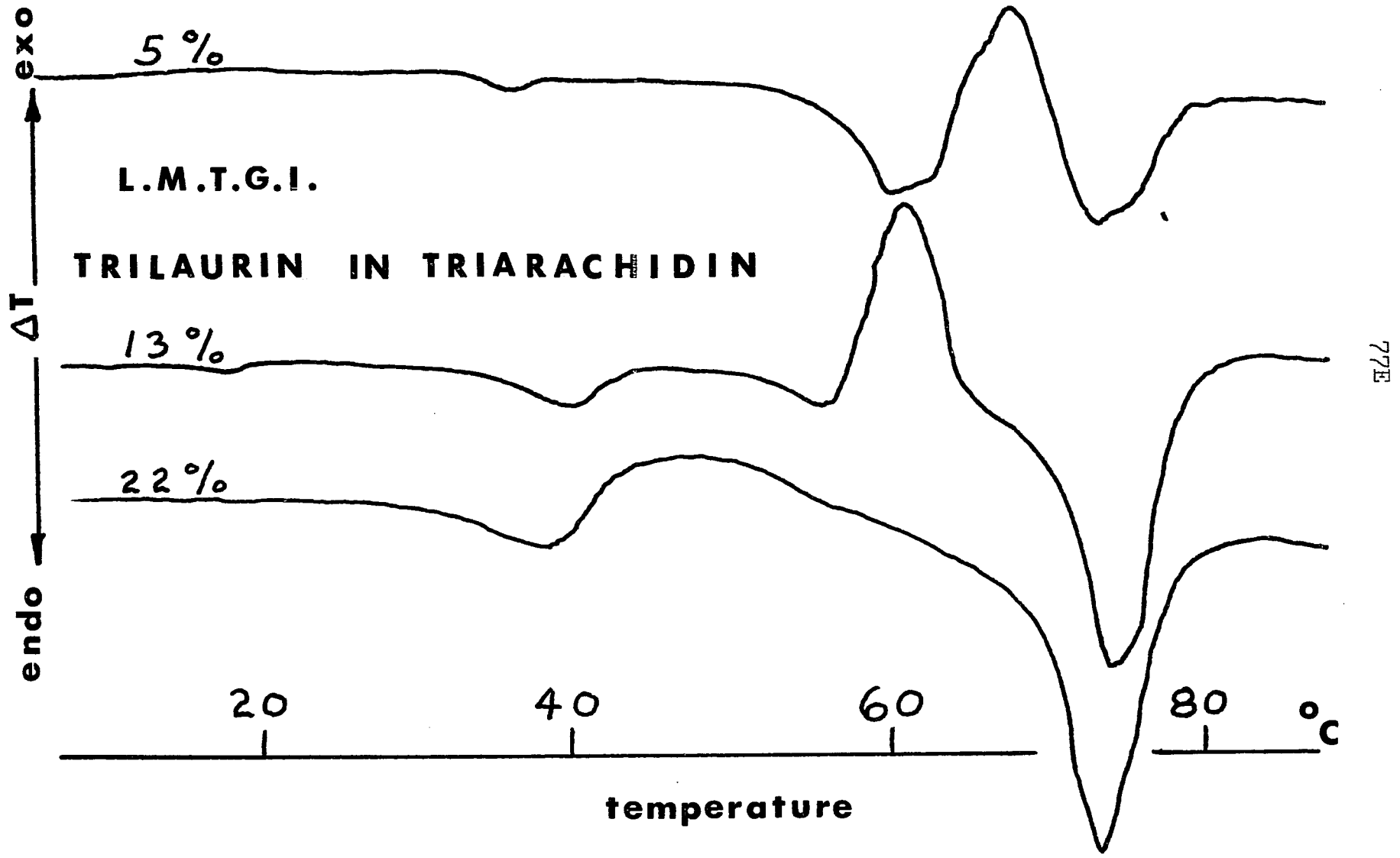
exo
5 %
L.M.T.G.I.
TRILAURIN IN TRIARACHIDIN
ΔT
13 %
22 %
endo
20
40
60
80
°C
temperature

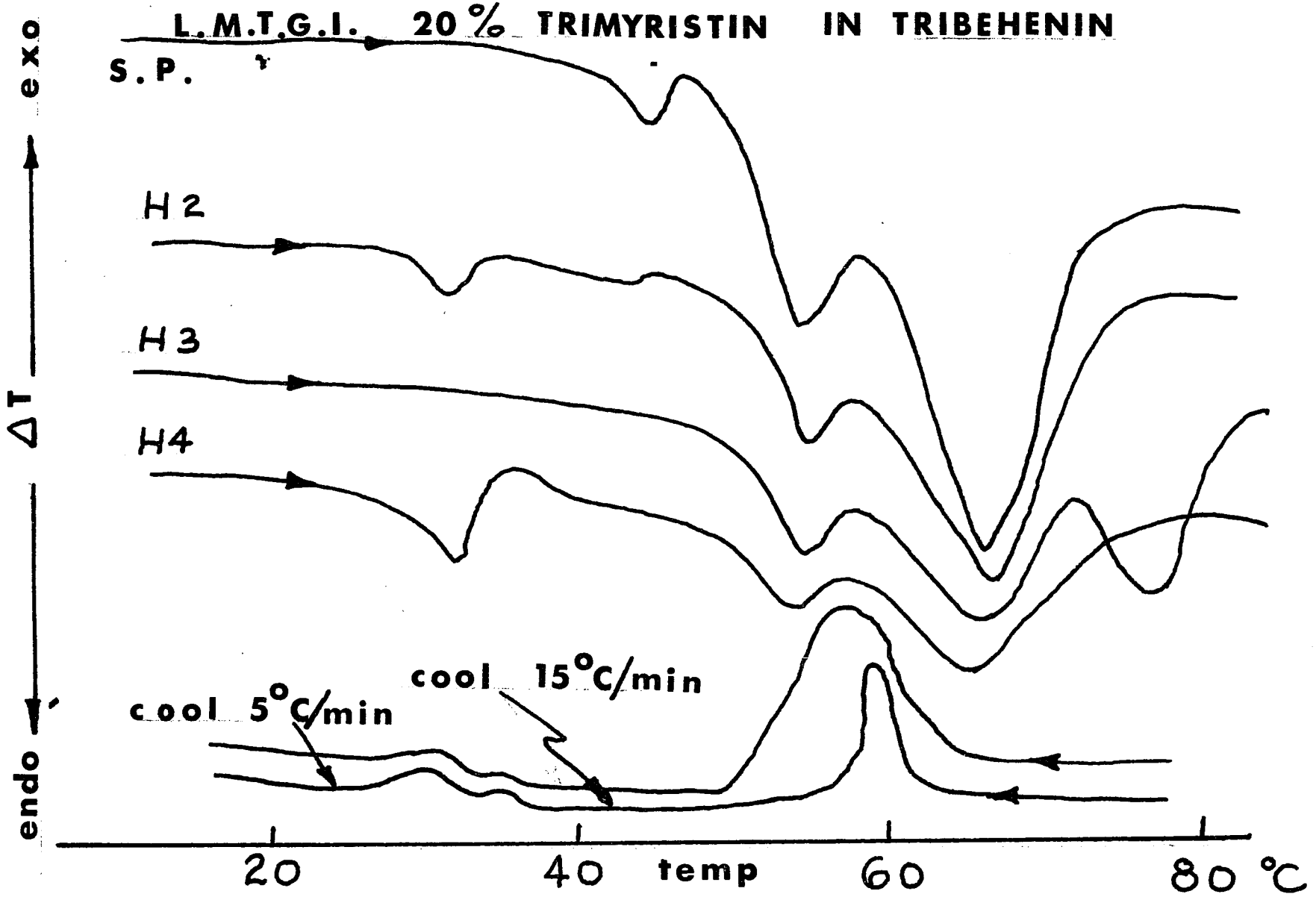
L.M.T.G.I. 20 % TRIMYRISTIN IN TRIBEHENIN
S.P.
H2
H3
H4
cool 5°C/min
cool 15°C/min
exo
endo
ΔT
20
40
temp
60
80 °C

systems. Essentially the following interesting effects should be noted:

1. The LMTGI appear to form rather easily in B' form when solvent prepared. The B' form of the bulk phase also forms more readily during a transition from the α polymorph. The thermogram of the pure triglyceride would generally show little β' when a transformation from α occurs.
2. A definite shift in the α exotherm DTA peaks occurs as a function of the trilaurin impurity concentration. Use of higher melting triglycerides as an impurity does not exhibit a significatnt peak shift.
3. Recrystallization of the α bulk phase is ~10°C below transition point for cooling rates between 5-15°C/min.
4. The change in properties (shift of DTA peaks, disappearance of a peaks) of the triglyceride upon the addition of LMTGI does not appear to be colligative in nature but rather dependent on the triglycerides used. For instance the α polymorph of triarachidin or tribehnin can be prevented from forming when trilaurin in excess of 15 weight per cent is used as an impurity. Otherwise adding trimyristin in excess of 25% does not completely eliminate the α forms of the larger triglycerides.
5. Addition of HMTGI does not drastically affect the DTA thermogram of the lower melting triglyceride.

systems. Essentially the following interesting effects should be noted:

1. The LMTGI appear to form rather easily in B' form when solvent prepared. The B' form of the bulk phase also forms more readily during a transition from the α polymorph. The thermogram of the pure triglyceride would generally show little β' when a transformation from α occurs.
2. A definite shift in the α exotherm DTA peaks occurs as a function of the trilaurin impurity concentration. Use of higher melting triglycerides as an impurity does not exhibit a significatnt peak shift.
3. Recrystallization of the α bulk phase is ~10°C below transition point for cooling rates between 5-15°C/min.
4. The change in properties (shift of DTA peaks, disappearance of a peaks) of the triglyceride upon the addition of LMTGI does not appear to be colligative in nature but rather dependent on the triglycerides used. For instance the α polymorph of triarachidin or tribehnin can be prevented from forming when trilaurin in excess of 15 weight per cent is used as an impurity. Otherwise adding trimyristin in excess of 25% does not completely eliminate the α forms of the larger triglycerides.
5. Addition of HMTGI does not drastically affect the DTA thermogram of the lower melting triglyceride.

c. Microspectrophotometry

The aging process of triglyceride mixtures maybe conveniently monitored by using the microspectrophotometer previously described. In addition D.T.A. and X-Ray determinations are also incorporated in the study to identify which phase the α form ages to.

Plots of absorbance versus wavelength of incident light were made of the glass microscope slides and of the various triglyceride materials sandwiched between the two slides. This enabled one to determine the optimum wavelength at which the absorbance due to the triglyceride was greater than the glass slides themselves. 320 mm appears to exhibit this optimum.

The results shown on Figure XXXIV indicate that aging of the alpha phase depends not only on the ΔT_E but also on the amount of triglyceride impurity and the nature of the particular triglyceride. LMTGI in general appear to enhance α stability for low concentrations. Trilaurin increases this stability up to a concentration of 15%. For trimyristin stabilization of the α phase was seen up to 26%. Above these concentrations the base triglyceride fails to form any α phase. This was observed in the D.T.A. studies, section B. Here again HMTGI impurities did not appear to affect the physical aging of the alpha phase at all.

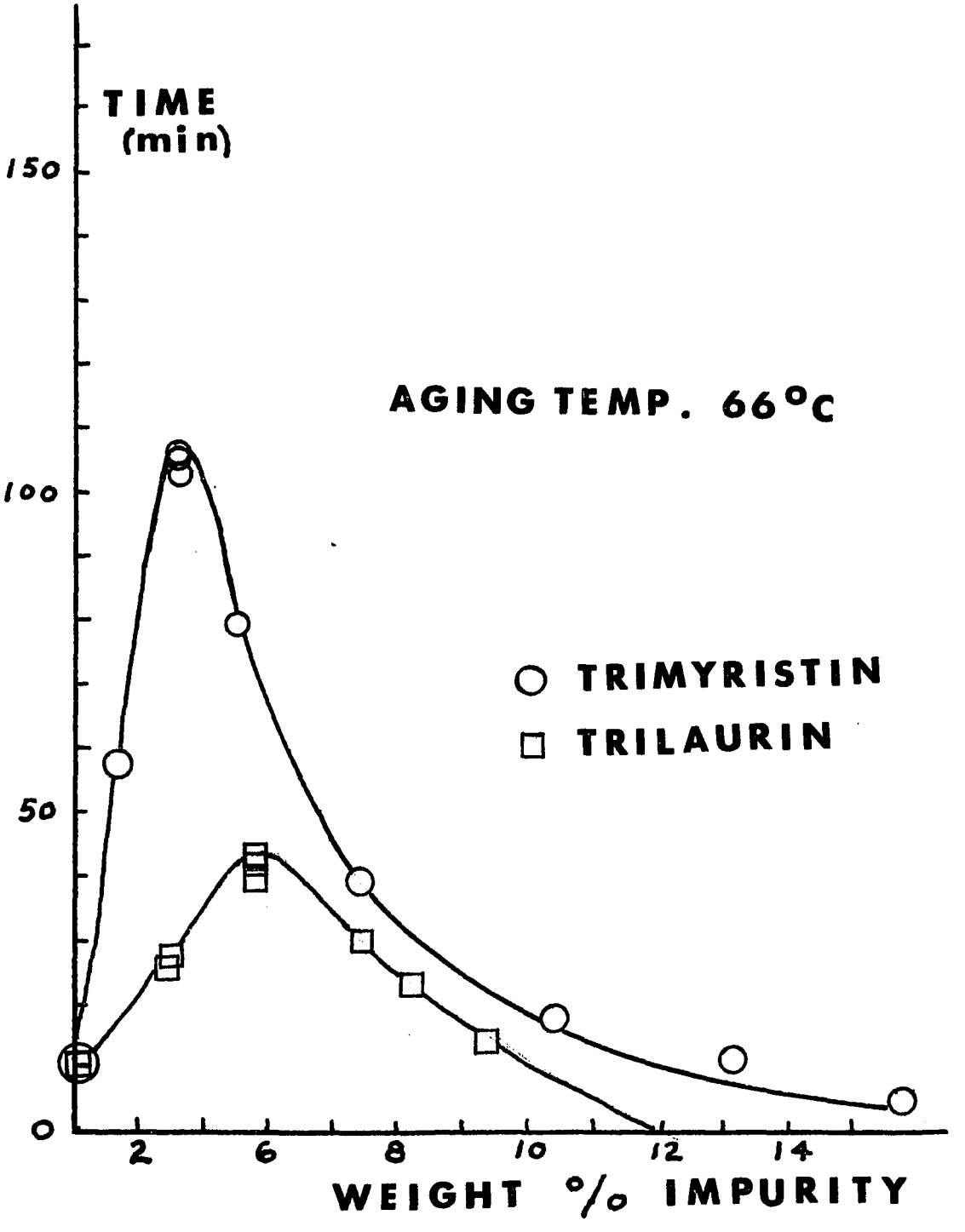

Figure XXXIV

Discussion

This study demonstrates that mixtures of triglycerides generally behave differently than the pure triglycerides. More specifically it is the Low Melting Triglyceride Impurities which alter the texture, phase properties and stability of the triglyceride.

From this evidence it is speculated that the reason the LMTGI are much more influential in altering these properties results from the increased mobility of these molecules in the crystal lattice. This accounts for the broader melting points and the α exotherm shift with increasing LMTGI.

The enhanced stability of the α polymorph at low concentrations of LMTGI is evidence of mixed crystal formation. Bailey (98) in his monograph series on fats and oils sites several examples of crystal habit differences in mixtures. Piper and co workers (99) studied the crystal habits of pure saturated fatty acid mixtures and reported various physical differences including melting point minimums for certain binary mixtures.

Chapter 5

Nucleation of Saturated Monoacid Triglycerides

5.1 Nucleation

It is known that a liquid can exist for a long time at a temperature well below its melting point. Triglycerides are no exception to this rule. Generally a condition that must be satisfied in order to supercool a liquid is that none of the solid be present.

At any temperature below that of equilibrium, the free energy of the solid is less than that of the liquid, this is a consequence of the thermodynamics of equilibrium. In the case of triglycerides the matter is further complicated since more than one solid phase may form. Furthermore the phase may or may not be thermodynamically stable.

According to standard nucleation theory, (See Section 1-3), the stability of a nucleus in an undercooled liquid depends on two factors: free energy of the liquid and the surface area of the solid. The free energy of the liquid decreases when it transforms to solid however for very small particles, the surface area is large relative to the volume so that the surface energy term dominates. Small particles can decrease the total free energy of the system (liquid plus particles) by shrinking and reducing their surface area. Large particles can reduce the free energy of the system by growing and creating more crystal. A balance between these tendencies defines the critical nucleus.

The change in free energy of the system due to a spherical particle of radius r as derived in section

1-3 is given by

$$G = -4/3\ \pi r^3 \Delta G_v + 4\pi r^2 \gamma \qquad 5\text{-}1$$

where ΔG_v is the difference between the volume free energy of the liquid and solid and γ is the specific surface free energy.

The basis for the rate of formation of nuclei having the given critical size has also been discussed in section 1-3. Many scientists have used this general relation for specific applications on the nucleation of crystals (86-89). Among the best known works are those of Turnbull 990) who using transition state theory developed an expression for the rate of homogeneous nucleation in condensed systems. His steady state nucleation rate per unit volume is given by:

$$dn/dt = N_o \exp(-E_d/RT)\exp(-\Delta G^{\ddagger}/RT) \qquad 5\text{-}2$$

where E_d is the free energy of activation for transport across a liquid nucleus boundary $\Delta G^{\ddagger}$ is the free energy change associated with nucleus formation and $N_o = M_o kT/h$ where M_o is the number of molecules per unit volume in the liquid, h is Blanck's constant and k is Boltzmann's constant. See Appendix III for derivation.

According to this theory, the nucleation is essentially controlled by two different rate processes. A plot of nucleation rate vs $1/T$ will give a maximum. At

temperatures below the nucleation rate maximum the process is diffusion or viscosity controlled. In this region, the molecules at the liquid crystal-crystal interface have enough energy to be activated (to cross an energy barrier to the face of the crystal); however, the microscopic viscosity of the medium retards this molecular realignment. At temperatures above the rate maximum, the microscopic viscosity of the medium is low enough so as not to be rate limiting and the thermal barrier becomes rate limiting.

Equation 5-2 may be further rewritten as:

$$dn/dt = I_o \exp\left[-b/T_r(\Delta T_r)^2\right] \qquad 5\text{-}3$$

where

$$I_o = M_o \frac{kT}{h} \exp\left(-E_d/RT\right) \qquad 5\text{-}4$$

$$b = 8\pi\left(\frac{\gamma}{L}\right)^3\left(\frac{L}{kT_E}\right) \qquad 5\text{-}5$$

$$T_R = T/T_E \qquad \Delta T_r = \frac{T_E - T}{T_E} \qquad 5\text{-}6$$

γ = interfacial free energy

It should be noted that heterogeneous nucleation also contributes to the term. Therefore $\Delta G^{\ddagger}$ should be replaced by $f(\theta)\Delta G$ and $f(\theta)$ varies from 0 to 1.

Since there is no accurate way to determine $f(\theta)$ it is assumed to be 1.

5.2 Experimental

The triglyceride samples were placed in glass tubes (1.0 mm I.D.). The samples were then heated to the isotropic state in a water bath 20°C above the melting point of triglyceride for five minutes. This was to ensure that all nucleating sites had been destroyed. After rotating the glass tubes to produce a thin liquid coating on the tube walls. The samples were placed in a thermostated bath. The time was noted at the first visual sign of crystallization which almost always occurred at the liquid air interface. These measurements obviously contain a contribution from crystal growth since it is impossible to observe initially stable nuclei. In addition heterogeneous nucleation in the sample has not been taken into account however it is felt that neither effect will alter the general trend of data.

The correction for heat transfer from the sample tube to the bath was estimated from temperature profiles for unsteady state heat conduction in a slab of finite thickness (91). The time was negligible ($\sim$1 sec). See appendix IV.

5.3 Results and Discussion of the Nucleation of Triglycerides

The nucleation data for the various saturated triglycerides is presented in Figure XXXV. A number of interesting facts emerge from this information.

a) There was no maximum nucleation rate as mentioned in Turnbull's equation. This implies that the major barrier in the nucleation process is due to the thermal free energy of formation of a nucleus. The diffusion or viscosity controlled term Ed is negligible. Vonnegut (93) also found this to be the case in his nucleation study of tin. Skoda and Van den Tempel (94) in a study on the crystallization of emulsified triglycerides also claim Ed to be negligible compared to b.

b) Essentially two points of discontinuity (or three separate slopes) are observed for each nucleation curve. This implies that the crystallization rates from supersaturated solutions depend not only on the ΔT of supercooling but more importantly on the polymorphic phase which forms. In each triglyceride tested the α polymorph nucleated and crystallized much more rapidly for a given degree of supercooling than the β' or β did for an equivalent Δ T.

c) Increasing the chain length of the triglyceride increased the nucleation time for the α phase at a given degree of supercooling. A smaller affect was noted on the β phase.

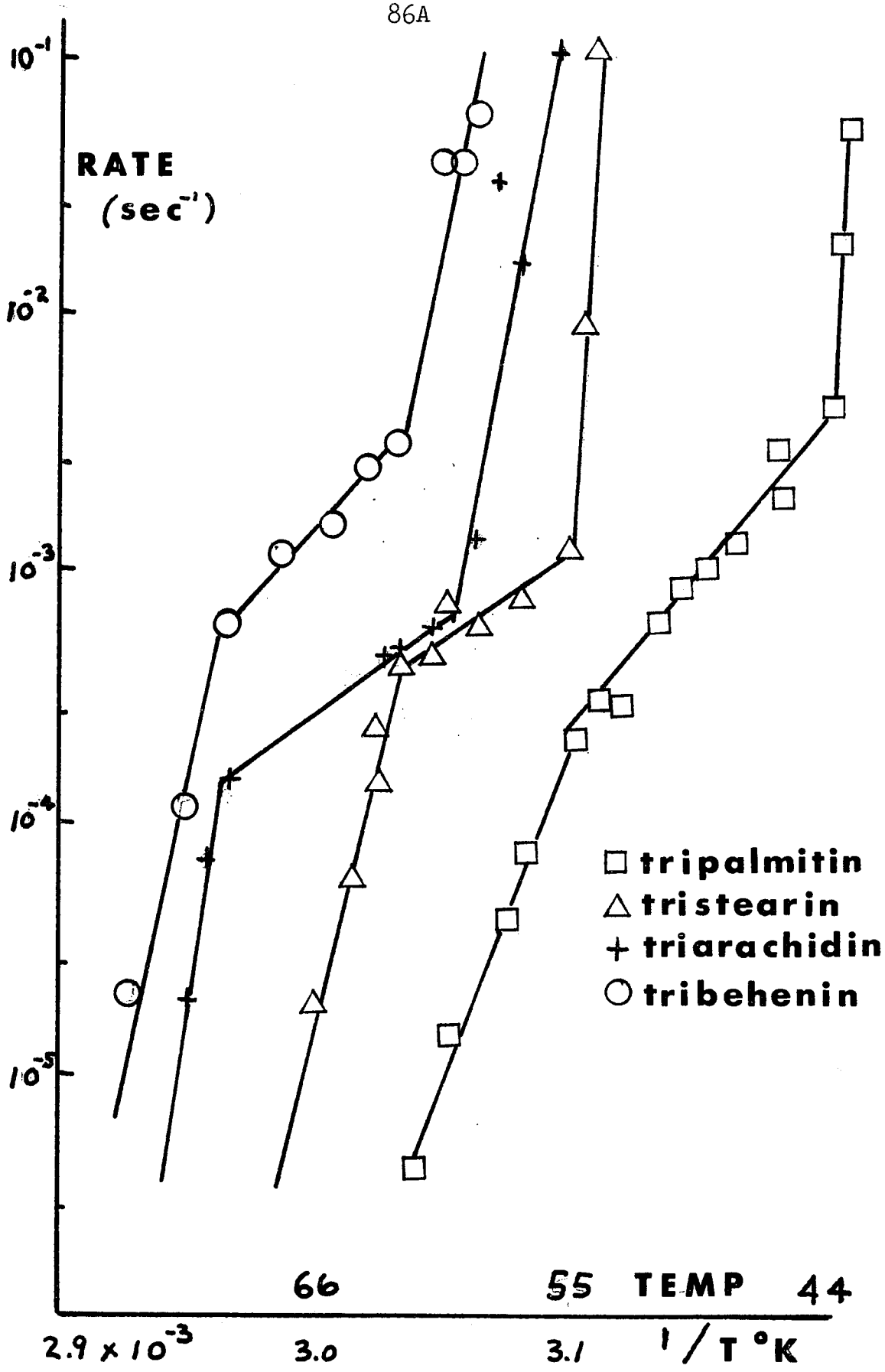
RATE
(sec⁻¹)
10⁻¹
10⁻²
10⁻³
10⁻⁴
10⁻⁵
tripalmitin
tristearin
triarachidin
tribehenin
66
55
TEMP
44
2.9 x 10⁻³
3.0
3.1
1/T °K

FigureXXXV

d) D.T.A. studies of various data points in the β' temperature range generally indicates that a mixture of β' and β or all β exists. A possible mechanism is that β' initially nucleates in that temperature region but transforms or ages to the β polymorph.

5.4 Estimation of Interfacial Free Energy

The β-liquid interfacial free energy may be estimated in theory from the nucleation equation 5-3 and the assumption that $dn/dt \sim 10^6$ cm $^{-3}$ sec $^{-1}$. This value was determined by Turnbull and serves as a reference for many estimates (95-97) of the number of nuclei formed per second per unit volume. To determine γ a graph of $\ln\left(\frac{\text{rate}}{T}\right)$ vs $\frac{T_e^2}{T\Delta T}$, Figure XXXVI is developed. The temperature T in the logarithmic term is due the pre exponential factor. Computing the slope yields b. γ is found by rewriting 5-5.

$$\gamma = \sqrt[3]{R\, b\, \rho^2 (\Delta H)^2 / 8\pi} \qquad 5\text{-}7$$

A compilation of results are summarized in Table
The values of γ show a slight decrease with decreasing chain length, which should be expected since the smaller chain triglycerides nucleate much more rapidly in the β form.

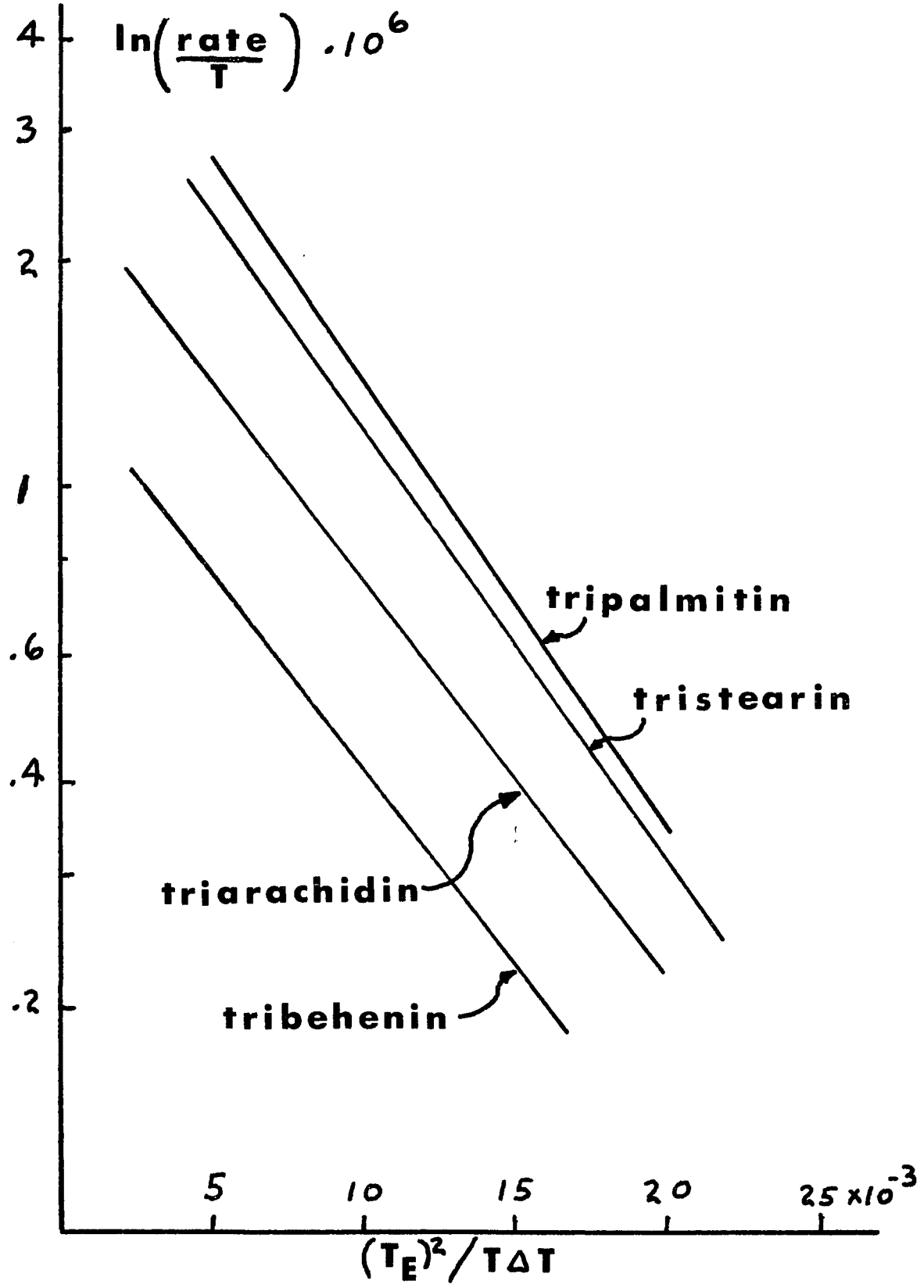

FigureXXXVI

Table VII

Estimated Surface Free Energy at the β/Liquid Interface

Compound	Chain Length	ΔH_f B form	ρ gms/cc	γ ergs/cm^2
Tribehenin	C_{22}	59.1	.830	17.4
Triarachidin	C_{20}	54.6	.843	16.8
Tristearin	C_{18}	51.4	.856	15.2
Tripalmitin	C_{16}	49.0	.875	14.6

5.5 Kinetics of α Phase Formation

In section 4.4 a schematic was developed on the types of polymorphic transformations which occur with saturated monoacid triglyceride. It was further indicated that not all transformations are reversible. Another question which one may ask is, What polymorphic phase forms most readily? The answer is usually vague (84-85) and generally indicates that a triglyceride on being cooled from the melt to below room temperature forms the α phase. This is the case only if the rate of cooling or solidification is fast enough..

One method to determine this rate is to use the temperature gradient microscope stage. The procedure is outlined as follows:

1. The reversible and variable DC Motor is calibrated i.e. rate of movement of stage vs. voltage.
2. The cell must be calibrated to determine the gradient during a constant rate of freezing and at a constant rate of melting. This must be done for each rate. The method is the same as that used to calibrate the cell at static equilibrium. (Figure X)
3. The system to be studied is placed on the stage and the solid/liquid interface is allowed to form. Due to the polymorphism that triglycerides exhibit one must be sure that a true solid/liquid

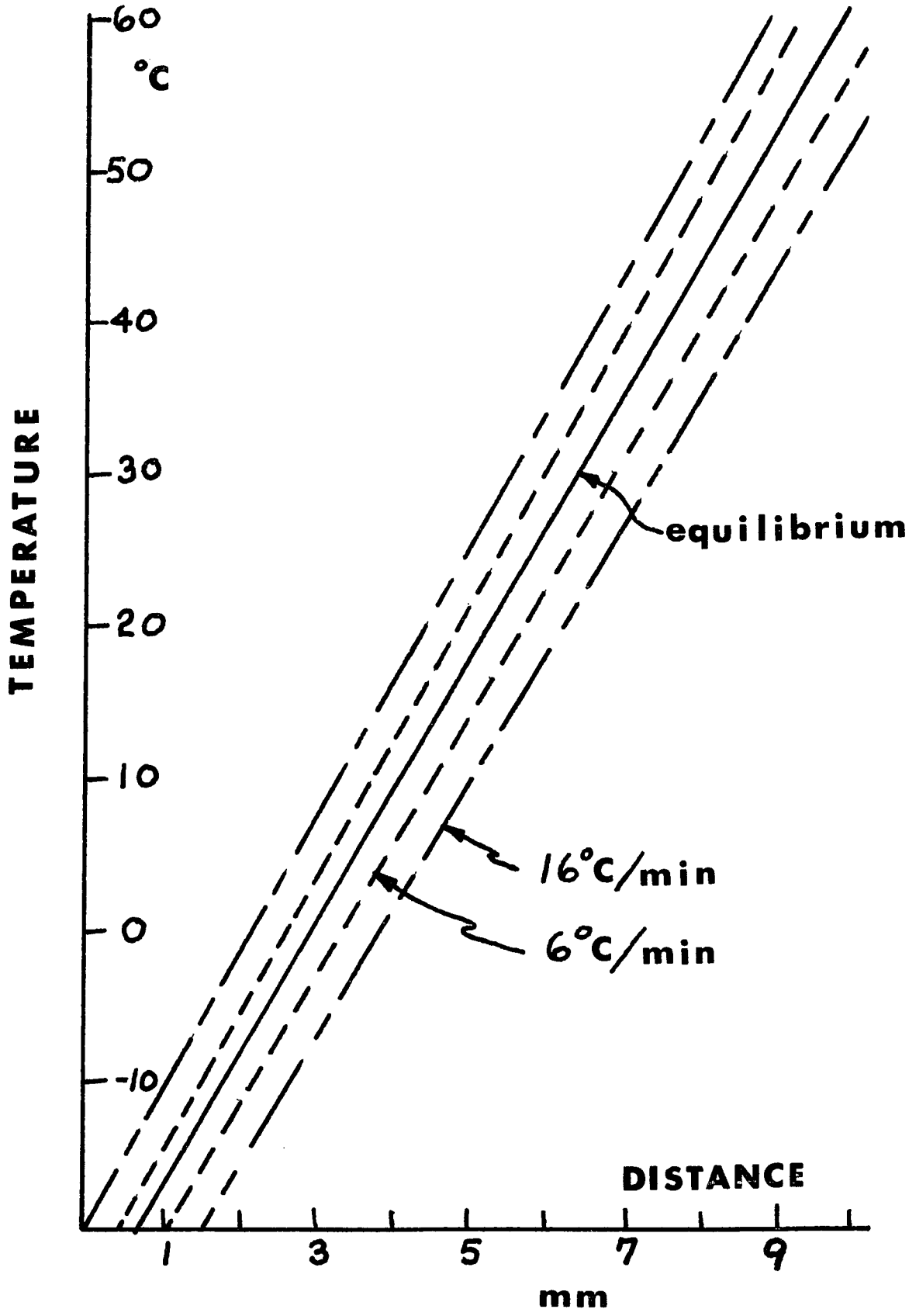
60
°C
50
40
30
20
10
0
-10
TEMPERATURE
equilibrium
16°C/min
6°C/min
DISTANCE
1
3
5
7
9
mm

Figure X

interface really exists and not a solid/solid or solid/liquid/solid nucleating site interface.

4. The system is then solidified or melted at a given date.
5. One can observe the solid changes by observing the system through cross polars.

Results and Discussion

The pure monoacid triglycerides were studied at five separate rates of freezing and thawing.

At a freezing rate of 2° C/min only tribehenin and triarachidin would form an alpha phase from the melt. At a freezing rate of 4°C/min tristearin would form the alpha phase. Tripalmitin appears to form a mixture of alpha and beta crystals. When the rate was increased to 6°C/min only alpha crystals were observed for the tripalmitin. At a rate of 14°C tripalmitin definitely formed the α spherulites. Trilaurin seemed to form the α phase when the rate of freezing was on the order of 16°/min (See Figure XXXVI)

It should be emphaxized that unlike many systems the triglycerides crystallize in more than one form and therefore not only will the rate depend on the degrees of supercooling but also the various phases. For instance at 2°C/min trilaurin and trimyristin did not even crystallize at -10°C. At a rate of 6°C min crystals were seen but they were not defined as alpha crystals. When the alpha crystals did form the degree of supercooling was on the order of -5°C $\pm$ 3°.

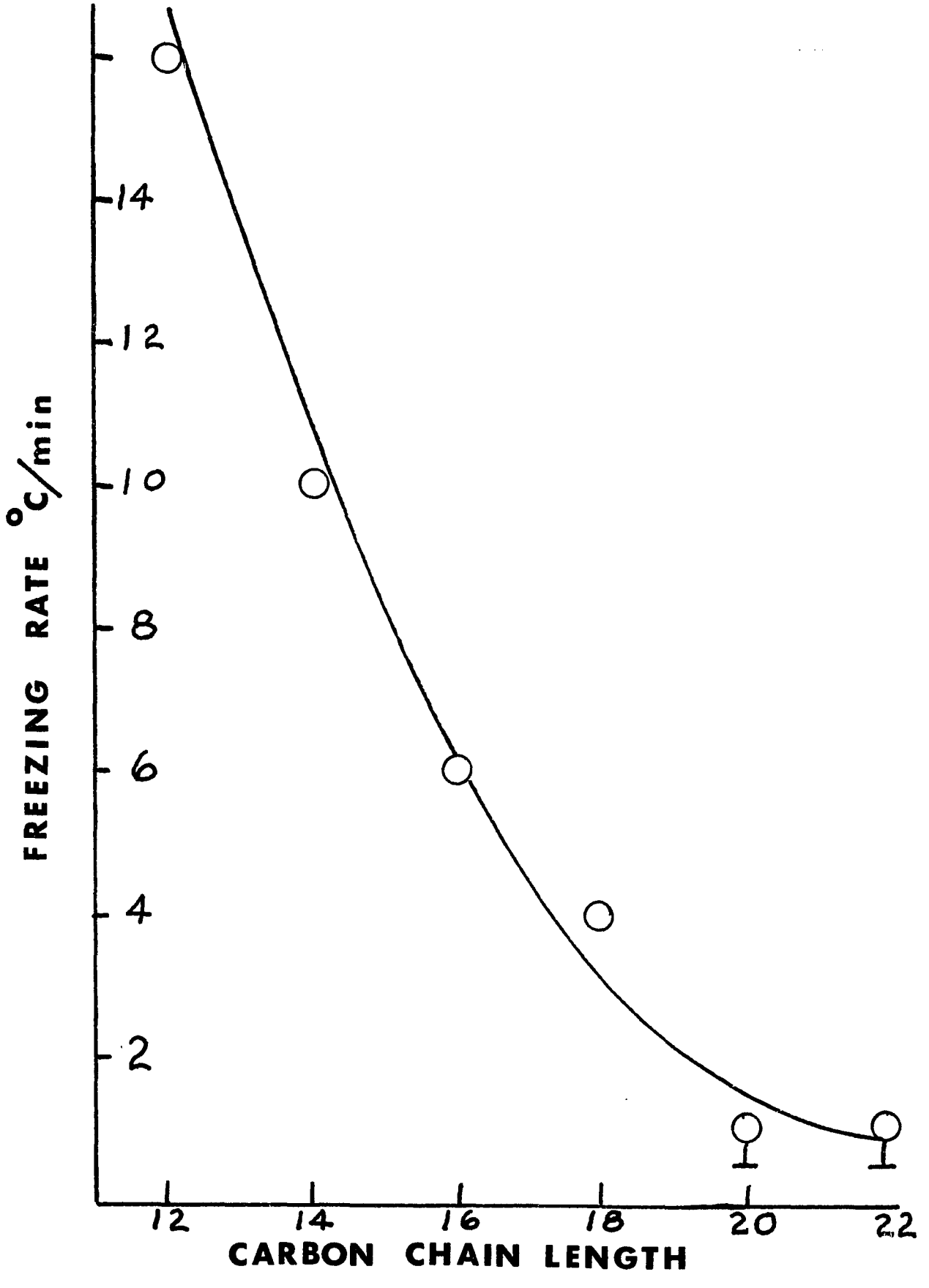

Figure XXXVII

From Figure XXXVII it is obvious that the α phase forms readily for the higher melting triglycerides. On the other hand trilaurin and trimyristin must be cooled considerably fast. This is why Lutton's (84) formulation for producing the α phase is to solidify the melt rapidly to approximately 20°C below the alpha transition temperature. The importance of this information is that the rate of solidification may be used as a means of producing only α polymorphs or eliminating this metastable phase from forming at all.

Chapter VI

Epilogue

The understanding of phase transformations and the solid/liquid interface has progressed immeasurably since Willard J. Gibbs' early thermodynamic treatment of phase equilibria. However, in order to investigate and prove experimentally the various theories in this field it must be possible to differentiate and separate problems of heat transfer from the actual physical problem. Unless this is accomplished three dimensional heat transfer problems will obscure any experimental observation. The work presented in this dissertation has differentrated this problem and allows one to observe the importance of the solid/liquid interface in three vital areas of concern.

A. Aqueous Solutions

Freezing of aqueous systems although simple in first thoughts is extremely complex on the molecular level. To elucidate these complexities a unique microscope stage for studying the freezing and freeze drying processes was developed. Using this stage it was possible to study dendrite growth as a function of concentration and the rate of freezing. Usually only two variables (diffusion and concentration) are taken into consideration when considering dendrite growth. This study has demonstrated that the heat extraction from the interface and associated or bound water play a significant role in interface structure.

The peak to peak distances for non electrolyte solutes has been found to be directly proportional to the rate of

freezing and concentration. Data on the peak to peak distances for salt solutions agrees with that of Rohatgi and Adams (36) ie. proportional to (rate) $^{-\frac{1}{2}}$.

B. Enzyme Systems

The activity of α amylase was found to be dependent on the rate of freezing, rate of thawing, and the concentration of various solutes. Evidence is presented which indicates that small concentration (10^{-3}%) of protective agents actually harm an enzyme. It is speculated that this is due to increased solute enzyme and enzyme-enzyme interactions at the solid/liquid interface.

C. Triglycerides

This final area of study is concerned with phase transformations, and the kinetics of phase transformations. It is known industrially that fatty materials may physically age rather than a chemical breakdown. However the how's and why's of this breakdown is not known.

Using the temperature gradient technique incorporated with x-ray diffraction pattern, D.T.A., Infra red spectra and wide line nuclear magnetic resonance it can be conclusively proven that the α and β' polymorphs of saturated triglycerides are thermodynamically unstable and their formation depends on the kinetics of solidification.

Further experimentation has yielded quantitative information regarding the stability of the alpha polymorph below its transition temperature. The implications of these

observations helps explain why many fatty materials (confectionary products, chocolate products, fat emulsions) will loose the physical properties they originally exhibited as a function of time and temperature even though their is no chemical degradation.

To prevent any unwanted transformation the object is to prepare the fat constituents in their most stable form. This may be accomplished (as seen in Chapter IV) by solidifying the fat at a slow enough rate or adding low melting point impurities (LMTGI) to the base fat. In the event it is desired to enhance the lifetime of the unstable polymorph, certain small concentrations of LMTGI are added.

Nucleation data for these triglycerides has shown that the α polymorph forms more rapidly than either the β' or β form for a given ΔT_E below the transition temperature and for a fast enough rate of freezing.

The technological importance of these findings are vast since it pinpoints the reasons why certain materials may physically age in the solid state and why certain physical processes may prevent this aging to occur at all.

Appendix

APPENDIX I

EMBRYO GEOMETRY

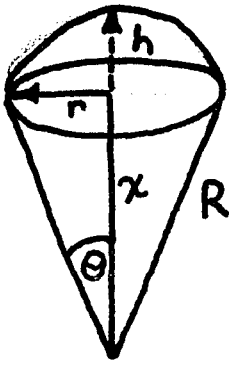

$$h + X = R$$
$$X = R\cos\theta$$
$$\therefore \quad h = R(1-\cos\theta)$$
$$r = R\sin\theta$$

$$V_{CAP} = \frac{1}{3}\pi h^2(3r-h)$$
$$= \frac{1}{3}\pi R^3(2-3\cos\theta+\cos^3\theta)$$

$$A_{CAP} = 2\pi r h = 2\pi R^2(1-\cos\theta)$$

$$A_{UNDER\ CAP} = \pi r^2 = \pi R^2\sin^2\theta$$

APPENDIX II

$$\Delta S_1 = k \ln P$$

WITH

$$P = \frac{N!}{N_A!\,(N-N_A)!}$$

USING STERLING APPROXIMATION

$$\Delta S_1 = k N \ln \frac{N}{N-N_A} + k N_A \ln \frac{N-N_A}{N_A}$$

APPENDIX III

ASSUMING BECKER'S APPROXIMATION FOR NUCLEATION RATE IN CONDENSED SYSTEMS (i.e. LIQUID - SOLID OR SOLID - SOLID)

$$I^* = K \exp\left[-(\Delta F_i^* + q)/kT\right]$$

ΔF_i^* - CRITICAL FREE ENERGY

q - ENERGY OF ACTIVATION FOR DIFFUSION

THE STEADY STATE I CORRESPONDS TO CONSTANT EQUAL NET FORWARD RATES

$$m\alpha_1 \rightleftharpoons \beta_m$$
$$\beta_m + \alpha_1 \rightleftharpoons \beta_{m+1}$$
$$\beta_{m+1} + \alpha_1 \rightleftharpoons \beta_{m+2}$$
$$\vdots$$

$\alpha \equiv$ ATOM OF PHASE α

$\beta_i \equiv$ NUCLEUS OF i ATOMS

CONSIDER THE FORWARD REACTION

$$\beta_i + \alpha_1 \longrightarrow \beta_{i+1}$$

THEN $$I_f = n_i a_1 i^{2/3} \left(kT/h\right) \exp\left(-\frac{\Delta f_i^*}{kT}\right)$$

WHERE $a_1 i^{2/3}$ = NUMBER OF α ATOMS IN CONTACT WITH A β NUCLEUS $i^* = i^{2/3}$

AND $\left(\frac{kT}{h}\right) \exp(-\Delta f_i^*/kT)$

IS THE SPECIFIC REACTION RATE

THE RATE OF THE REVERSE REACTION

$$\beta_{(i+1)} \rightarrow \beta_i + \alpha_1$$

$$r^- = n_{i+1}\, a_2\, i^{2/3} \left(\frac{kT}{h}\right) \exp(-\Delta f_2^*/kT)$$

$\therefore$ THE NET FORWARD REACTION IS

$$r^* = r^+ - r^- = \left(\frac{kT}{h}\right) i^{2/3} \left[n_i a_1 \exp(-\Delta f_1/kT) - n_{i+1} a_2 \exp(-\Delta f_2/kT) \right.$$

TURNBULL AND FISHER J. CHEM PHYSICS 17, 71, (1949) MAKE THE FOLLOWING ASSUMPTIONS

① THE NUMBER OF α ATOMS IN CONTACT WITH β_i NUCLEUS IS NOT EQUAL TO THE β ATOMS IN CONTACT AT THE α SURFACE

② n_i AND ΔF_i ARE SMOOTH FUNCTIONS

③ $\frac{1}{kT} \frac{d(\Delta F_i)}{di}$ and $\frac{1}{n_i} \frac{dn_i}{di}$ ARE SMALL

THE $\Delta f_1^* = \Delta f^* + \frac{1}{2} d(\Delta F_i)/di$

$\Delta f_2^* = \Delta f^* - 1/2\, d(\Delta F_i)/di$

REWRITING r^* AND DEFINING R

$= r^* \left(\frac{\omega kT}{h}\right) \exp(-\Delta f^*/kT)$

$$\frac{d\, n_i}{di} + \left(\frac{2}{3} A_i^{-1/3} - B\right) n_i = -R\, i^{-2/3}$$

SOLVING FOR n_i WITH THE BOUNDARY CONDITIONS

$$\lim_{i \to \infty} \exp(-\Delta F_i/kT) = \infty$$

$$\lim_{i \to \infty} n_i = 0$$

AND REPLACING $\Delta F_i/kT$ BY A TAYLOR SERIES

$$r^* \approx \left(\frac{NkT}{h}\right) \exp\left[-(\Delta f^* + \Delta F^*)/kT\right]$$

USING THE INTIAL CONDITIONS AND INTEGRATING

$$\frac{T_1 - T}{T_1 - T_0} = 2 \sum_{n=0}^{\infty} \frac{(-1)^n}{(n+\frac{1}{2})\pi} e^{-(n+\frac{1}{2})^2 \pi^2 \alpha t / b^2} \cos (n+\tfrac{1}{2}) \frac{\pi y}{b}$$

THIS EQUATION HAS BEEN GRAPHICALLY PLOTTED BY H. CARSLAW AND J. JAEGER - CONDUCTION OF HEAT IN SOLIDS, OXFORD PRESS (1959)

KNOWING Θ, b AND α t MAY BE SOLVED FOR.

APPENDIX IV

FOR SOLIDS, THE ENERGY EQUATION AFTER INSERTION OF FOURIER'S LAW OF HEAT CONDUCTION IS

$$\rho C_p \frac{\partial T}{\partial t} = (\nabla \cdot K \nabla T)$$

ASSUMING THERMAL CONDUCTIVITY IS INDEPENDENT OF TEMPERATURE AND POSITION

$$\frac{\partial T}{\partial t} = \alpha \nabla^2 T \; ; \quad \alpha = \frac{k}{\rho C_p}$$

IF THE WALL OF THE SAMPLE TUBE IS ASSUMED TO BE A FINITE SLAB THEN THE FOLLOWING DERIVATION IS TRUE:

DEFINE DIMENSIONLESS TERMS

$$\Theta = \frac{T_1 - T}{T_1 - T_0} \qquad \text{TEMP.}$$

$$\eta = \frac{y}{b} \qquad \text{LENGTH}$$

$$\Gamma = \frac{\alpha t}{b^2} \qquad \text{TIME}$$

THEN $$\frac{\partial \Theta}{\partial \tau} = \frac{\partial^2 \Theta}{\partial \eta^2}$$

INTIAL COND @ $\tau = 0$ $\Theta = 1$

BOUND COND @ $\eta = \pm 1$ $\Theta = 0$

BY CLASSICAL SOLUTION METHODS ASSUME

$$\Theta(\eta, \tau) = f(\eta) g(\tau)$$

THEN BY SEPARATION OF UARIABLES

$$\frac{1}{g}\frac{dg}{d\tau} = \frac{1}{f}\frac{d^2 f}{d\eta^2}$$

SOLVING $$\frac{dg}{d\tau} = -c^2 g \Rightarrow g = A \exp(-c^2 \tau)$$

$$\frac{d^2 f}{d\eta^2} = -c^2 f \Rightarrow f = B \sin c\eta + C \cos c\eta$$

APPLYING B C

$$\Theta_n = A_n C_n e^{-(n+1/2)^2 \pi^2 \tau} \cos(n+\tfrac{1}{2})\pi\eta$$

THE MOST GENERAL SOLUTION IS FOUND BY Σ FOR ALL n FROM $-\infty \rightarrow +\infty$

$$\Theta = \sum_{n=0}^{\infty} D_n e^{-(n+\frac{1}{2})^2 \pi^2 \tau} \cos(n+\tfrac{1}{2})\pi\eta$$

$$D_n = A_n C_n + A_{-(n+1)} C_{-(n+1)} .$$

REFERENCES

1. Gibbs, J. W.; Scientific Papers, Vol I, Dover, New York (1961)

2. Chalmers, B.; Trans. A.I.M.E. 200 519 (1954)

3. Frenkel, J.; Kinetic Theory of Liquids, Oxford University Press London (1946)

4. Pound, G. M.; Liquid Metals and Solidification A.S.M. Cleveland (1958)

5. Kanenelskaga, D.S.; Reports at the First Conference on Crystal Growth. USSR 4 March 10, (1956)

6. Jackson, K. A.; Growth and Perfection of Crystals; Wiley 1958 p.319.

7. Burton, W.K.; Cabrerra, N.; Franck, P.; Trans. Roy.Soc. 243 209 (1951)

8. Burton, W.K.; Cabrerra, N.; Disc. Faraday, Soc. 5 33 (1949)

9. Mullins, W. W.; Acta. Met. 7 786 (1959)

10. Jackson, K. A.; Liquid Metals and Solidification; ASM Cleveland 1958 (p. 174)

11. Jackson, K. A.; Acta Met. 7 148 (1959)

12. Turnbull, D.; Thermodynamics in Physical Metallurgy. Am. Soc. for Metals Cleveland (1958) p. 282

13. Wilson, H. A.; Phil. Mag. 50 238 (1900)

14. Frenkel, J.; Physik. Z der Soviet Union 1 498 (1932)

15. Chalmers, B.; Jackson, K.A.; Can J. Phys. 34 473 (1956)

16. Pfann, W.G.; Zone Melting; J. Wiley & Sons, N.Y. (1958)

17. Tiller, W.A.; Liquid Metals and Solidification; Am. Soc. of Metals, Cleveland (1958)

18. Rutter, J. W.; Chalmers, B.; Jackson, K.A.; Tiller, W.A.; Con. J. Phys. 31 15 (1953)

19. Walton, J.H.; Judd, R.C.; J. Phys. Chem. 18 725 (1914)

20. Harrison, J.D.; Tiller, W.A.; Nat. Acad. Sci. Nat. Res. Publ. #942 312-316 (1963).

21. Macklin, W.C.; Ryan, B.F.; Phil. Mag. 14 30 (1966)

22. MacKenzie, A.P.; Proc. Int. Conf. on Refrig. Munich Annals N.Y. Acad. Sci. 125 522 (1965)

23. Chaufford, F.; Revue Generale du Fiord 15, 8 1967

24. Hunt, J.D.; Jackson, K.A.; Brown, H.; Rev. Sci. Instru. 37 6 (1966)

25. Roehl, E.; Soap and Per. Cos. 45 343 (1972)

26. Rosano, H. L.; Whittam, J.H.; Freedman, M.: Journal of Food Science 37 492 (1972)

27. Brescia, F.; Arents, J; Meislich,H.; Turk, A.; Fundamentals of Chemistry A Modern Introduction Academic Press N. Y. (1967) p.384

28. Papatreou, A.; Z von Kristallographie 92 89 (1935)

29. Macklin W. C.; Ryan, B; Phil. Mag. 14 # I 30 (1966)

30. Ivantson G.P.; Growth of Crystals (Consultants Bureau Inc.) I p. 76 (1958)

31. Horvay, G.; and Cahn, J.W.; Acta Met. 9 695 (1961)

32. Bolling, G. F.; Tiller, W.A.; J. Appl. Physics 32 2587 (1961)

33. Weast, R.; Handbook of Chemistry & Physics, Chemical Rubber Co. (Ohio) (1972) F 47

34. Kahn, A.; and Philibert, J.; Revue de Metallurgie 14 303 (1960)

35. Tiller. W.A.; and Rutter J.W. Westinghouse Scientific Paper No 60-8-08- P W East Pittsburgh, Pa.

36. Rohatgi, P.; and Adams Jr. C.L.; AIME 239 1729 (1967)

37. Melnick, J.; Cryobiology 1 2, 140 (1964)

38. Neurath, H.; Cooper. G. R.; and Erickson, J. O.; J Biol. Chem. 142 249 (1942)

39. Bruce, T.C.; and Butler, A.R.; Fed. Proc. 24 Suppl. 15 S-45 (1965)

40. Finn, D. B.; Proc. Roy. Soc. B 111 396 (1932)

41. Lovelock, J.E.; Proc. Roy. Soc. B 147 427 (1957)

42. Klotz, I. M.; Fed. Proc. 24 S-24 (1965)

43. Chilson, O.P.; Costello, L.A.; Kaplan, N.C.; Fed. Proc. 24 Suppl 15, S-55 (1965)

44. Keith, S. C.; Science 37 877 (1913)

45. Kavanau, J.L.; Water and Water Solute Interactions Holden Day San Francisco (1964)

46. Frank, H.S. and Evans, M.J.; J. Chem. Phys. 13 507 (1945)

47. Nash, T.; Gen. Physical, 46 167 (1962)

48. Doebbler, F.G.; and Infret, A.P.; Biochem. Biophys. Acta 58 499 (1962)

49. Prigogine, I.: The Molecular Theory of Solutions p 305-322 Interscience Pub. N.Y. (1957)

50. Rowlinson, J.S.; Liquids and Liquid Mixtures, Butterworths, London (1959)

51. Rowlinson, J.S.; In Hydrogen Bonding, D Hadzi ed. p 423-27 Pergamon Press N.Y. (1959)

52. Podolsky, R.J. J.A.C.S. 80 4442 (1958)

53. Merryman, H.T.; Cryobiology 8 173 (1971)

54. Heber, U.; Cryobiology 5 188 (1968)

55. Hanafusa, N.; Int. Conf. Low Temp. Sci. 2 33 (1967)

56. Kaplan, N.O.; Brookhaven Nat. Lab. 2 215 (1964)

57. Market C.L.; Science 140 1329 (1963)

58. Greiff, D.; and Kelly, R.; Cryobiology 2 335 (1966)

59. Chilson, O.P.; Costello, L.A.; and Kaplan, N.O.; Fed. Proc. 24 555 1965

60. Ashwood-Smith, M.J., and Warby C.; Cryobiology 9 137 (1972)

61. Doebbler, G.F.; Cryobiology 3 2 (1966)

62. Lovelock, J.E.; and Bishop, M.W.; Biochem J 56 265 (1954)

63. Luget, B.S. and Keane J.F.; Biodynamics 7 119 (1952)

64. Heber, U.; Cryobiology 5 188 (1968)

65. Mayar, P.; Science 168 939 (1970)

66. Wagner,R Trans. A.I.M.E. 200 154 (1954)

67. Heintz, W.; Jahresber. 2 349 (1849)

68. Duffy, P.J.; J Chem Soc. 5 197 (1853)

69. Besthelot, M.; Liebigs Annalen der Chemie, 88, 304 (1853) 92, 301 (1854)

70. Guth, F.; Z Biology 44, 78 (1902)

71. Lantz, H., Z Phys. Chem. 84, 611 (1913)

72. Weygand, C.; Gruntzig, W.Z.; Anorg. Chem. 206, 304 (1932)

73. Malkin, T.; Clarkson, J.; J. Chem. Soc. 666 , (1934)

74. Clarkson And Malkin, JACS, 60 985 (1948)

75. Ravich, C., Zurinov, Volnova and Petrov; Act Physicochimica 21, 101 (1946)

76. Lutton, E.S.; JACS, 67, 524 (1945)

77. Bailey, A.E.; Jefferson, M.E.; Kreeger, F.B.; and Bauer, S.T.; Oil and Soap 22 10 (1945)

78. Chapman, D.; J Chem. Soc. 56 2524 (1956)

79. Santoro, A.; Esposito, M.; J Thermal. Anal. 6 101 (1974)

80. Barrall II, E.; Guffy, J.C.; Ordered Fluids and Liquid Crystals A.C.S. Series #63

81. Chapman, D.; Richards, R. E.; Yorke, R.W.; J Chem.Soc. 60 436 (1960)

82. Charbonnet, G.H.; and Singleton, W.S.; J.A.O.C.S. 6 140 (1947)

83. Vand, V. and Bell, I.P.; Acta Cryst. 4 104 (1951)

84. Lutton, E.S.; and Fehl, A.J.; Lipids 5 90 1972

85. Chapman, D.; Structure of Lipids. Wiley,New York, (1965)

86. Becker, R.; Doering,W.; Ann Physik 24 719 (1935)

87. Buckle, E.R.; Proc. Roy. Soc. London A261 189 (1961)

88. Volmer, M.; Flood,H.; Z Physik Chem A 170 273 (1934)

89. Turnbull, D.; Solid State Physics 3 225 (1956)

90. Turnbull, D.; Fisher, J.C.; J Chem Physics 17 71 (1949)

91. Bird, R.; Stewart, W.; Lightfoot, E.; Transport Phenomena p 356 Wiley, New York (1960)

92. N.R.C. International Critical Tables McGraw Hill Co. New York (1948)

93. Vonnegut, B.; Bull, Am. Met. Soc. 29 175 (1949)

94. Skoda, W.; Van den Tempel, M.; J.O.C.S. 18 568 (1963)

95. Pochan,J.M.; Gibson, H.W.; J.A.C.S. 93 1279 (1971)

96. Phipps, L.W.; Farad Soc. 60 1873 (1964)

97. Mandelkern, L.; Crystallization of Polymers, McGraw Hill N.Y. (1964) p.214

98. Bailey, A.E.; Melting and Solidification of Fats. Interscience Publishers (1950)

99. Piper, S. H.; Chibnail, A.C.; and Williams, E.F; Biochem J. 28 2175 (1934)

JAMES HENRY WHITTAM

Date of Birth: April 23, 1949
5' 11" 170lbs
U. S. Citizen

Home: 2031 Palmetto St.
Ridgewood, New York
11227
(212) VA. 1-8824

EDUCATION

College

The City University of New York
Doctor of Philosophy: Chemistry
June 1975

The City College of New York
Bachelor of Chemical Engineering
June 1972

High School

Brooklyn Technical High School
Academic Technical Diploma--Chemistry

Honors

Graduate

1. Curtman Award Recipient 1975
2. Myron Pantzer Award Recipient 1974
3. Member of Sigma XI

Under Graduate

Magna Cum Laude
Dean's list for four years
Honor Society: Tau Beta Pi (Engineering)
Omega Chi Epsilon (Chem. Engineering)

High School

Awarded three year Chemistry Medal June 1967
Member Arista

FIELD OF SPECIALTY

Physical Chemistry

Thesis: Solid/liquid Phase Transformation
Faculty Supervisor: Dr. Henri L. Rosano

EXPERIENCE

Summer 1969
Consolidated Edison Company of New York
4 Irving Place New York, N.Y. 10003
Production technician in chemical bureau of a power station.

Summer 1970
Consolidated Edison Company of New York
4 Irving Place, New York, N. Y. 10003
Technician in technical service division
Trouble Shooting and testing of various equipment in a power station

Summer 1971
Research for General Foods Corporation-Maxwell House Division, Hoboken, New Jersey
Conducted experiments on freeze drying of coffee
Development of temperature gradient freeze drying microscope stage

Summer 1972
Lever Bros. Company, Research Division, 45 River Road Edgewater, New Jersey
Study of structural changes and phase transformations using techniques of election microscopy, x-ray diffraction patterns and differential thermal analysis

1973-74
General Foods Corporation, Tarrytown, New York
Consultant to Physical Chemistry Division

1972 to Present
Instructor at the City College of New York
Department of Chemistry

EXTRA CURRICULAR ACTIVITIES

Graduate
Member AI Che & ACS
Chemistry Dep't Executive Comm. 1973-75
CUNY Doctural Students Council

Under-Graduate
Research Honor's Program-project involved study of the mechanism of freeze drying.
Member of AICHE
Student Chapter Vice President, Omega Chi Epsilon
Student Chapter Secretary Tau Beta Pi 1972
Member of Amateur Athletic Union
Member U. S. Handball Association

PUBLICATIONS

1. Freezing of Aqueous Systems Using a Temperature Gradient Microscope Stage
   with H. L. Rosano and M. Freedman
   Journal of Colloid & Interface Science 40, 123 (1972)

2. Temperature Gradient Freeze Drying Microscope Stage
   with H. L. Rosano and M. Freedman
   Journal of Food Science 37, 492 (1972)

3. Effect of Freeze Thaw Process on Amylase
   with H. L. Rosano
   Cryobiology 10, 240 (1973)

4. Surface Drag Viscosity of Bovine Serum Albumin Monolayers
   with H. L. Rosano and S. H. Chen
   Journal of Physical Chemistry 78,2266 (1974)

5. Etude Microscope Du Vieillissement De la Tripalmitive
   with H. L. Rosano
   Revue francaise des Corps Gras 21,605 (1974)

6. Physical Aging of Pure Even Monoacid Triglycerides
   with H. L. Rosano
   Journal of The American Oil Chemist
   52, 128 (1975)

7. Role of the Bovine Serum Albumin Subphase in Relation to Surface Viscosity and Film Transfer
   with H. L. Rosano and S. H. Chen
   N. K. Adam Memorial Monograph
   Accepted for publication

PRESENTATIONS

May 1972

Metrochem 72
New York North Jersey Regional ACS Meeting
Temperature Gradient Freeze Drying Microscope Stage

Sept. 1974

168th ACS National Meeting
Atlantic City, New Jersey

1. Phase Transformations and Aging of Monoacid Triglycerides
2. Surface Drag Viscosity of Monolayers

April 1975

169th ACS National Meeting
Philadelphia, Pennsylvania

1. Physical Aging of Mixed Monoacid Triglycerides